2012

Signals Delivered By Interleukin-7 Regulate The Activities Of Bim And Jund In T Lymphocytes

Shannon Moore Ruppert
University of Central Florida

SIGNALS DELIVERED BY INTERLEUKIN-7 REGULATE THE ACTIVITIES OF BIM AND JUND IN T LYMPHOCYTES

by

SHANNON MOORE RUPPERT
B.S. University of Central Florida, 2006

A dissertation submitted in partial fulfillment of the requirements
for the degree of Doctor of Philosophy
in the Burnett School of Biomedical Sciences
in the College of Medicine
at the University of Central Florida
Orlando, Florida

Summer Term
2012

Major Professor: Annette R. Khaled

ABSTRACT

Interleukin-7 (IL-7) is an essential cytokine for lymphocyte growth that has the potential for promoting proliferation and survival. While the survival and proliferative functions of IL-7 are well established, the identities of IL-7 signaling components in pathways other than JAK/STAT, that accomplish these tasks remain poorly defined. To this end, we used IL-7 dependent T-cells to examine those components necessary for cell growth and survival. Our studies revealed two novel signal transducers of the IL-7 growth signal: BimL and JunD.

IL-7 promoted the activity of JNK (Jun N-terminal Kinase), and that JNK, in turn, drove the expression of JunD, a component of the Activating Protein 1 (AP-1) transcription factors. Inhibition of JNK/JunD blocked glucose uptake and HXKII gene expression, indicating that this pathway was responsible for promoting HXKII expression. After a bioinformatics survey to reveal possible JunD-regulated genes activated early in the IL-7 signaling cascade, our search revealed that JunD could control the expression of proteins involved in signal transduction, cell survival and metabolism, including Pim-1. Pim-1, an IL-7 induced protein, was inhibited upon JNK or JunD inhibition. Our hypothesis that JunD positively regulated proliferation was confirmed when the proliferation of primary CD8+ T-cells cultured with IL-7 was impaired upon treatment with JunD siRNA. These results show that the IL-7 signal is more complex than the JAK/STAT pathway, activating JNK and JunD to induce rapid growth through the expression of metabolic factors like HXKII and Pim-1.

When metabolic activities are inhibited, cells undergo autophagy, or cell scavenging, to provide essential nutrients. Pro-apoptotic Bim was evaluated for its involvement in autophagy. Bim is a BH3-only member of the Bcl-2 family that contributes to T-cell death. Partial rescue of

T-cells occurs when Bim and the interleukin-7 receptor are deleted, implicating Bim in IL-7-deprived T-cell apoptosis. Alternative splicing results in three different isoforms: BimEL, BimL, and BimS. To study the effect of Bim deficiency and define the function of the major isoforms, Bim-containing and Bim-deficient T-cells, dependent on IL-7 for growth, were used. Loss of Bim in IL-7-deprived T-cells delayed apoptosis, but blocked the degradative phase of autophagy. The conversion of LC3-I to LC3-II was observed in Bim-deficient T-cells, but p62, which is degraded in autolysosomes, accumulated. To explain this, BimL, was found to support acidification of lysosomes associated with autophagic vesicles. Key findings showed that inhibition of lysosomal acidification accelerated death upon IL-7 withdrawal only in Bim-containing T-cells, indicating that in these cells autophagy was protective. IL-7 dependent T-cells lacking Bim were insensitive to inhibition of autophagy or lysosomal acidification. BimL co-immunoprecipitated with dynein and Lamp1-containing vesicles, indicating BimL could be an adaptor for dynein to facilitate loading of lysosomes. In Bim deficient T-cells, lysosome-tracking probes revealed vesicles of less acidic pH. Over-expression of BimL restored acidic vesicles in Bim deficient T-cells, while other isoforms, BimEL and BimS, associated with intrinsic cell death. These results reveal a novel role for BimL in lysosomal positioning that may be required for the formation of functional autolysosomes during autophagy.

This dissertation is dedicated to my loving, patient parents, and my wonderful, supporting husband, Chase.

ACKNOWLEDGMENTS

I am extremely thankful and indebted to a number of people for their support. Firstly, I must thank my mentor, Dr. Annette Khaled, for seeing my potential and giving me an opportunity to study under her guidance. Thank you to all of the people in my lab: Dr. Christina Kittipatarin, Dr. Mounir Chehtane, Dr. Kathleen Nemec, Dr. Michael Lee, Rebecca Boohaker, Ge Zhang, Rania Bassiouni, Arati Limaye, Ashley Iketani, and the friends that I've made while working late into the evenings. I would also like to thank my committee members, Dr. William Self, Dr. Kenneth Teter, and Dr. Antonis Zervos, for providing invaluable criticism and unfailing patience as I've continued in this journey. Lastly, I'd like to thank my husband, my family, and the Brandywiners for their understanding and helping me to maintain my sanity.

TABLE OF CONTENTS

LIST OF FIGURES

LIST OF ACRONYMS AND ABBREVIATIONS

2-DOG: 2-Deoxy-Glucose

3-MA: 3-Methyladenine

AP-1: Activating Protein-1

BCL-2: B-cell Lymphoma 2

BCL-XL: B-Cell Lymphoma-Extra Large

BCR: B-Cell Receptor

BH3: Bcl-2 Homology Domain 3

BIM: Bcl-2 interacting protein

BimEL: Bim Extra Long

BIMKO: Bim Knock Out

BimL: Bim Long

BimS: Bim Short

BrdU: Bromodeoxyuridine

Cdc25A: Cell division cycle 25 homolog A

ChIP: Chromatin Immunoprecipitation

CQ: Chloroquine

DN: Double Negative

ERK: Extracellular-signal Regulated Kinase

FBS: Fetal Bovine Serum

FITC: Fluorescein isothiocyanate

FKHR-L1: Forkhead Transcription Factor

FSC: Forward Scatter

GFP: Green Fluorescent Protein

GLUT1: Glucose Transporter 1

HXKII: Hexokinase II

HRP: Horse Radish Peroxidase

HTLV-1: Human T-Lymphotrophic Virus 1

IL-7: Interleukin-7

IL-7R: Interleukin 7 receptor

JAK1: Janus Activating Kinase 1

JAK3: Janus Activating Kinases 3

JNK: C-Jun N-terminal Kinase

Lamp1: Lysosomal-associated membrane protein 1

LC3: Microtubule-associated protein light chain 3

LC8: Dynein Light Chain 8

LN: Lymph Node

miRNA: micro RNA

MAPK: Mitogen Activated Protein Kinase

NGF: Nerve Growth Factor

PI: Propidium Iodide

PI3K: Phospho-Inositide 3 Kinase

PE: Phosphatidylethanolamine

rhIL-7: recombinant human IL-7

RUNX1: Runt-related Transcription Factor 1

siRNA: small-interferring Ribonucleic Acid

SCID: Severe Combined Immunodeficiency

SMAD: Sma and Mad related family

SOCS: Suppressors of Cytokine Signaling

SRSF1: Serine/Arginine-Rich Splicing Factor 1

SSC: Side Scatter

STAT: Signal Transducers and Activator of Transcription

TCR: T Cell Receptor

TGF: Transforming Growth Factor

WT: Wild Type

CHAPTER 1: INTRODUCTION

Cytokines are necessary messenger molecules for the immune system, involved in functions ranging from promoting lymphocyte expansion, and differentiation, to the maintenance of homeostasis. In general, cytokines are low molecular weight proteins, having a four-alpha helical bundle structure, that regulate the growth, proliferation, and differentiation of cells composing the immune system. Typically, cytokines function by binding to specific receptors on the membranes of targeted cells, regulating the diverse activities that mediate immunity. Cytokine receptors are composed of two or more polypeptide chains. Typically, one chain is specific to the individual cytokine receptor and the other chain(s) is shared with multiple cytokines within the same family. For example, the common γ chain (γc), expressed by most hematopoetic cells, is essential to establishment of the immune system, and recognizes cytokines including, but not limited to, interleukins (IL-) 2, 4, 7, 9, and 15.

Alterations to the cytokine signaling cascade can most easily be seen in mice lacking γc-containing receptors. For example, IL-2 is necessary for Treg development [1] and IL-7 is involved in T cell development and memory T cell homeostasis [2]. IL-4 is essential for the development and function of T helper 2 cells [3] and IL-15 is required for T cell activation [3]. However, when the receptor for IL-2, IL-4, or IL-15 is deleted, minor phenotypical defects occur, whereas deletion of IL-7, or a deficiency in its receptor, results in reduced thymic and peripheral T cell development and lymphopenia, making IL-7 a non-redundant cytokine [4-8]. Deficiencies in the γc receptor chain result in decreased NK and T cell numbers similar to Severe Combined Immunodeficiency in humans [9, 10].

The IL-7 receptor is composed of two chains, the common cytokine-receptor γ chain, and the IL-7Rα, which is expressed exclusively on cells of lymphoid origin [11]. Regulation of IL-7α receptor expression occurs through a negative feedback loop, in which the transcription of IL-7 suppresses IL7Rα [3]. Mice lacking IL-7 or the IL-7 receptor display reduced lymphoid progenitor development [12, 13], and impaired expansion and maintenance of naïve T cells [14, 15]. Conversely, excess IL-7 results in the development of lymphoma or leukemia [16]. Taken together, these studies illustrate the importance of IL-7 in T cell development.

IL-7 itself, is an essential, non-redundant cytokine that is made by stromal and non-lymphoid cells [17], and is produced at such low doses (in the pictogram per milliliter range) [18] in circulation, that T-cells encounter this signal infrequently. However, the synthesis of IL-7 is increased in response to infection [19] or during sepsis [20], or upon T cell depletion [21]. After binding IL-7, the IL-7 receptor heterodimerizes, bringing together the Janus kinases, Jak1 and Jak3, by association between the IL-7Rα and γc, respectively (Fig. 1). Jak1 and Jak3 phosphorylate each other, increasing their kinase activities, and in turn, phosphorylate Y449 on IL-7Rα to create a docking site for Stat5a/b [22]. Stat5a/b are phosphorylated by JAKs, and undergo further activation upon forming a homodimer. The Stat5 homodimer translocates to the nucleus to initiate transcription of various pro-survival genes, such as SOCS1 and Bcl-XL [23]. Previous studies describe Stat5 as the main transducer of the IL-7 signaling pathway, and so less knowledge exists concerning other pathways induced by IL-7.

IL-7-mediated signaling initiates pathways at multiple stages in the life of a T cell. For example, IL-7 contributes to the diversity of the thymocyte TCR (T Cell Receptor) repertoire through de-methylation and histone acetylation of target DNA [24, 25]. This activity permits

V(D)J recombinase, an enzyme that facilitates transposition events, access to V(D)J genes, inducing δγ TCR rearrangement [25, 26]. IL-7-mediated signaling is also necessary for mature T cell survival. IL-7 sustains this T cell pool by up-regulating pro-survival genes and their respective proteins, and in addition to those mentioned previously, up-regulates Bcl-2, primarily through activation of PI3-kinase and AKT and limits expression of pro-apoptotic Bcl-2 family proteins, Bax and Bad [27]. Questions remain as to whether these are the only targets that IL-7 regulates transcriptionally and post-translationally. In fact, evaluation of immediate response genes using a cDNA array of IL-7 dependent T cells after a two hour pulse with IL-7, reveals the potential for many other IL-7-mediated signaling targets, especially those involved in growth [28].

One homeostatic function of IL-7 is to promote lymphocyte development. IL-7 is essential for the survival, proliferation and differentiation of immature thymocytes. In the thymus, thymocytes undergo progressive phases of maturation to establish tolerance of self and eliminate tolerance of foreign antigens. IL-7R is expressed on the surface of double-negative (DN) (CD4-CD8-) thymocytes, and IL-7 signaling promotes survival of DN thymocytes to develop a diverse TCR repetoire, by maintaining a balance between Bcl-2 family members and promoting the recombination of the T cell receptor γ-chain (TCRγ) [29-31]. To transition to a double-positive (DP) phase, T cell selection must occur. Essentially, the avidity of the TCR interaction with the self-peptide:major histocompatibility complex on antigen presenting cells determines whether a cell will survive [32]. Without the presence of the IL-7R on double-positive (CD4+CD8+) thymocytes, cells unable to recognize self-peptide:MHC undergo death by neglect through downregulation of Bcl-2, and reduced inhibition of pro-apoptotic Bim [33, 34].

IL-7R is once again expressed on single-positive (CD4+ or CD8+) thymocytes and permits maintenance of the population [35].

IL-7 is also involved in the maintenance of memory T cells. Following antigen-activation of naïve T cells, cells undergo clonal expansion, otherwise known as proliferation of target T cell subsets. Once invading antigens are destroyed, the immune cell population undergoes contraction, eliminating excess lymphocytes through apoptosis [36]. What remains is a subset of antigen-specific T-cells that retain IL-7R expression and develop into memory T cells and enter a resting phase [7, 37]. IL-7 supports this basal population through promoting metabolic rate [38] in addition to balancing Bcl-2 and Bim expression [39]. In fact, the level of IL-7R expression also assists in the differentiation of memory cells. IL-7Rhi effector cells have potential for further development as memory cell precursors, whereas IL-7Rlo cells are senescent effector cells [7].

IL-7 signaling and Bim

Homeostasis is in part, maintained through induction of apoptosis. One activity of IL-7 is to promote pro-survival factors. IL-7 signaling up-regulates the expression of the anti-apoptotic protein, Bcl-2 [40, 41]. The Bcl-2 family includes anti-apoptotic proteins, such as Bcl-2 and Bcl-xL, pro-apoptotic members, such as the multi-domain proteins, Bax and Bak, and BH3-only proteins, Bad, Bid, Bim or Bmf [42] (Fig. 2). Due to the important roles of the Bcl-2 family in T cell survival, IL-7R-/- immunodeficiency can be partially rescued by overexpression of Bcl-2 [43], and depletion of Bim [44], or Bax [45]. Mice lacking Bim are unable to delete autoreactive T cells, but coupled with the absence of IL-7R, Bim deficiency can restore partial T cell volumes

[33, 34, 44]. Being that the addition of IL-7 or Bim (or Bax) deficiency, does not completely rescue cells from death, indicates involvement of additional factors.

Originally, interest surrounded the involvement of Bim in apoptosis since it was discovered as a possible antagonistic binding partner for Bcl-2. The *bim* gene was found by screening a bacteriophage lambda cDNA expression library constructed from a p53 deficient T cell lymphoma line [46], with a recombinant Bcl-2 protein probe [47]. Additionally, the *C. elegans* BH3-only homologue, EGL-1, was found to be essential for programmed cell death and bound a Bcl-2 like protein, CED-9 [48]. In experiments with BimKO mice, these mice had increased numbers of B and T cells, enlarged lymph nodes, and these cells survived longer in the absence of essential cytokines [33]. These findings led others to evaluate the role of Bim in cytokine withdrawal *in vitro*. For example, in pro-B cells, Bim protein levels increased upon IL-3 deprivation [49]. However, healthy cells maintain basal Bim mRNA and protein levels, but at such low concentrations that Bim was initially undetectable until cell numbers surpassed 10^7 [50]. Other studies have shown that Bim associates with mitochondrial Bcl-2 in healthy, resting T cells and in cells undergoing apoptosis [51, 52].

Since basal levels of Bim protein were maintained in healthy cells, and sequestered under non-apoptotic conditions, it was possible that regulation of Bim occurred transcriptionally. The promoter of Bim is unique in that the region lies before the unencoded exon 1, lacking TATA or CAAT boxes, but contains three RUNX sites and 1 SMAD site [53]. Bim is induced by many extracellular stressors, including growth factor deprivation, and serum starvation [33, 54-56]. For example, in neuronal cells, NGF deprivation induced c-Jun-dependent upregulation of BimEL mRNA and protein production [57]. Bim can be transcriptionally activated through

alternative means. In some healthy cells, PI3K-mediated activation of AKT, increases phosphorylation of Foxo3a, inhibiting its nuclear translocation, thereby reducing Bim transcription [58]. In pro-B cells withdrawn from IL-3, up-regulation of Bim mRNA synthesis occurs through FKHR-L1 [49]. TGF-beta up-regulates RUNX1 expression, binds and regulates Foxo3 levels, and up-regulates Bim transcription [53, 59]. TGF-beta can also inhibit ERK, preventing phosphorylation-dependent degradation of Bim [60]. Interestingly, the IL-7Rα promoter also contains a RUNX1 site, and up-regulation of IL-7Rα expression in T cells is, in part, activated by RUNX1 [61]. Taken together, these studies indicate that regulation of the transcription of Bim may be cell specific.

Alternative splicing of Bim results in over 18 isoforms, the three major isoforms being BimEL, BimL, and BimS [47, 62, 63], with focus on canonical isoforms of Bim, with a lack of study on physiological relevance, and protein products of the novel splice variants. Indeed, even intron retention within BimEL cDNA can lead to increased BimL protein expression [64]. In fact, in studies done with individually induced Bim proteins, an unintended side effect of up-regulated BimL protein levels upon BimEL induction, can be seen [62, 65]. Recent studies have concluded that BimEL and BimL are interchangeable for apoptotic function in homeostatic hematopoiesis [66], but have not evaluated the individual isoforms in other context other than degree of apoptosis upon treatment with immunosuppressors. There exist non-apoptotic isoforms of Bim as well. Overexpression of the splicing activator, SRSF1, which is upregulated in breast cancers, promotes alternative splicing of non-apoptotic isoforms of Bim lacking the BH3 domain. In fact, overexpression of one of these isoforms, Bim-γ1, resulted in reduced apoptotic cell numbers compared to controls [67]. Alternative splicing also contributes to the

phosphorylation state of Bim. Indeed, phosphorylation sites encoded by alternative splicing of exon 3 contribute to increased BimL expression [68].

Bim activity is also regulated through phosphorylation. Two of the three major isoforms of Bim (BimEL, BimL) contain phosphorylation sites, which garner control over its activity and degradation. Currently, there is debate as to whether the phosphorylation of Bim, inhibits or activates its activity. Previous studies have shown that JNK and p38 MAPK mediated phosphorylation of BimEL, increases apoptosis [68-71]. Additionally, the loss of IL-7 leads to phosphorylation of BimEL and an increase in its pro-apoptotic activity, in T cells [52]. However, others have shown that phosphorylation by ERK [72-74] leads to ubiquitylation and further, proteosomal degradation of BimEL.

In addition to regulation by alternative splicing mechanisms, and phosphorylation, Bim can be regulated through its interaction with other proteins. Pro-apoptotic activities of Bim are blocked through the inhibitory binding of pro-survival Bcl-2 [75]. However, in equal molarities, BimL cannot overcome Bcl-2 protection [76]. In some healthy cells, BimL and BimEL are bound to the dynein light chain [77] and upon encountering stress, such as UV light, BimL detaches from LC8, and is released into the cytosol [78]. In fact, BimL can be found localized to intracytoplasmic membranes independently of association with Bcl-2 [47].

In addition to mediating cell survival, IL-7 could regulate the maintenance of T cell populations. Previous work has shown that Bim, a pro-apoptotic member of the Bcl-2 family, participates in activated T cell death [39]. However, there is little study on the individual isoforms produced through alternative splicing of Bim. In our own studies, we have confirmed the involvement of Bim in apoptosis, and furthermore, the binding Bim to the dynein light chain

[77], but we have also discovered an anti-apoptotic role for Bim in the maintenance of lysosomes.

IL-7 signaling in metabolism and growth

The mechanism by which IL-7 regulates the metabolism of certain T cell populations is less known. Earlier work suggested that IL-7 promoted glucose uptake, independent of Stat5 activation [79], whereas others later found this function specifically mediated by Stat5 [80]. In both cases, IL-7 induced up-regulation of glucose transporter, GLUT-1, trafficking to the cell surface [79, 80]. However, activated T-cell glucose uptake is increased before GLUT-1 expression [81]. This led to our finding that HXKII, a glycolytic enzyme involved in glucose metabolism, and the retention of intracellular glucose, was transcriptionally regulated by IL-7 [82].

In addition to the IL-7 signal transduction that occurs through Jaks activation, Stat5 can be phosphorylated and activated by two Src kinases, Lck and Fyn [83, 84]. Other early work suggested that Mitogen Activated Protein Kinase (MAPK) participated in the context of IL-7 signaling as well [85, 86]. Lck-mediated TCR signaling was shown to operate independently of, or amplify IL-7 signaling to facilitate T cell proliferation [87]. Previously, we reported that an IL-7 signal skewed T-cell subset proliferation, and trafficking [88, 89]. In fact, inhibition of Lck modulated the IL-7 dose response of CD4 but not CD8 T-cells by regulating STAT5 activation [88]. Concerning MAPKs, IL-7 could induce T cell proliferation without participation by ERK [85] but p38 MAPK activation was required [86]. In contrast, we and others reported that IL-7 deprivation induced p38 MAPK and c-Jun N-terminal Kinase (JNK) activities and contributed to

cell death [90, 91] as well as cell cycle arrest as a result of both the phosphorylation and degradation of Cdc25A [89], and the up-regulation of the cyclin-dependent kinase inhibitor, p27Kip1 [92]. Cdc25A, a phosphatase required for progression through the cell cycle, is also activated through phosphorylation by Pim-1 [93], an IL-7 responsive kinase transcribed through Stat5 [94]. Pim-1 contributes to the proliferation of T cells and can reconstitute thymic cellularity in IL-7 and γc mutant mice [95]. In fact, in studies done in Pim TKO mice, reduced T cell proliferation and response to growth factor signaling resulted [96]. However, Pim-1 can negatively regulate the Jak/Stat pathway by phosphorylating and stabilizing the suppressor of cytokine signaling, SOCS1 [97].

It is possible that growth and proliferation can be mediated by IL-7 in a Stat5 independent manner. Analysis of the HXKII promoter reveals putative binding sites for the transcription factor complex, Activating Protein-1 (AP-1). Usually, AP-1 is composed of two or more DNA-binding proteins, including those belonging to the Jun, Fos, Maf, and ATF protein families [98]. Regulation of AP-1 is critical as its targets include genes involved in cell proliferation, growth, transformation, DNA repair, and apoptosis [99]. The activity of AP-1 can be regulated through phosphorylation of its components, with a feedback loop contributing to its activation. For example, AP-1 initiates c-Jun transcription, and further enhancement through rapid phosphorylation by JNK, perpetuates c-Jun activity and expression [100]. JNK also activates another component of the AP-1 complex, JunD. JunD was initially described as a negative regulator of proliferation [101, 102], although more recently, JunD was found to stimulate anti-apoptotic protein expression in HTLV-1-infected T cells [103]. Taken together,

these data suggest that IL-7 could alternatively activate HXKII through a mechanism other that mediated by Stat5.

Recent Developments

Over the last few years, IL-7 has been considered for therapeutic development for a diverse group of diseases. Animal studies have demonstrated that the administration of IL-7 stimulates reconstitution of immune cells in treatments such as stem cell transplants, and chemotherapy [104-106]. Viral infection studies in mice have shown that administration of IL-7 increases the numbers of antigen-specific memory T cells [107]. Recently, a group has shown adaptive regulatory T cells (Tregs), that normally repress the immune response, have the ability to reverse diabetes, but require IL-7 for maintenance of population size [108]. Additionally, administration of IL-7 has been used in an attempt to counteract T cell depletion in immunodeficiencies. While recombinant IL-7 (rhIL-7) did expand and diversify the TCR repertoire of naïve T cells in pre-clinical trials [109], supraphysiological doses very different from limited *in vivo* amounts were used. Additionally, IL-7 has the potential to be used to treat HIV, idiopathic CD4 T cell lymphocytopaenia, and congenital immunodeficiency, as well as supplementation after haematopoietic stem cell transplantation, or after chemotherapy for cancer (reviewed in [110]). One challenge of using rhIL-7 is that this therapy has not been evaluated for its impact upon functions of the individual cell subsets. Specifically, which cell activities are stimulated, and how rhIL-7 contributes to their metabolism and maintenance of their population. Recently, our studies have demonstrated that IL-7 dosing has an effect on the development of T

cell subsets [88], indicating that there is a need to better understand the consequences of IL-7 signaling and its impact upon T cell gene expression.

The studies included here contribute to the understanding of the diverse and complex pathways of metabolism and survival that the IL-7 signal directs in T cells. We attempt to fill in the gaps in knowledge about how other signaling pathways, other than those transduced through JAK/STAT, are involved in T cell growth, and how the multiple isoforms of Bim have separate functions, particularly, in "housekeeping" and cell maintenance. Additionally, we explain how IL-7 contributes to T cell metabolism through regulation of HXKII, eventual glucose consumption, and cell scavenging to prevent premature death. Furthermore, we evaluate how JNK, Bim, and other effectors of the IL-7 signaling pathway, can have various activities, contrary to previous understanding. Without a further understanding of how IL-7 impacts T cell survival and homeostasis, development of effective therapies cannot be achieved, nor the consequences known by modulating IL-7 signaling.

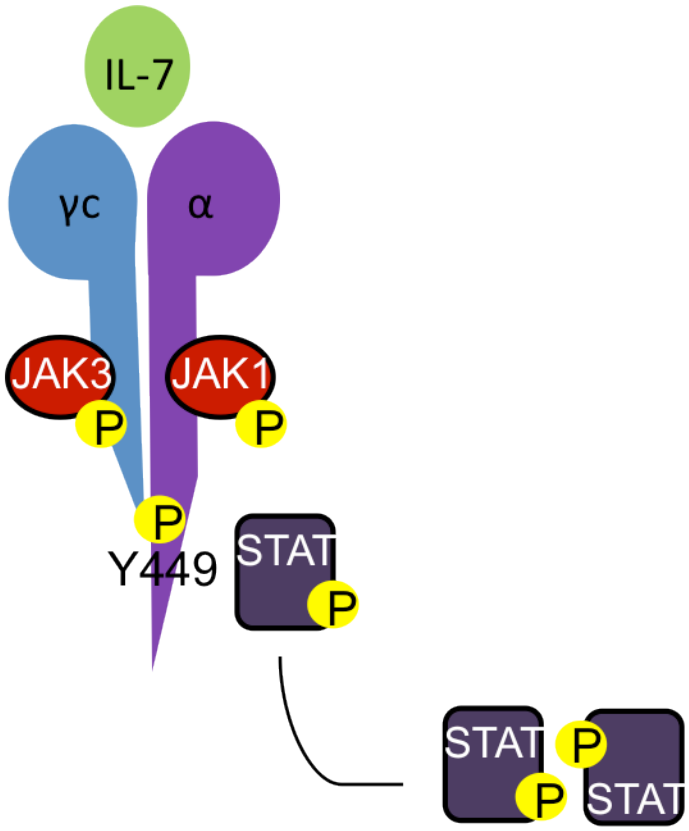

Figure 1. The IL-7 Receptor.
The heterodimeric IL-7 receptor is composed of two chains, the IL-7Rα chain (CD127) and the common γ chain. The common γ chain is shared by receptors that recognize the IL-2 family of cytokines. Binding of IL-7 to its receptor activates JAK1 and JAK3, after which self-phosphorylation increases their kinase activities. JAK1 and 3 phosphorylate the tyrosine (Y) residue at site 499, creating a docking site for STAT5a/b. The JAKs phosphorylate and activate STAT5, leading to STAT5 homodimerization, and further, translocation to the nucleus to transcribe pro-survival genes.

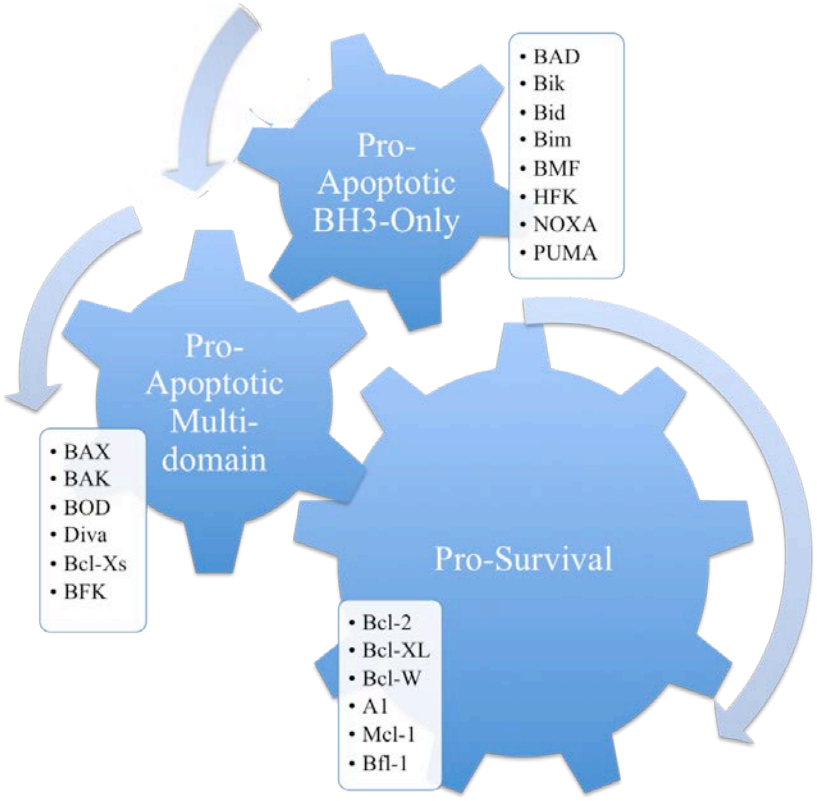

Figure 2. The Bcl-2 Family of Proteins.
The Bcl-2 family of proteins consists of pro-survival proteins, such as Bcl-2 and Bcl-XL, and pro-apoptotic members, which are either multidomain or BH3-only proteins. Pro-survival proteins bind antagonistically to apoptotic proteins, and when an imbalance occurs, apoptosis results.

CHAPTER 2: JUND/AP-1-MEDIATED GENE EXPRESSION PROMOTES LYMPHOCYTE GROWTH DEPENDENT ON INTERLEUKIN-7 SIGNAL TRANSDUCTION

Introduction

Interleukin-7 (IL-7) plays a major role in lymphocyte survival, development and proliferation [2]. Because of its importance as a lymphocyte growth factor, IL-7 has potential use as a therapeutic agent in cancer therapy [109], bone marrow transplantation [111] and treatment of infectious diseases like sepsis [112] and HIV [113]. IL-7 is a 25 kDa protein that is not produced by lymphocytes but was discovered as a product of a thymic stromal cell line [114]. Tissues that produce IL-7 include the generative lymphoid organs [115], [116]; however, the regulation of IL-7 production remains unclear but could be induced in nonlymphoid tissues upon infection [19]. The receptor for IL-7 (IL-7R), expressed by lymphocytes, consists of the IL-7Rα chain and the common cytokine γ chain (γc) [117]. Upon binding of IL-7, the two receptor chains heterodimerize and initiate signaling mediated through receptor-associated kinases, Janus kinases, Jak1/Jak3, which phosphorylate and activate the transcription factor, STAT5a/b [2]. The most recent biological information on IL-7 signal transduction focuses on the JAK/STAT pathway, with scant new information on probable crosstalk with other signaling pathways.

Descriptions of the IL-7R interacting with Fyn or Lyn were published in the early 1990's [118, 119], while other early work revealed aspects of Mitogen Activated Protein Kinase (MAPK) signaling in the context of IL-7 [85, 86]. Lck-mediated T-cell receptor (TCR) signaling was shown to both synergize and operate independently of IL-7 signaling to promote T-cell proliferation [87]. We found that inhibition of Lck modulated the IL-7 dose response of CD4 but not CD8 T-cells by regulating the activation of STAT5 [88]. In regards to the MAPKs, IL-7

could induce T cell proliferation in the absence of ERK (Extracellular signal-Regulated Kinase) activity [85] but required p38 MAPK [86]. In contrast, we and others reported that IL-7 withdrawal induced the activity of p38 MAPK and JNK (Jun N-terminal Kinase) and promoted apoptosis [90, 91] as well as cell cycle arrest [89]. How MAPKs, like p38 MAPK and JNK, can have both growth-promoting and apoptotic functions that are controlled by IL-7 remains unknown.

One of the functions of the MAPK family is the post-translational regulation of Activating Protein 1 (AP-1) transcription factors. AP-1 are dimeric transcription factors composed of proteins with basic leucine zipper domains needed for dimer formation and DNA-binding [120]. The major subfamilies that form AP-1 are Jun (c-Jun, JunB and JunD) and Fos (c-Fos, FosB, Fra1 and Fra2). Activating Transcription Factor (ATF) proteins and Maf proteins can also be components [121]. The potential for multiple combinations gives the AP-1 family its specificity and capacity for a large repertoire of regulated-genes [122]. The activity of AP-1 is mediated in part by ERK, JNK, or FRK (Fyn-Related Kinase) - each of these kinases phosphorylates different substrates. Three distinct JNK gene families have been described: JNK1, JNK2, and JNK3. JNK1 and 2 are ubiquitously expressed, while JNK3 is selectively expressed in neuronal and cardiac tissues [123]. The Jun family is activated through phosphorylation by JNKs, with c-Jun and JunD being recognized targets [124]. While c-Jun and JunB are considered activating factors and expressed as early genes [125-127], JunD was first described as a negative regulator of cell proliferation [101, 128, 129].

There exists a number of IL-7 functional targets [28]. To name a few, IL-7 promotes cell survival through Bcl-2 upregulation and repression of Bax [29, 130, 131], Bim [44] or Bad [30].

IL-7 drives proliferation through cell cycle regulators such as Cdc25A [89] and p27 kip [92]. IL-7 also regulates glucose metabolism [80, 131], and this function is partially fulfilled through transcriptional control of Hexokinase II (HXKII) [82]. How other signaling pathways augment the JAK/STAT signal and contribute to T-cell growth is unknown. In this study, we investigated the activity of the JNK pathway in IL-7- dependent T-cells and found that it involved the activation of JunD-containing AP-1 complexes. JunD/AP-1 drove the expression of HXKII. Using a bioinformatics approach, we discovered other JunD-regulated genes that included the oncogene, Pim-1, which was induced by IL-7. The importance of these findings is the demonstration that, in T-cells, JunD can modulate positive growth in response to IL-7, enhancing the initial cytokine signal transduced by JAK/STAT.

Materials and Methods

Mice, Cell Lines and Culture Reagents

C57Bl/6 mice were purchased from Jackson Laboratory (Bar Harbor, Maine) and housed at the University of Central Florida, Orlando, FL. Mice were used in accordance with the recommendations in the Guide for the Care and Use of Laboratory Animals of the National Institutes of Health. The protocol was approved by the Institutional Animal Care and Use Committee at the University of Central Florida (Assurance # A4135-01). All efforts were made to minimize suffering. The IL-7 dependent T cell line, D1, was established from pro-T lymphocytes isolated from a $p53^{-/-}$ mouse as previously described [28]. Since its establishment in 1997, the D1 cell line has been used to study regulatory pathways controlled by IL-7 [22, 29, 30, 82, 89]. D1 T-cells were grown in RPMI 1640, 10% fetal bovine serum (FBS), 5%

Penicillin/Streptomyocin (Fisher), 0.1% B-mercaptoethanol (Invitrogen) (complete medium) and 50 ng/mL IL-7 (Peprotech). Early passages of D1 cells were frozen as stocks and cells used at less than 10 passages from stocks. Primary lymph node (LN) T cells were isolated from 8- to 12-week-old C57Bl/6 mice as previously described [132]. To enrich for IL-7 dependent cells, we used our published method of *ex vivo* expansion, culturing LN T cells with 150 ng/mL IL-7 for 5 days [132]. Reagents used as described in Figure Legends include: JNK inhibitor II (Calbiochem, 20 μM), p38 MAPK inhibitor (Calbiochem, 20 μM), Wortmannin (Calbiochem, 5 nM), PD169316 (Calbiochem, 20 μM), MEK1/2 inhibitor (Calbiochem, 20 μM) and STAT5 inhibitor (Calbiochem, 50 μM).

Plasmids and Nucleofection for Transient Gene Expression

Generation of the chimeric IL-4 receptor/IL-7 receptor plasmids were previously described [22] and pcDNASTAT5a-CA was a kind gift from Dr. Wenqing Li, NCI-Frederick. To transiently express the plasmids, T-cells were “nucleofected” using the Murine T-cell Nucleofection kit (Amaxa), following the manufacturer's protocol. Briefly, 1×10^6 D1 cells were incubated with (4 μg) plasmid DNA in 100 μl of the mouse T-cell solution, and electroporated with the specific program optimized for mouse T-cells. Nucleofected D1 cells were incubated in the supplemented media with or without IL-7 for 4–8 hours prior to analysis. In D1 cells nucleofection efficiency averaged approximately 40–50% expression of the target gene with viabilities ranging 60–80%

Glucose Uptake Assay

Cells were incubated in glucose-free, serum-free RPMI 1640 supplemented with or

without IL-7 for 1 hour. 2-Deoxy-D-[$_3$H] glucose (2-DOG)(2 μCi/reaction) (Sigma) was added for 3 min. Reactions were stopped by adding 250 μl of ice-cold 0.3 mM phloretin (Sigma). Cells were then centrifuged through a cushion of 10% bovine serum albumin, and lysed with 0.1% Triton X-100. Radioactivity was measured with scintillation counter (LS6500, Beckman Coulter).

Real Time PCR

Ten million cells per experimental condition were re-suspended in 1 ml of TRIzol reagent (Invitrogen). Total RNA was extracted from the cells using the reagent according to the manufacturer's instructions. Each cDNA template was synthesized from total RNA by reverse transcription with iScript cDNA Synthesis kit (BioRad) according to manufacturer's instructions. Quantitative analysis of cDNA amplification was assessed by incorporation of SYBR Green (ABI) into double-stranded DNA. Primer sets were used as follows: for mouse Pim-1: 5′-CCC GAGCTATTGAAGTCTGA-3′, 5′-CTGTGCAGATGGATCTCA GA-3′ (sense and antisense, respectively) [133], for mouse JunD: 5′-ATGGACACGCAGGAGCGCAT-3′ and 5′-AGCAGCTGGCAGCCGCTGTT-3′ (sense and antisense, respectively) [134], for mouse HXKII: 5′-CACTGGGTACTAAGGCTCAA-3′ and 3′-CGGAGTTGTTCTGCTTTGGA-5′ [82], and for β-Actin: 5′-GAAATCGTGCGTGACATCAA AG-3′ and 5′-TGTAGTTTCATGGATGCCACAG-3′ (sense and antisense, respectively) [135]. Reactions contained Fast SYBR Green Master mix (1×), β-Actin primers (50 nM), or Pim-1 or JunD primers (100 nM), and 3–4 μg cDNA template. Thermal cycling conditions were as follows: enzyme activation for 20 seconds at 95°C, followed by 40 cycles of 3 seconds at 95°C, and 30

seconds at 62°C at annealing and extension temperatures. All cDNA samples were processed using the ABI Fast 7500 and analyzed using ABI Sequence Detection Software version 1.4. The difference in mRNA expression was calculated as follows: fold change = $2^{-\Delta\Delta Ct}$, $\Delta\Delta Ct$ is equal to the change in ΔCt values over time after normalization to β-actin.

Detection of Proteins by Immunoblotting

For preparation of whole cell lysates, $20–25\times10^6$ D1 cells (per experimental sample) were lysed using the Cell Lysis buffer (Cell Signaling) in the presence of protease and phosphatase inhibitors (Roche). Lysates were immunoblotted for Pim-1 and JunD as described below. For immunoblotting, whole cell lysate samples were run in 12% SDS-PAGE gels, and proteins transferred to nitrocellulose membranes (Invitrogen) following manufacturers' protocols. Membranes were washed and probed with primary antibodies (see below) and incubated with horseradish peroxidase (HRP)-conjugated (Santa Cruz) or fluorescence-conjugated secondary antibodies (LICOR). Signal was detected using either chemiluminescent substrate (SuperSignal West Fempto; ThermoSci) or the LICOR Odyssey detection system. The primary antibodies used in this study were as follows: a mouse monoclonal antibody against Pim-1 (Abcam), and rabbit polyclonal antibodies against p38 (Santa Cruz Biotechnology), and JunD (Abcam).

JunD Inhibition by Small Interfering RNAs (siRNAs)

Four million D1 cells (per experimental condition) were treated with JUND1 SMART pool siRNA (Dharmacon) and Accell delivery media (Dharmacon) supplemented with 1% FBS, and IL-7 (50 ng/ml) for 52 hours. After 52 hours, cells were washed and re-plated in media containing the siRNA alone, for 18 hours with or without IL-7. In addition, a subset of IL-7

deprived cells was re-pulsed with the cytokine. SMART pool siRNA contains four sequence variations of siRNAs to eliminate non-specific interactions. Non-targeting siRNA (NT siRNA) and NT siRNA containing a FAM reporter, were used as controls and to determine delivery efficiency, respectively.

Detection of JNK Activity

Whole cell lysates from 10×10^6 D1 cells (per experimental sample) were prepared using the Kinase Extraction Buffer provided within the JNK kinase assay kit (KinaseSTAR JNK Activity Assay Kit, BioVision) and assayed for protein concentration by absorbance at 280 nm (Nanodrop 8000). To measure JNK activity, cell lysates were pre-cleared with Protein A/G Sepharose beads (Santa Cruz) and then incubated with the kit provided JNK-specific antibody and agarose beads to pull down JNK. Phospho-c-Jun was used as a substrate to measure JNK activity following the manufacturer's protocol. Total JNK protein in lysates was measured using a JNK-specific antibody (Cell Signaling) following the immunoblot procedure described above.

Chromatin Immunoprecipitation (ChIP) Assay

ChIP assay was performed using the ChIP-IT kit (Active Motif) according to manufacturer's protocol. Briefly, 100×10^6 D1 cells were incubated overnight with or without IL-7, and treated with 37% formaldehyde to crosslink protein to DNA. Cells were then treated with the kit-provided lysis buffer supplemented with protease inhibitors and dounce homogenized. Nuclear pellets were sonicated and pre-cleared using the Protein G beads provided within the kit. Pre-cleared chromatin was incubated with anti-JunD antibody (Abcam) and immunoprecipitated using Protein G beads according to the manufacturer's protocol. DNA was eluted and purified. To

determine the DNA sequence to which JunD bound, PCR analysis of the DNA was performed using AP-1 primers for the HXKII promoter sequence (Primer3 software): forward Primer 5′GGGCTCTAGGCGCTGATT3′ and reverse Primer: 5′GGAGTTGGTGCAACAATGTG3′. PCR products were analyzed by non-denaturing agarose gel (1%) electrophoresis.

Electrophoretic Mobility Shift Assay (EMSA)

Nuclear extraction and EMSA were performed according to the method described by Jaganathan et al. [136] and a modified Dignam protocol [137]. Briefly, 60×10^6 cells were washed and cell lysates prepared with hypotonic buffer (20 mM HEPES (pH 7.9), 1 mM EDTA, 1 mM EGTA, 1 mM Na3VO4, 1 mM Na4P2O7, 0.5 mM PMSF, 0.1 mM aprotinin, 1 mM leupeptin, 1 mM antipain, and 1 mM DTT). NP-40 was added to a final concentration of 0.2% and the solution was centrifuged. The supernatants were retained as cytosolic controls and the nuclear pellets lysed with hypertonic extraction buffer (20 mM HEPES (pH 7.9), 0.42 M NaCl, 1 mM EDTA, 1 mM EGTA, 1 mM DTT, 20 mM NaF, 20% glycerol, 1 mM Na3VO4, 1 mM Na4P2O7, 0.5 mM PMSF, 0.1 mM aprotinin, 1 mM leupeptin, 1 mM antipain). The nuclear fractions were then recovered by centrifugation. Transcription factors bound to specific DNA sequences were examined by EMSA. Normalized extracts, containing 3–8 µg of total protein, were incubated with a double-stranded ^{32}P-radiolabeled AP-1 oligonucleotide probe (Santa Cruz) prepared by radiolabeling the AP-1 probe with [α^{32}P]dCTP (3000 Ci/mmol) and [α^{32}P]dATP (3000 Ci/mmol). Protein-DNA complexes were resolved by non-denaturing polyacrylamide gel electrophoresis (PAGE) and detected by autoradiography. To establish the specificity of the AP-1 probe, unlabeled AP-1 oligonucleotides or mutant AP-1 nucleotides (Santa Cruz) were incubated with

nuclear extracts for 15 min before incubation with radiolabeled probes. To identify components of the AP-1 transcription factor in the DNA–protein complex shown by EMSA, we used protein-specific supershift antibodies, c-Fos, c-Jun and JunD (Active Motif), to detect the formation of a supershift DNA–protein complex. These antibodies were incubated with the nuclear extracts for 30 min at room temperature before incubation with radiolabeled probe.

Analysis of JunD ChIP-seq Data

The JunD ChIP-seq (chromatin immunoprecipitation followed by high throughput parallel sequencing) data for three cell lines, GM12878, Helas3, and K562, was downloaded from http://hgdownload.cse.ucsc.edu/goldenPat h/hg18/encode DCC/wgEncodeYaleChIPseq/. Narrow peaks provided by this website were used as the binding regions of JunD. These narrow peaks are regions enriched with JunD binding segments in ChIP-seq experiments, and are selected with a false discovery rate [138] of 0.001. In total, 12958, 45893, and 1500 JunD binding regions were obtained from the GM12878, Helas3, and K562 cell lines, respectively. These JunD binding regions were compared with all annotated refseq genes in the human genome. By assuming that the genes closest to the above binding regions were target genes of JunD, we obtained 6754, 15577, and 1643 target genes in the above three cell lines, respectively. For example, we obtained 1643 target genes in the K562 cell line with only 1500 binding regions because some binding regions were located in multiple annotated genes. To understand the function of these target genes, we performed gene ontology analysis by using the GOTermFinder software [139]. Results are found in supplemental files, Figure S2 and Data S1. A previous cDNA array, using IL-7 dependent D1 cells [28], identified 179 genes that were immediate

responders to a two hour pulse with IL-7. We found that 116 out of the 179 IL-7-responsive genes were target genes of JunD in the three cell lines. However, 108 out of the 116 genes are not annotated.

Proliferation Assay for Primary Lymphocytes

Five to ten million primary LN T-cells, enriched by 5 day culture with IL-7 and treated with control or JunD siRNA as described above, were examined for proliferative capacity. Viability of cultured cells was determined based on cell shrinkage and granularity by gating on FSC/SSC parameters acquired by flow cytometry (Accuri C6 Flow Cytometer). IL-7-cultured primary T-cells treated with siRNAs were pulsed with 10 µM BrdU for 48 hours. DNA synthesis was evaluated through BrdU incorporation, using a PE-tagged, anti-BrdU antibody for detection of DNA content with a commercially available kit according to manufacturer's protocol (BD Biosciences). Surface expression of CD4 and CD8 on the primary T cells were assessed by flow cytometry using the following conjugated antibodies: PerCP-anti-CD4 (clone RM4-5), and PerCP-anti-CD8 (clone 53-6.7) (BD Biosciences). Cells were incubated with antibodies for 20 min on ice, washed in RPMI+10% FBS, prior to BrdU analysis, and analyzed by flow cytometry on a C6 flow cytometer (Accuri).

Statistics

Statistical analysis and significance was determined using Prism 5 (Graphpad) for Windows, Version 5.02.

Results

Previously, using an IL-7 dependent T-cell line, D1, and primary T-cells, we reported that HXKII gene expression was regulated by an IL-7 signal [82]. However, we found that inhibition of STAT5 did not prevent the expression of HXKII in response to IL-7 (Fig. S1). To demonstrate that a STAT5-independent, but still an IL-7 dependent signal, controlled HXKII gene expression, we nucleofected D1 cells with a chimeric IL-4/IL-7 wild-type receptor or with a chimeric IL-4/IL-7 receptor bearing a mutation in the STAT5 binding site, Y449. Normally, when Y449 is phosphorylated it binds STAT5; therefore mutation of this site would prevent STAT5 activation. D1 cells, nucleofected with the chimeric receptors, were cultured with human IL-4. Gene expression of HXKII was measured by quantitative PCR and glucose uptake was measured by 2-DOG uptake. We found that the IL-4-induced HXKII gene expression and glucose uptake in nucleofected cells was not affected by the Y449 mutation and that cells were comparable to those incubated with IL-7, suggesting that these events were STAT5-independent [140]. Examination of the mouse HXKII promoter region showed that the proximal promoter region contained most of the transcription factors binding motifs that regulate HXKII expression [141]. Some of the recognized factors included SP-1, NF-Y, CREB, Glucose binding site, and the AP-1 complex. To study this, we examined the activity of the MAPK pathway and induction of AP-1 transcription factors in response to IL-7.

JunD/AP-1 complexes are activated upon IL-7 stimulation through the JNK Pathway

A limited number of studies showed that IL-7 withdrawal up-regulated p38 MAPK [91] and JNK [90], and that ERK signaling was dispensable in IL-7 dependent T-cells [85]. Because

of the importance of JNK in AP-1 activation [120], we examined JNK activity in response to IL-7. Previously, we and others established that D1 cells express all the known components of the IL-7 signaling pathway and are representative of the primary T-cell response to IL-7 [30, 45, 52, 82, 89, 92]. Because of this and the fact that primary T-cell subsets are not equally responsive to IL-7 [88, 132], in the current study we used D1 cells, which uniformly respond to the cytokine, to study the functional outcomes of IL-7 signal transduction. Our goal was to identify novel molecular events driving the lymphoproliferative activity of IL-7. A JNK activity assay was performed that involved immunoprecipitation of the kinase from whole cell lysates and detection of the phosphorylated c-Jun substrate as a read out for kinase activity. As shown in the immunoblot for phosphorylated c-Jun substrate in Figure 3, D1 cells incubated with IL-7 had higher levels of JNK activity than those deprived of IL-7 (Fig. 3). In IL-7-deprived D1 cells, JNK activity was initially observed through 6 hours of cytokine withdrawal and was undetectable after 18 hours of cytokine withdrawal. As control for protein input, JNK levels were detected in lysates prior to immunoprecipitation. These results support that JNK activation is a part of the IL-7 signaling pathway.

Since JNK is known to regulate the components involved in AP-1 activation, a gel shift assay was performed to determine whether IL-7 induced AP-1 DNA-binding activity. An oligonucleotide probe containing the AP-1 DNA-binding consensus site was incubated with nuclear extracts from D1 cells grown with or without IL-7 for 18 hours. EMSA results revealed that more AP-1 bound to DNA in D1 cells incubated with IL-7 [140]. This suggested that IL-7 induced the formation of AP-1 complexes that bound to the consensus DNA sequence. To confirm specific binding of the protein to the AP-1 probe, a competition assay with excess cold

AP-1 probe (unlabeled) as well as with a mutant AP-1 probe was performed. Addition of cold AP-1 probe effectively reduced binding of protein to the radiolabeled AP-1 probe, while addition of mutant AP-1 probe had little effect [140]. To identify the components that formed the IL-7-induced AP-1 complex, nuclear extracts, made from D1 cells grown with IL-7, were co-incubated with supershift-specific antibodies against c-Fos, c-Jun and JunD, and added to the AP-1 radiolabeled DNA probe. We found that the c-Fos and c-Jun antibodies did not produce a supershift or impede protein binding to DNA, whereas the JunD antibody caused steric hindrance, preventing protein binding to the AP-1 DNA probe [140]. This illustrates that IL-7 stimulation resulted in an AP-1 complex containing JunD.

To determine whether the JNK pathway was involved in synthesis and activation of JunD in response to IL-7, we examined, by quantitative PCR, JunD gene expression levels in response to IL-7 and in the presence of JNK (and, as control, p38 MAPK) pharmacological inhibitors. Note that doses of inhibitors used were experimentally determined. D1 cells were grown with or without IL-7 for 18 hours, and, to a separate population of cytokine-deprived cells, IL-7 was added back for 2 hours to induce expression of IL-7-dependent gene products. Loss of IL-7 caused a decrease in the gene expression of JunD that was restored upon a two hour re-addition of IL-7 (Fig. 4A). This IL-7-driven increase in JunD mRNA was inhibited by treatment with the JNK but not the p38 MAPK inhibitor (Fig. 4A). To confirm this result, protein lysates from similarly treated cells revealed that JunD protein decreased in the absence of IL-7 and increased upon IL-7 re-addition (Fig. 4B) in the manner observed for the mRNA levels (Fig. 4A). Inhibition of JNK caused a reduction in protein levels of JunD (Fig. 4B); a result consistent with

the gene expression data (Fig. 4A) and the decrease in JNK activity noted after IL-7 withdrawal (Fig. 3).

IL-7-dependent JNK activity drives glucose uptake through the synthesis of HXKII

To investigate a functional consequence of JNK activity, D1 cells were deprived of IL-7 for 18 hours and IL-7 added back to the culture with the addition of either PD169316, (p38 MAPK/JNK inhibitor), MEK1/2 inhibitor, or wortmannin (PI3K (Phosphoinositide 3-kinase) inhibitor). As an indicator of cell metabolism, glucose uptake was measured using 2-DOG [82]. Figure 5A showed decreased glucose uptake in D1 cells that were stimulated with IL-7 and incubated with PD169316, an inhibitor of the p38/JNK pathway, but not with inhibitors of the MEK1/ERK pathway or the PI3K pathway. To differentiate between the p38 MAPK and JNK pathways, glucose uptake was then measured in IL-7-stimulated D1 cells cultured with specific inhibitors for JNK or p38 MAPK. Figure 5B demonstrates that D1 cells incubated with a JNK inhibitor, but not a p38 MAPK inhibitor, had decreased glucose uptake upon IL-7 addition. To show that, upon IL-7 stimulation, JunD/AP-1 complexes mediated the uptake of glucose, D1 cells were treated with JunD siRNA and assayed for the uptake of 2-DOG. The efficacy of siRNA knockdown of JunD mRNA (~60%) and protein (~50%) are shown in later figures. Inhibition of JunD reduced the uptake of glucose in IL-7-stimulated D1 cells to levels approaching those observed in the cells cultured without IL-7 (Fig. 5C). Note that background levels of 2-DOG uptake are indicated by the IL-7 deprived controls and are the point of comparison for the other experimental samples. These results indicate that JNK and JunD/AP-1

complexes were in part responsible for regulating the activity of factors that promoted glucose uptake upon IL-7 stimulation.

In our previous study, we reported that HXKII gene expression increased after two hours of IL-7 re-addition to deprived cells [82]. We also found that a STAT5-independent mechanism with driving the synthesis of HXKII [140]. Since the gene expression of JunD was dependent upon JNK and IL-7 (Fig. 5A), it was possible that the increase of HXKII gene expression that followed IL-7 re-addition was also associated with the activity of JNK. Therefore, the synthesis of HXKII was evaluated in D1 cells stimulated with IL-7 and treated with a JNK inhibitor. Quantitative PCR results demonstrated that HXKII synthesis was reduced by about 60% compared to vehicle control upon treatment with JNK inhibitor (Fig. 6A). D1 cells incubated with the p38 MAPK inhibitor showed little effect (Fig. 6A). This data confirmed that the IL-7-driven increase in HXKII gene expression is likely mediated by JNK. To establish a role for JunD-containing AP-1 complexes in HXKII gene expression, D1 cells were stimulated with IL-7 and treated with JunD siRNA. Shown in Figure 6B is a representative experiment in which loss of JunD reduced the IL-7-driven expression of HXKII. A graph alongside shows that treatment with JunD siRNA reduced JunD mRNA levels by approximately 60% as compared to the non-targeting control siRNA. Hence, JunD/AP-1 complexes were contributing to the synthesis of HXKII in response to IL-7.

The binding of JunD/AP-1 complexes to the AP-1 site on the HXKII promoter was examined to validate our conclusions. To this end, a chromatin immunoprecipitation assay (ChIP) was performed. Nuclear lysates of D1 cells cultured with and without IL-7 for 18 hours were incubated with JunD antibody to immunoprecipitate JunD-bound DNA. Quantitative PCR

was then performed, using primers specific to the AP-1 region on the HXKII promoter to amplify a DNA sequence of approximately 150 base pairs. We reported the cycle threshold (Ct) values of cells cultured with (31.219) and without (37.374) IL-7, indicating that amplification of the HXKII promoter DNA, immunoprecipitated with the JunD antibody, from IL-7-cultured cells, occurred 6 cycles faster than from IL-7 deprived cells and was thus significantly more abundant. Endpoint DNA from the amplification reactions was run on a non-denaturing agarose gel, and visualized using ethidium bromide staining, to demonstrate that more HXKII promoter DNA was amplified from samples of D1 cells cultured with IL-7. Controls for the reaction are the total DNA inputs, showing equivalent amounts of starting materials. This representative experiment confirms that JunD-containing AP-1 complexes bound to the AP-1 site within the HXKII promoter region in an IL-7 dependent manner.

Bioinformatics Approach Reveals Novel IL-7 Induced Genes Induced by AP-1/JunD

To identity novel IL-7-regulated genes whose synthesis was driven by JunD/AP-1 complexes, we performed a bioinformatics analysis. Previously, we identified a number of genes whose expression was induced upon IL-7 stimulation or deprivation [28]. A comparison of these genes with potential JunD-targeted genes (identified in a bioinformatics screen, see Methods and [140]) yielded a number of targets containing putative JunD binding sites that were potentially IL-7-responsive. The diagram, shown in Figure 7, organizes the information by function. Of the three cell lines characterized, gene functions were separated into suppressive (red) or supportive actions (green). Many of the gene products identified were involved in signal transduction, survival or adhesion (Fig. 7). Among these, JunD emerged as a self-regulated and IL-7 dependent

gene (Fig. 7). Suppressive genes were generally involved in blocking inflammatory processes (Fig. 7). The cell line databases assessed for potential JunD target genes were also evaluated for functional homology, whether inhibitory or stimulatory. The most significant gene ontology terms, according to cell line, are listed in order by P-value and are provided as Data S1. Gene ontology ID (GO), significance by p-value, and the number of genes annotated with that term are found in supplemental files. Also included under each cell line are the number of annotated target genes and the number of target genes for the specific cell line. This approach revealed that a variety of functions can be ascribed to JunD-mediated transcription, specifically, regulation of signal transduction, cell cycling and cellular metabolic processes. Of those genes, ones initiated early in the IL-7 signaling cascade, which could drive additional growth pathways, were of interest for study.

Pim1 is an IL-7-Inducible Gene Product through the Activity of AP-1/JunD

One of the genes that emerged from the bioinformatics analysis as a JunD target and IL-7 dependent was the proto-oncogene, Pim-1. Hence, Pim-1 was chosen for evaluation to validate the bioinformatics approach and provide insight on a novel aspect of the IL-7 signal. The repetitive blot in Figure 8A revealed detectable levels of Pim-1 protein in D1 cells grown continuously with IL-7 for 18–24 hours, while withdrawal of IL-7 for 2–24 hours caused a decline in Pim-1. Next, we examined the effect of JNK inhibition upon Pim-1 protein levels in D1 cells grown with or re-stimulated with the cytokine. Our data in Figure 8B indicates that the basal levels of Pim-1 protein expressed in D1 cells, continually growing in IL-7, were only slightly decreased by inhibition of JNK; however, the increased amounts of Pim-1 that were

induced upon re-stimulation with IL-7 for 2 or 4 hours after deprivation were almost completely inhibited by blocking JNK activity. These results suggest that basal levels of Pim-1 were in part JNK-dependent, but that induction of Pim-1 protein upon IL-7 re-addition was almost completely dependent upon JNK signaling (Fig. 8B). To establish that JunD/AP-1 factors were transducing the JNK signal that induced Pim1, we repeated the experiment using JunD siRNA and observed a measureable decrease in Pim-1 protein induction after IL-7 re-addition (Fig. 8C) when JunD expression was impaired. Levels of JunD protein in these cells are shown for comparison.

These studies were followed by examining Pim-1 gene expression in response to either JNK or AP-1/JunD inhibition. In Figure 9A, re-addition of IL-7 caused an increase in Pim1 mRNA supporting that increase previously detected by protein assay (Fig. 8B). Inhibition of JNK decreased the levels of Pim-1 mRNA in D1 cells stimulated with IL-7, while little or no effect was observed in D1 cells continually grown in IL-7. Likewise, as observed for protein levels of Pim-1, inhibition of JunD with siRNA decreased Pim-1 gene expression in cells re-stimulated with IL-7 after deprivation (Fig. 9B).

Proliferation of Primary Lymphocytes in Response to IL-7 Depends on JunD Activity

Our studies with the D1 cell line revealed the specifics of the IL-7 signaling pathway from activation of JNK through induction of the JunD/AP-1 transcription factors and increased gene expression of HXKII and Pim-1. The expected outcome of IL-7 signal transduction through this pathway would be T-cell proliferation. To examine this, we used our *ex vivo* expansion protocol [132] to isolate IL-7-dependent primary T-cells. This expansion method is needed

because freshly isolated lymphocytes contain only a small number of T-cells that proliferate in response to IL-7 (~10–20%, Khaled, unpublished data). To confirm the results observed with D1 cells, that JunD and Pim1 expression was dependent on the JNK pathway, we treated IL-7 stimulated T-cells with a JNK inhibitor and assessed the effect upon protein levels of JunD and Pim-1. Results in Figure 10A show that JNK inhibition resulted in decreased JunD and Pim-1 proteins (34% and 64% respectively), substantiating the data from D1 cells. Note that primary T-cells under IL-7-deprived conditions cannot be evaluated because these fail to expand and die in culture. To evaluate IL-7-driven proliferation, we measured the incorporation of BrdU in CD4 and CD8 T-cells. As shown in Figure 10B, continuous culture with IL-7 caused CD8 T-cell expansion (16%) to occur more rapidly as compared to CD4 T-cells (2%) – an observation previously published [88]. The addition of JunD siRNA had a modest inhibitory effect (Fig. 10B). However, examining the proliferation of CD4 and CD8 T-cells, re-stimulated with IL-7, revealed that JunD inhibition reduced IL-7 driven growth by more than 60% - more so for the actively dividing CD8 T-cells (from 13% to 5%) (Fig. 10C). These results suggest that IL-7 signaling promotes T-cell proliferation in part through JunD-mediated transcription of gene products such as Pim-1 or HXKII.

In summary, we have shown that IL-7 promotes growth signals through other transcriptional components in addition to STAT5. We found that the JunD/AP-1 transcription factors are activated in response to JNK and drive the synthesis of at least two essential mediators of lymphocyte growth, HXKII and Pim-1, in response to IL-7 stimulation. These results establish a novel approach employing bioinformatics to discover new transducers of the IL-7 metabolic and proliferative signals.

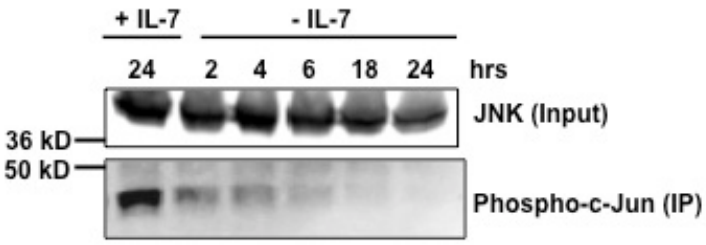

Figure 3. IL-7 signaling induces JNK activity.
JNK activity was determined by the capacity to phosphorylate the substrate, c-Jun. JNK was immunoprecipitated from whole cell lysates prepared from D1 cells cultured in the presence or absence of IL-7 for the times indicated. Pre-immunoprecipitation levels of JNK (input) in lysates are shown. Results are representative of three or more independent experiments.

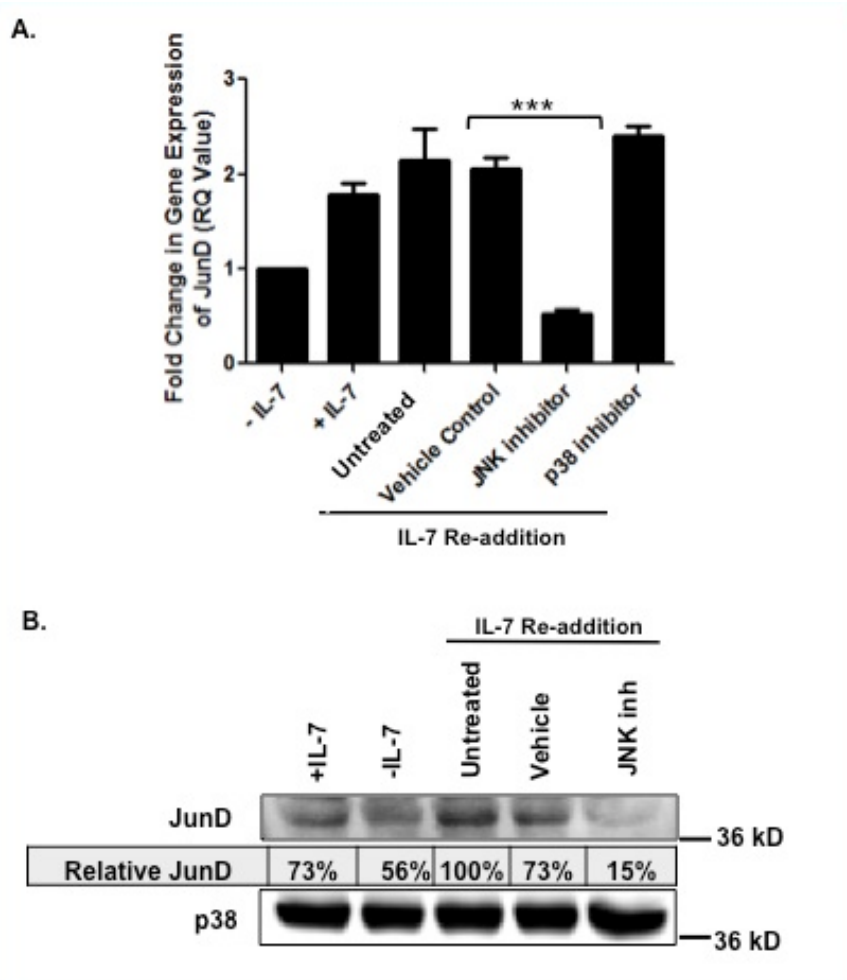

Figure 4. JNK activity promotes JunD expression.
(A) Quantitative PCR evaluation of JunD expression in the IL-7 dependent T-cell line, D1. Cells were continuously cultured with IL-7 or without IL-7 for 18 hours, or withdrawn from IL-7 (18 hours) and then re-stimulated for two hours (IL-7 Re-addition). Re-stimulated cells were untreated, treated with DMSO (Vehicle Control), 20 μM JNK inhibitor (JNK inhibitor), or 20 μM p38 MAPK (p38) inhibitor. (***) indicates $P < 0.0001$. (B) Western blot analysis of JunD protein and p38 MAPK protein content, as loading control, of whole cell lysates from D1 cells cultured as stated above. Relative JunD protein indicates JunD protein levels normalized to p38 MAPK (loading control) and compared relative to the untreated, re-stimulated sample. Results (A, B) are representative of four independent experiments (values in graphs are mean ± SD).

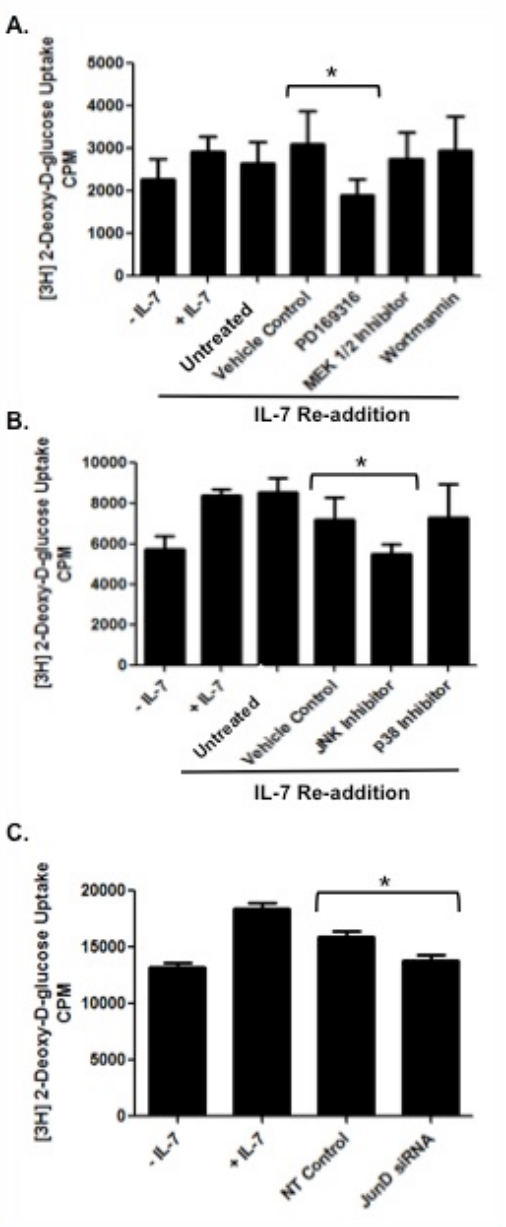

Figure 5. A functional consequence of JNK/JunD signaling is the IL-7 dependent uptake of glucose.
D1 cells continuously cultured with or without IL-7 for 18 hours, or withdrawn (18 hours) and then stimulated with IL-7 for four hours (IL-7 Re-addition), were untreated or treated with DMSO (Vehicle Control), 20 μM MAPK inhibitor, 20 μM PD169316, 20 μM MEK1/2 inhibitor or 5 nM PI3K inhibitor, wortmannin. Glucose uptake was assessed by measuring the accumulation of radiolabeled 2-DOG as stated in Methods. (*) indicates P = 0.0348. (B) D1 cells were treated similarly as those in (A) except that cells were pulsed for two hours and specific inhibitors for JNK (20 μM) or p38 MAPK (20 μM) were used. (*) indicates P = 0.0342. (C) D1 cells were cultured with or without IL-7 after introduction of non-specific control (NT) or JunD siRNA as described in Methods. Glucose uptake was assessed as above by measuring the accumulation of radiolabeled 2-DOG. (*) indicates P = 0.0320. Results (A, B, and C) are representative of three or more experiments performed (values in graphs are mean ± SD). Glucose experiments were performed by Mounir Chehtane, and analysis and interpretation by Shannon Ruppert.

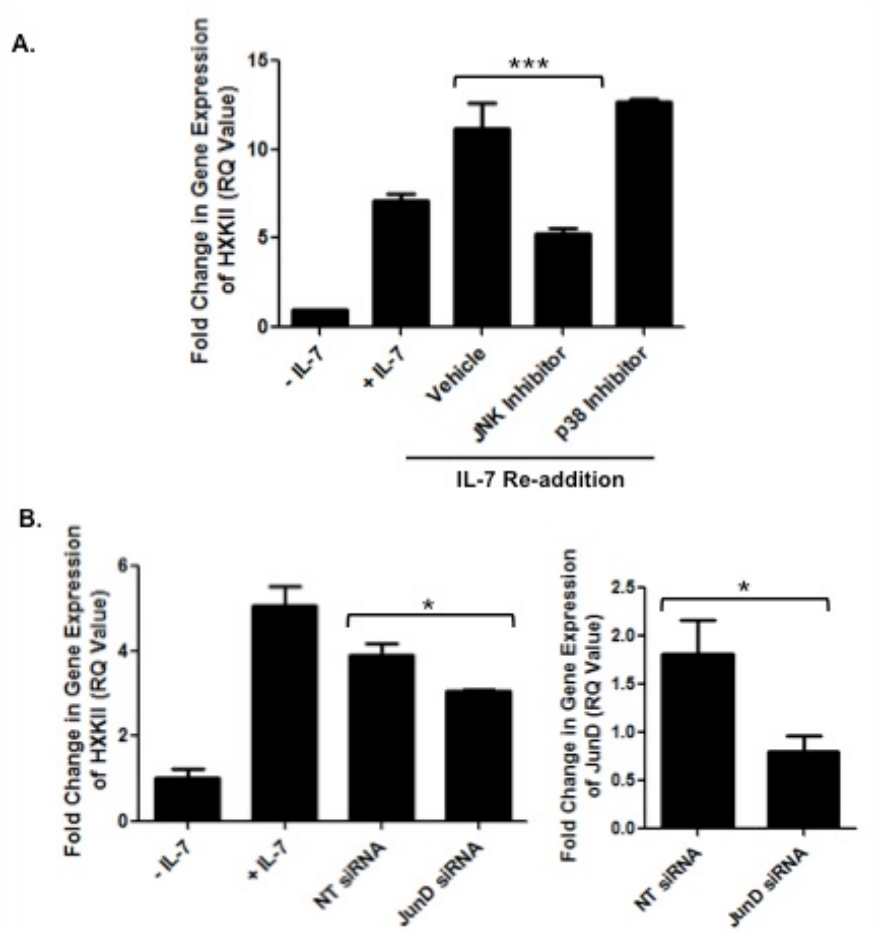

Figure 6. HXKII gene expression is dependent upon JNK/JunD signaling.
(A) HXKII gene expression in the IL-7 dependent T cell line, D1, was measured by quantitative PCR as described in Methods. Cells were cultured with or without IL-7, or after an IL-7 pulse for 2 hours (IL-7 Re-Addition), in presence of a vehicle control, 20 µM JNK inhibitor, or 20 µM p38 inhibitor. RQ (Fold change) = $2^{-\Delta\Delta Ct}$. (***) indicates $P < 0.001$. (B) HXKII gene expression in D1 cells cultured with or without IL-7 and the non-targeting control (NT) or JunD siRNA, as described in Methods, was measured as described above. (*) indicates $P = 0.0254$. Efficacy of JunD siRNA upon JunD mRNA levels (right panel) was established through measuring total JunD gene expression by quantitative PCR. (*) indicates $P = 0.0336$. RQ (Fold change) = $2^{-\Delta\Delta Ct}$. Results are representative of three experiments performed in triplicate (values in graphs are mean ± SD). HXKII gene expression experiments were performed by Mounir Chehtane, and JunD gene expression experiments, and analysis and interpretation of each were completed by Shannon Ruppert.

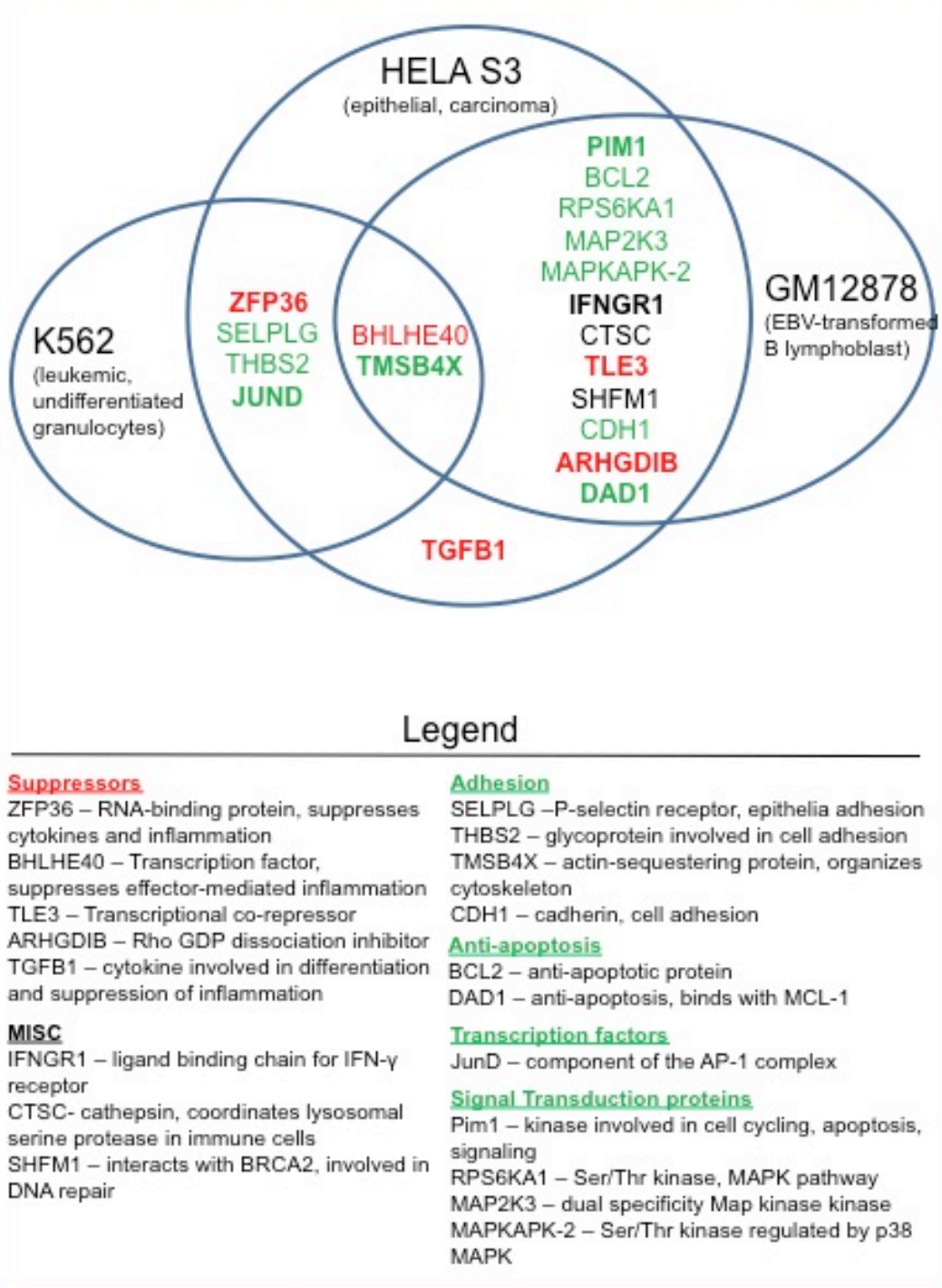

Figure 7. Bioinformatics evaluation of potential IL-7 dependent genes transduced through JunD.
Three cell lines (GM12878, Helas3, and K562) were evaluated for genes containing putative JunD binding sites that are potentially IL-7-responsive, as described in Methods. Gene functions were determined using gene ontology analysis as described in Methods, and were separated into suppressive (red) or supportive actions (green).

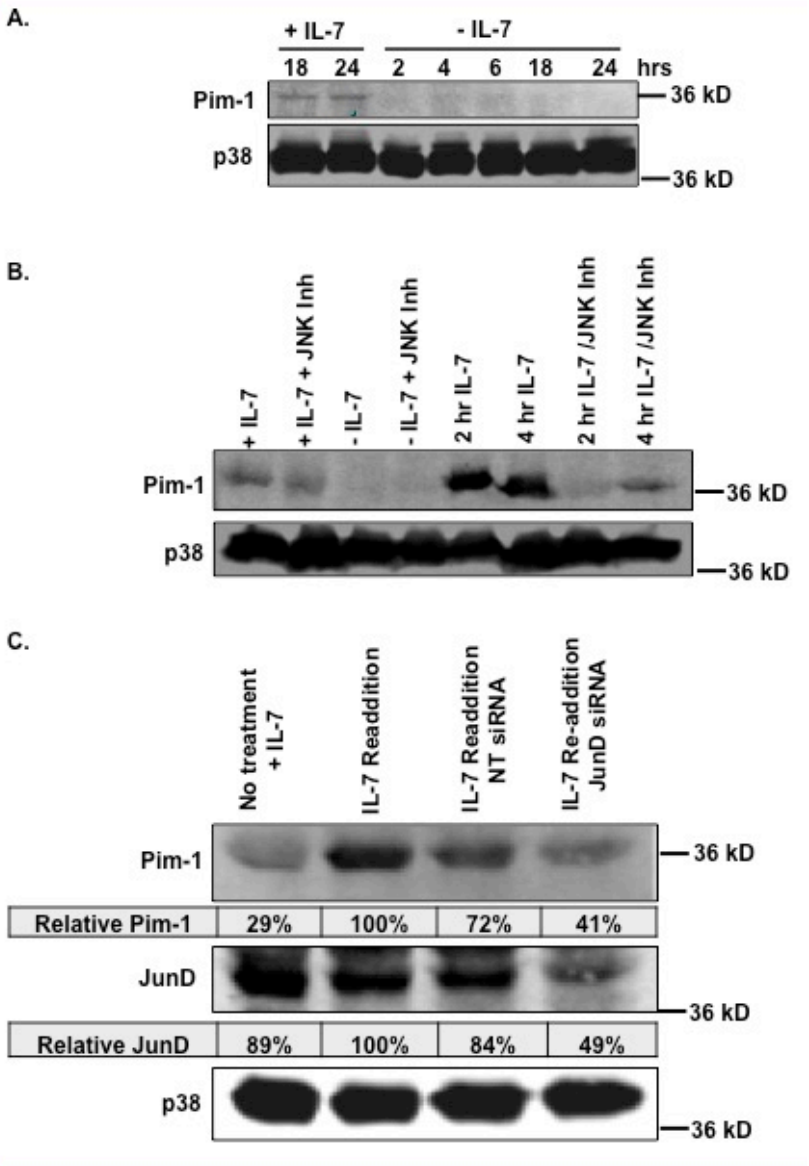

Figure 8. Pim-1 protein is dependent on IL-7 and JNK/JunD.
(A) Immunoblot analysis of Pim-1 was performed. Whole cell lysates were prepared from D1 cells cultured in the presence or absence of IL-7 for the indicated time points. p38 MAPK was measured as a loading control. (B) Immunoblot analysis of Pim-1 was performed. Whole cell lysates were prepared from D1 cells cultured in the presence or absence of IL-7 and/or with JNK inhibitor (20 μM), or 2-4 hour IL-7 stimulation after 18 hour deprivation, alone, or with 20 μM JNK inhibitor. p38 MAPK was used as a loading control. (C) Whole cell lysates of D1 cells were cultured for 52 hours with IL-7 in the presence of non-targeting control (NT) or JunD siRNA, then cells were withdrawn from IL-7 for 18 hours as described in Methods. A separate group was also deprived of IL-7, and then re-stimulated with IL-7 for two hours in the presence of either siRNA (Re-addition). Whole cell lysates were subjected to SDS-PAGE and immunoblotted for Pim-1, JunD, and p38 as loading control. Tables indicate relative amounts of protein normalized to p38 content and shown relative to the IL-7 re-addition sample. Results are representative of three experiments performed.

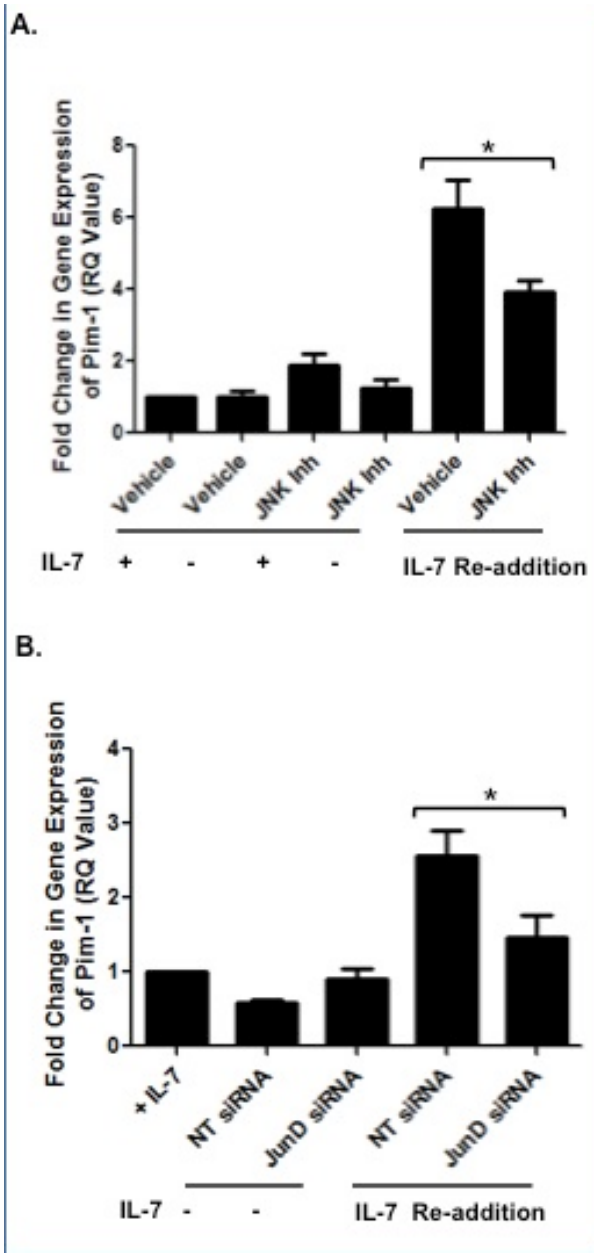

Figure 9. IL-7 inducible Pim-1 gene expression is dependent on JNK/JunD.
(A) Pim-1 gene expression in the IL-7 dependent T cell line, D1, was measured by quantitative PCR as described in Methods. D1 cells were cultured with or without IL-7 (+/- IL-7), in the presence of a vehicle control (Vehicle) or 20 µM JNK inhibitor (JNK Inh). In some samples, after an 18 hour deprivation, IL-7 was added back to the culture for 2 hours in the presence of a vehicle control (IL-7 Re-addition, Vehicle) or 20 µM JNK inhibitor (IL-7 Re-addition, JNK Inh). (*) indicates P = 0.0104. (B) Quantitative PCR of Pim-1 gene expression was performed using D1 cells cultured for 52 hours with and 18 hours without IL-7 in the presence of non-targeting control (NT) or JunD siRNA. A separate group was also deprived of IL-7, and then re-stimulated with IL-7 for two hours in the presence of either siRNA (IL-7 Re-addition). RQ (Fold change in gene expression normalized to β-actin) = $2^{-\Delta\Delta Ct}$. Results are representative of three experiments performed in triplicate (values in graphs are mean ± SD). (*) indicates P = 0.0140.

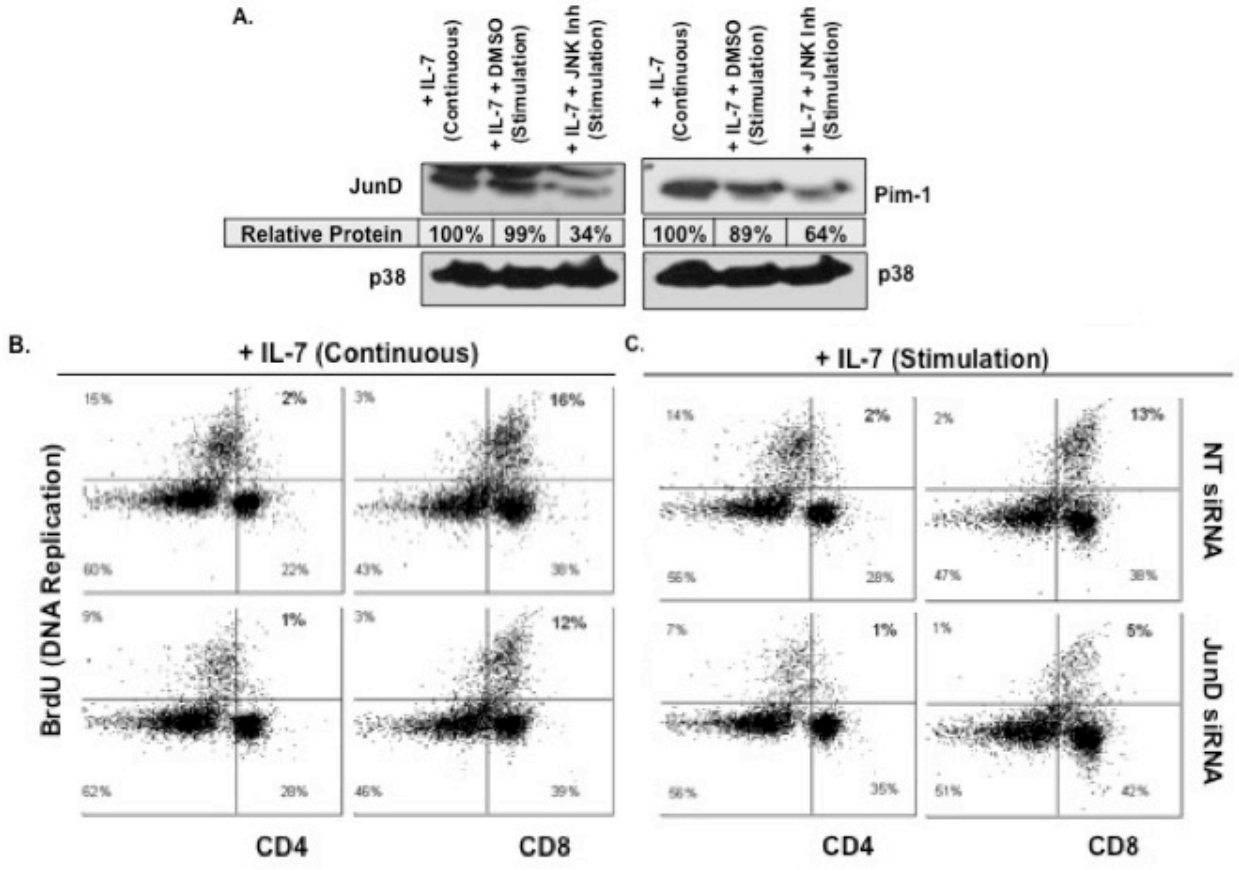

Figure 10. Inhibition of JunD prevents IL-7 induced proliferation of primary lymphocytes.
(A, B) Proliferation was measured by BrdU incorporation. Lymph node T cells were isolated from WT C57Bl/6 mice, cultured continuously with 150 ng/ml of IL-7 for 7 days (A), or for 5 days, then deprived from IL-7 for 18 hours, and stimulated for 24 hours (B) as described in Methods, Cells were assessed for BrdU incorporation and surface expression of CD4 and CD8 as determined by flow cytometric analysis of BrdU-PE and CD4- or CD8-PerCp fluorescence. Dot blots show percentages representing the population of cells that are non-proliferating (BrdU negative), proliferating (BrdU positive), and CD4+ or CD8+ as indicated by the quadrants. Quadrants were established using controls. Gating was performed to remove autofluorescent cells. Results are representative of duplicate samples.

Discussion

Our results suggest that IL-7 in part contributes to the metabolism and growth of T-cells by promoting HXKII and Pim-1 gene expression through the JNK activation of JunD/AP-1. This conclusion was reached by finding that JNK was active in response to IL-7, and that IL-7 induced the binding of AP-1 transcription factors, containing JunD, to DNA sequences such as the HXKII promoter. Using a bioinformatics approach to discover previously unrecognized JunD gene targets that were IL-7-responsive, we identified Pim-1. Confirmation that Pim-1 expression was IL-7- and JunD-dependent, validated the bioinformatics results. Physiological relevance of our findings was established when inhibition of JNK in primary lymphocytes decreased the levels of Pim-1 and JunD and inhibition of JunD prevented the proliferation of CD8 T-cells stimulated with IL-7. This work achieves the goal of demonstrating that other regulators of gene expression, in addition to the JAK/STAT5 pathway, can respond to the IL-7 signal in T-cells and indicates that a bioinformatics approach can be used to discover novel IL-7 signal transducers.

To support T-cell growth, IL-7 signaling leads to the activation of transcription factors, such as STAT5. STAT5 can mediate T-cell survival by inducing anti-apoptotic proteins of Bcl-2 family [142, 143]. STAT5 also promotes glucose metabolism by enabling GLUT1 trafficking to the cell surface [80]. However, we found that the IL-7-mediated increase of HXKII gene expression used a STAT5 independent mechanism to regulate glucose uptake in T-cells. We identified JunD-containing AP-1 complexes as key factors that controlled the synthesis of HXKII in response to IL-7. Pim-1 is also a recognized gene transcribed by STAT5 [94] and a possible JunD-target. We found that T-cells deprived and then re-stimulated with IL-7, which mimics the *in vivo* conditions in which T-cells encounter IL-7, immediately increased Pim-1 levels in a

JunD/AP-1 dependent manner. This is consistent with the proliferative function of Pim-1, since it phosphorylates and induces the activity of proteins involved in cell cycling, including Cdc25A [93] and Skp2 [144]. Our conclusions are supported by the fact that Pim-1 is an effector of the IL-7 signaling pathway, as its expression reconstituted thymic cellularity in IL-7 deficient mice [95], and that Pim-1, 2 and 3 are required for proliferation of peripheral T-cells [96].

JunD was initially described as a negative regulator of proliferation. Early studies showed that over expression of JunD in immortalized fibroblasts increased the numbers of cells in the G0/G1 phase of the cell cycle, promoting growth arrest [101]. JunD also suppressed transformation by Ras [101]. Immortalized cells lacking JunD had higher levels of cyclins and increased proliferation, but also were more sensitive to death-inducing agents, suggesting that JunD could have both negative and positive effects upon cell growth [145, 146]. Concerning the latter activity, JNK and JunD were shown to work with NF-kB to increase the expression of the caspase inhibitor, cIAP-2 [146]. While these studies were performed using immortalized cells and fibroblasts, the evaluation of JunD activity in lymphocytes revealed different results and demonstrated that JunD activity can be cell specific. JunD over expression did not protect lymphocytes from apoptosis and caused reduced growth and activation, while $JunD^{-/-}$ T-cells hyperproliferated upon stimulation [147]. These findings seemed in apparent conflict with our data that HXKII, a key enzyme in the glycolytic pathway, was a JunD target gene. To explain this, we performed a bioinformatics evaluation of potential JunD-regulated genes and found that many critical effectors of cell signaling and growth (like Pim-1), survival (like Bcl-2), and metabolism were possible JunD targets. Further, we found that inhibition of JunD impaired the proliferation of T-cells in response to IL-7. While, JunD remains a negative regulator of growth

in many cells, like intestinal epithelial cells in which JunD repressed gene expression of cyclin dependent kinase 4 (CDK4) [102], in IL-7-pulsed T-cells, as shown in our studies, JunD promotes the expression of essential growth effectors.

Regulation of JunD gene expression is not typical of other AP-1 components. Contrary to results with other AP-1 proteins, JunD protein levels were detected in quiescent immortalized cells; JunD protein then initially declined upon serum stimulation and later steadily increased [101]. Coupled to the constitutive activity of the JunD promoter, this suggests that JunD may be controlled by different post-transcriptional or post-translational mechanisms. As example, the JunD transcript is intronless, is G/C rich, has a long 5′ untranslated region (UTR) and produces two isoforms, a full-length and truncated form (reviewed in [148]). Moreover, the presence of a unique post-transcriptional control element (PCE) and the potential interaction with RNA helicase A (RHA) suggests that JunD could be efficiently translated under the right growth conditions [149]. Post-translational modifications also contribute to the activity of JunD in different cellular environments. JunD is poorly ubiquitinated and has a long half-life [150]. The JunD transcript is also positively regulated by JNK activity [151], as we have shown in the IL-7-dependent D1 cells. In fact, JNK could stimulate an auto-regulatory loop that controls the gene expression of JunD.

In summary, JunD emerges as an important transducer of the IL-7 signal in T-cells and, along with the JAK/STAT pathway, could promote gene expression to drive survival and growth when cells are stimulated with IL-7. The importance of this conclusion is appreciated when considering that T-cells normally exist in an IL-7-limited environment (with picograms levels of the cytokine normally detected in serum [152]). To be stimulated, T-cells must traffic to IL-7-

containing tissues. When a T-cell receives an lL-7 signal, the JNK/JunD pathway may function to enhance the JAK/STAT mechanism and induce expression of genes like HXKII and Pim-1 as a rapid response to the initial growth signal. Because the therapeutic use of IL-7 involves application of superphysiological dosing of the cytokine that is very different from the *in vivo* state of limited IL-7 availability, there is a need to better understand the consequences of IL-7 signal transduction and the impact upon gene expression in T-cells. The fact that the JNK/JunD pathway can have positive outcomes in IL-7 dependent T-cells highlights the need for continued research in this area. The bioinformatics approach presented could provide a means to identify potential gene expression changes that result from activation of JunD/AP-1 complexes in the context of IL-7 signaling that can be tested for validation in different animal models of immunological responses.

CHAPTER 3: THE MAJOR ISOFORMS OF BIM CONTRIBUTE TO DISTINCT BIOLOGICAL ACTIVITIES THAT GOVERN THE PROCESSES OF AUTOPHAGY AND APOPTOSIS IN INTERLEUKIN-7 DEPENDENT LYMPHOCYTES

Introduction

Cell death is an essential process needed for tissue homeostasis. Central to the modulation of apoptotic death are members of the B-cell lymphoma-2 (Bcl-2) family, which includes pro-survival proteins, such as Bcl-2 and Bcl-xL, pro-apoptotic members, like the multi-domain proteins, Bax and Bak, and a number of BH3-only proteins, such as Bad, Bid, Bim or Bmf [42]. Of the BH3-only proteins, Bim emerges as an important regulator of T-lymphocyte (T-cell) apoptosis. Bim is necessary for the death of autoreactive T-cells and is upregulated in T-cells upon death induced by T-cell receptor re-stimulation or growth factor withdrawal [39, 55]. Therefore, the key to understanding Bim's role in the apoptotic program is appreciating its relationship to T-cells.

In order to receive stimulatory and growth signals, T-cells need to migrate to environments where these signals are found [153]. An example of one essential signal is the cytokine, interleukin-7 (IL-7). IL-7 is mainly found in generative lymphoid organs as well as some nonlymphoid tissues [19] and is produced in large part by accessory cells [115, 154]. The heterodimeric IL-7 receptor (IL-7R), composed of both IL-7Rα and γc chains, is expressed by T-cells [155]. IL-7 is necessary for T-cell development, since disruption of either IL-7 or its receptor resulted in defects in mice [12, 156] similar to the SCID (Severe Combined Immunodeficiency Syndrome) phenotype in humans [157]. Evidence of the importance of IL-7

is the fact that excess IL-7 underlies lymphoproliferation and lymphoma formation [158, 159], indicating a role in the maintenance of peripheral T-cell homeostasis [15]. IL-7 supports T-cell survival by maintaining a balance between the anti-apoptotic and pro-apoptotic Bcl-2 family members [29, 160]. Indicative of a function in T-cell biology, loss of Bim could partially rescue the immunodeficient phenotype of IL-7R$^{-/-}$ mice [44].

How the activity of Bim is regulated remains the focus of study. In some healthy cells, Bim is sequestered by LC8, the light chain element of the microtubule-associated dynein motor complex [77, 161], or is bound to anti-apoptotic proteins such as Bcl-2 or Bcl-xL at the mitochondrial interface as was shown in T-cells [51]. Other regulatory mechanisms include transcriptional regulation by FHKR (forkhead) through Foxo3a [56, 162], the gastric tumor suppressor, RUNX [53] the post-translational phosphorylation of Bim at multiple sites [54, 68, 72, 78, 163-165]. We recently showed that IL-7 mediates the phosphorylation of BimEL, contributing to its pro-apoptotic activity [52]. While a role for Bim as a pro-apoptotic protein is well-recognized, Bim may also have unknown functions that go beyond its described death-promoting activity. Bim exists as multiple isoforms generated through alternative splicing, with the three major isoforms, BimEL, BimL, and BimS, part of a larger cohort of spliced forms [47, 62]. Some isoforms lack the BH3 domain or the dynein light-chain binding site, while others lack phosphorylation sites [166], which result in the possibility that isoforms may have different functions.

When extracellular nutrient sources are limiting, autophagy can support T-cell activation through intracellular scavenging [167], but, under less well-understood conditions, autophagy can also induce T-cell death, for example that of CD4 T-cells [168]. The individual contribution

of the major isoforms of Bim to the processes of autophagy or apoptosis in T-cells is unknown. To study this, we used Bim-containing and Bim-deficient T-cells, responsive to IL-7, to examine the activity of the major isoforms in response to the cytokine. A novel role in lysosome positioning was found for BimL that was dependent upon IL-7 and supported the degradative phase of autophagy. In contrast, BimEL and BimS promoted IL-7 withdrawal-induced apoptosis. These results demonstrated that Bim isoforms can participate in distinct apoptotic and lysosomal/degradative activities in T-cells. While Bim has long been recognized as an inducer of apoptosis, its role in supporting lysosome acidification suggests that controlled manipulation of Bim isoforms could lead to novel applications in diseases like cancer.

Materials and Methods

Mice, Cell Lines and Culture Reagents

C57BL/6 mice were purchased from Jackson Laboratory (Bar Harbor, Maine) and housed at the University of Central Florida, Orlando, FL. Bim knockout (BimKO) mice (C57BL/6 background) [52], $Rag^{-/-}$ and $IL\text{-}7^{-/-}/Rag^{-/-}$ mice were housed at NCI-Fredrick as previously described [52]. This study was carried out in accordance with the recommendations in the Guide for the Care and Use of Laboratory Animals of the National Institutes of Health. The protocol was approved by the Institutional Animal Care and Use Committee at the University of Central Florida and NCI-Frederick. All efforts were made to minimize suffering.

The IL-7 dependent T-cell line, D1, was established from one clone that arose from T-cells isolated from a $p53^{-/-}$ mouse and immortalized as previously described [28]. Since its establishment in 1997, the D1 cell line has been extensively used to study regulatory pathways

controlled by IL-7 in T-cells [22, 29, 30, 82, 89] and was used to reveal the role of IL-7 in the phosphorylation of BimEL [52]. To uncover the functional consequences of Bim deficiency and evaluate the function of each Bim isoform, we needed a T-cell line that was IL-7 dependent and also Bim deficient. To this end, we generated the SMoR T-cell line. Briefly, lympn node T-cells were isolated from BimKO mice (see above). Cells were resuspended in RPMI 1640, 10% fetal bovine serum (FBS), 5% Penicillin/Streptomyocin (Fisher), 0.1% B-mercaptoethanol (Invitrogen) (complete medium), and 200 ng/mL IL-7 at a concentration of 5 x 10^5 cells/ml. Using twenty 96-well, round bottom plates, 100 μl or approximately 10^4 cells/well were plated. In total, almost 2 x10^7 cells were used for mutagenesis as follows. Ethyl-N-nitrosurea (0.64 mM, ENU) in phosphate/citrate buffer was added to the cultures at 0, 7, 14, 21, and 28 days from initial isolation. Mutagenized T-cells were grown with complete media and IL-7. After 3 months, one BimKO T-cell clone emerged that was immortalized and IL-7-dependent. This outcome recapitulated the same observed when the original D1 cells line was cloned, in that a single line emerged from the selection process for IL-7 dependency [28]. This experience showed that generating immortalized IL-7 dependent T-cells is not possible unless underlying mutations, such as Bim or p53 deficiency, are present. D1 and SMoR T-cell lines, both derived from mice with a C56BL/6 background, were grown in complete medium and 50-200 ng/mL IL-7. Early passages of D1 and SMoR cell lines were frozen as stocks and cells were used at less than 10 passages from stocks.

Primary lymph node and splenic T-cells were isolated from both wild-type (WT) and BimKO C57BL/6 mice as previously described [132]. Phoenix cells (see below) were maintained in DMEM medium that was supplemented with 10% FBS.

Reagents used as described in Figure Legends include pifithrin-α (p53 inhibitor) (Sigma-Aldrich), 3-Methyladenine (3-MA) (Class III phosphatidylinositol 3-kinase (PI3K) inhibitor) (Sigma-Aldrich), Cathepsin III Inhibitor (pan cathepsin inhibitor, EMD), Pepstatin A (cathepsin D inhibitor, EMD), Ca074 (Cathepsin B inhibitor, EMD), and Chloroquine (CQ) diphosphate salt (Sigma-Aldrich).

Viability and Proliferation Assays

To quantitate cells undergoing apoptosis, the FITC Annexin-V Apoptosis Detection Kit (BD Pharmingen) was used following manufacturer's protocol. This kit utilizes a FITC-conjugated Annexin-V antibody that recognizes phosphatidyl serine exposed on cells undergoing early apoptosis, and contains PI (propidium iodide) which can permeate necrotic, membrane-damaged cells. The Annexin-V/PI kit could not be used with cells expressing GFP (see below) as the kit contains a FITC-conjugated antibody whose emissions would overlap the emission of GFP-containing cells. To address this, the SYTOX® AADvanced™ dead cell stain solution and the Violet Ratiometric Membrane Asymmetry Probe/Dead Cell Apoptosis Kit (Invitrogen) was used following the manufacturer's protocol. Apoptosis was indicated by membrane asymmetry using the violet ratiometric dye, and membrane permeability was measured by Sytox uptake. Sytox was visualized at 488nm and emissions collected at 695nm. The violet ratiometric probe was visualized at 405nm and emissions collected at 450nm and 510nm. Cells were analyzed by flow cytometry using the BD FACSCanto II flow cytometer. Analysis was completed using FCSExpress (DeNovo) software. Viability was also assessed by determining morphological

changes, cell shrinkage and granularity, using forward scatter (FSC) and side scatter (SSC) gating by flow cytometry with an Accuri C6 flow cytometer.

Proliferation was measured by labeling cells with CFSE as previously described [88, 132, 169]. For CFSE labeling, one million cells were treated with 2 μM CFSE (Molecular Probes) staining solution (PBS + 0.1% BSA) for 10 minutes and then washed to remove excess label. The division of cells was determined by measuring CFSE fluorescence by flow cytometry after 72 hours of culture with or without IL-7. The generation number for the population was determined from a best fit of these data using the Proliferation module for the FCS Express software (DeNovo). Unstimulated CFSE-containing cells were used to determine the peak corresponding to the undivided population.

Bim inhibition by small interfering RNAs

One-to-two million D1 cells were treated with 1-2 nM BCL2L11 SMART pool siRNA (Dharmacon) and Accell delivery media (Dharmacon) supplemented with 1% FBS, and IL-7 (50 ng/ml) for 24 hrs. After 24 hours, cells were deprived of IL-7 and re-plated in media containing the siRNA alone, for 48 hours. SMART pool siRNA contains four sequence variations of siRNAs to eliminate non-specific interactions. Non-targeting siRNA (NT siRNA) containing a FAM reporter sequence was used as a delivery control, and was comparable to treatment with Accell media alone. Cells were analyzed using flow cytometry and confocal microscopy.

Quantitative PCR

Ten million D1 cells, per experimental condition, were cultured with or without IL-7 as described above, were re-suspended in 1 ml of TRIzol reagent (Invitrogen). Total RNA was

extracted from the cells using the reagent according to the manufacturer's instructions. Each cDNA template was synthesized from total RNA by reverse transcription with iScript cDNA Synthesis kit according to manufacturer's instructions. Quantitative analysis of cDNA amplification was assessed by incorporation of SYBR Green (ABI 4385370) into double-stranded DNA. For mouse Bim: forward 5'- CGACAGTCTCAGGAGG AACC-3', reverse 5'-CCTTCTCCATACCAGA CGGA-3'. For β-Actin, forward primer 5'-GAAA TCGTGCGTGACATCAAAG-3' and 5'-TGTAG TTTCATGGATGCCACAG-3' reverse primer were used. Reactions contained Fast SYBR Green Master mix (1X), β-Actin primers at 50 nM or Bim primers at 100 nM, and 3-4 μg cDNA template. Thermal cycling conditions were as follows: 40 cycles of 30 sec at 95 °C followed by 45 sec at 57 °C, and 60 sec at 72 °C, denaturing, annealing and extension temperatures, respectively. All cDNA samples were processed using the ABI Fast 7500 and analyzed using ABI Sequence Detection Software Version 1.4. The difference in mRNA expression was calculated as follows: fold change = $2^{-\Delta\Delta Ct}$, ΔΔCt is equal to the change in ΔCt values over time after normalization to β-actin. ΔCt is equal to the difference between the endogenous control Ct and target gene Ct values.

Immunoprecipitation and Immunodetection

For preparation of whole cell lysates, 37-45 million cells were lysed using the Cell Lysis buffer (Cell Signaling) in the presence of protease inhibitors (Roche). In the case of primary cells, 1 to 3 million cells per condition, were used. For immunoprecipitation, cell lysates were pre-cleared with Protein A/G Sepharose beads (Santa Cruz), incubated with anti-dynein antibody and immunoblotted for Lamp1 and Rab5 as described below. For immunoblotting, subcellular

fractions (from gradients, see below), whole cell lysate samples, or co-immunoprecipitated samples were run in 10% or 12-15% SDS-PAGE gels, and proteins transferred to nitrocellulose membranes by semi-dry transfer (BioRad) or wet transfer (Novex) following manufacturers' protocols. Membranes were washed and probed with primary antibodies (see below) and incubated with horseradish peroxidase (HRP)-conjugated (Santa Cruz) or fluorescence-conjugated secondary antibodies (LICOR). Signal was detected using either chemiluminescent fempto substrate (SuperSignal West Fempto; ThermoSci) or the LICOR Odyssey detection system. The primary antibodies used in this study were as follows: a rabbit polyclonal antibody against amino acids 22 to 40 of human Bim protein (anti-Bim; Calbiochem), Bim (rat monoclonal 14A8; Calbiochem), Lamp1 (mouse monoclonal 1D4B; developed by J. Thomas August, Developmental Studies Hybridoma Bank, University of Iowa), Prohibitin (rabbit polyclonal ab28172; Abcam), p38 (Santa Cruz), Bcl-2 (Santa Cruz), Rab5, an early endosome marker (Abcam), Cathepsin B (Abcam), Dynein (Abcam), p62 (Cell Signaling), and LC3B (Abcam). Quantitation of the bands was performed using ImageJ software, taking the average of the three separate measurements for each band.

Cell surface protein analysis

Surface expression of IL-7R expressed on T-cells was assessed by flow cytometry using a PE-conjugated anti-IL-7R antibody (BD Biosciences) as previously described [88, 132, 169]. A PE-conjugated isotype matched antibody was used as a control for non-specific staining. One–two million D1 or SMoR cells were incubated with or without IL-7 for 18 hours and then

treated with saturating amounts of the appropriate antibody for 20 minutes, washed in buffer (PBS + 0.1% BSA) and analyzed by flow cytometry on the Accuri C6 flow cytometer.

Measurement of intracellular pH

Cells (D1, SMoR, primary C57BL/6 and BimKO) were resuspended in Hanks supplemented with 25mM HEPES (Invitrogen), 1% FBS, and 1µM BCECF-AM (Molecular Probes). Intracellular pH-dependent changes in fluorescence were measured by flow cytometry, using methods previously described [170, 171]. To establish a pH calibration curve, cells were re-suspended in high-potassium HEPES buffer (25 mM HEPES, 145 mM KCl, 0.8 mM MgCl2, 5.5 mM glucose, and DDH2O) at pH standards (5.9, 6.5, 7.0, 7.2, and 7.8) and nigericin (10 µM) added followed by BCECF-AM. Measurements were acquired using a BD FACSCanto II cytometer excited with a 488 nm laser, with emissions were filtered through 525 nm and 610 nm. Dead cells were excluded by forward- and side-scatter gating. pH values were determined by measuring the absorbance ratio between 525 nm (green fluorescence) and 610 nm (red fluorescence), the latter of which compensates for dye concentration, volume, and cell size.

Live Cell Imaging/ Microscopy

For imaging, cells were plated in 24-well glass bottom dishes (MatTek) that had been washed with 1N HCl and PBS. Cells were supplemented with 1 µM LysoSensor immediately before imaging. LysoSensor probe is cell membrane permeant and exhibits pH-dependent increases in fluorescence intensity upon acidification. For imaging of retrovirus-infected cells, dishes were coated with 8 µg/mL Retronectin (Takara), followed by the retroviral supernatant, prior to adding cells. At 20 hours post-infection, 1 µM LysoTracker (Molecular Probes) was

added to cell culture in RPMI complete media immediately prior to imaging. LysoTracker probes are also cell membrane permeant and contain a fluorophore bound to a weak base that becomes partially protonated upon neutral pH exposure and selectively stains acidic organelles in live cells, although fluorescence is independent of pH changes. Fluorescent images were acquired with the UltraView spinning disc confocal system (PerkinElmer) with AxioObserver.Z1 (Carl Zeiss) stand, and a Plan-Apochromat 40x/1.4 Oil DIC objective. Z-stacks and extended focus of scanned images were created and modified using the Volocity 5.5 image processing program (PerkinElmer). LysoSensor-treated samples were excited at 405 nm. To detect Lysosensor fluorescence, emissions between 445 nm and 615 nm were collected for more neutral pH vesicles (assigned an arbitrary yellow color), and between 525 nm and 640 nm for acidic vesicles (assigned an arbitrary blue color). LysoTracker stained samples were excited at 561 nm and emissions collected between 525 nm and 640 nm. Transmitted light images were collected for DIC. For SMoR cells transfected with pMIG, BimEL, or BimL plasmids, total fluorescence and the number of GFP positive events, with the removal of auto fluorescent outliers, per field, were obtained using Volocity 5.5. GFP was acquired using a 488 nm laser, and emissions were collected at 525 nm and 640 nm.

Retroviral Transfection

The bi-cistronic plasmids, pMIG, pEco, BimEL-pMIG, BimS-pMIG, and BimL-pMIG were made as previously described [52]. The retroviral infection technique was optimized specifically for the D1 and SMoR cell lines [52]. A Phoenix-Eco packaging cell line (Orbigen) was transfected with bi-cistronic plasmids containing a Bim isoform (or none, termed pMIG) and

GFP. Cells were transfected using TransIT-LT1 reagent (Mirus). The supernatant containing the retrovirus was harvested after 48 hours and loaded onto Retronectin (Takara)-coated plates. One million cells per mL were incubated in supplemented media containing Polybrene (Santa Cruz, 8 μg/mL), either in the presence or absence of IL-7, and added to the plates for several hours.

Adoptive transfer of T-cells and Chloroquine in vivo treatment

C57BL/6 and BimKO LN cells were isolated and suspended in PBS containing 5% FBS. Cells were incubated for 10 min with CFSE (Invitrogen) following previously established methods [52]. $Rag^{-/-}$/IL-$7^{-/-}$ double knockout or $Rag^{-/-}$ recipient mice were irradiated with 3 Gy whole body γ-irradiation 4 hours prior to injection. Five million CFSE-labeled cells were then suspended in PBS and adoptively transferred into the previously irradiated $Rag^{-/-}$, and $Rag^{-/-}$/IL-$7^{-/-}$ double knockout mice. Mice were intraperitoneal injected with 60 mg/kg chloroquine within 24 hours, and again, after 48 hours. Mice were euthanized within 72 hours, spleens and lymph nodes recovered, and T-cells isolated and utilized for analysis as previously mentioned [88]. Recovered cells were analyzed for loss of CFSE label by flow cytometry (Accuri C6 flow cytometer) and calculation of generation times performed using FSC Express (DeNovo) proliferation module software.

Subcellular Fractionation

Cells were seeded to 80-90% confluence. For lysosome preparations: 200 mg (140 million) cells were harvested by isotonic lysis buffer according to protocol from the Lysosome enrichment kit (Pierce) and prepared for density gradient ultracentrifugation. Enriched lysosomal fractions were layered onto an iodixanol gradient (17%, 23%, 25%, 27%, 29%, and 30%

Optiprep) and subjected to ultracentrifugation using an Optima L-100XP Ultracentrifuge. Gradients were fractioned in 500 µL aliquots (Fractions 1-10) using an Auto Densi-Flow (Labconco). Enriched preps were utilized for downstream processing or re-suspended in sample buffer for gel-electrophoresis (see above).

Statistics

Statistical analysis and significance was determined using Prism 5 (Graphpad) for Windows, Version 5.02. P values determined are shown in Figure Legends.

Results

Bim has multiple functions, promoting death as well as growth in IL-7 responsive cells

It is generally accepted that Bim inhibits the survival activity of anti-apoptotic members of the Bcl-2 family [172], and that it has an important, although poorly understood, role in T-cell biology [44]. Our previous studies showed that in T-cells, IL-7 regulated the activity of BimEL through phosphorylation [52], but the activity of other major isoforms, BimL and BimS, relative to IL-7 signaling remained unknown. Using primary LN T-cells from C57BL/6 or BimKO mice, we evaluated the effect of *in vitro* culture with IL-7, using methods we previously established [88, 132]. Shown in Figure 11A are representative results indicating in the absence of IL-7 that the loss of Bim provided short-term protection (3 days) from death, although such LN cells eventually died in *in vitro* culture. Viability of cells was determined by assessing cell shrinkage and increased granularity detected by forward scatter (FSC) and side scatter (SSC) gating using flow cytometry. Because primary T-cells do not uniformly respond to an IL-7 signal (i.e. CD8

T-cells proliferative at the expense of CD4 T-cells) [88, 132] and may need additional signals through the T-cell receptor (TCR) for optimal growth [87], we used an IL-7-dependent T-cell line, D1, to examine the activity of Bim in response to IL-7. The generation of the D1 cell line has been previously described [28] and a number of studies have demonstrated its biological relevance in the context of IL-7 signaling [22, 29, 30, 82, 89, 92]. Upon IL-7 withdrawal, cell death, as indicated by increased Annexin-V/PI staining, was detected in D1 cells within 36 hours, and death was maximal by 48 hours (Fig. 11B) [28]. To determine whether loss of Bim could protect D1 cells from IL-7 deprivation, cells were treated with Bim siRNA, to inhibit total Bim. We observed a 40% reduction in Bim mRNA levels in cells treated with Bim siRNA as compared to cells treated with control siRNA (Fig. 11C). Note that the siRNA methodology limits cell numbers to a few million, which is below the threshold for detection of endogenous Bim protein. The siRNA-induced decrease in Bim expression led to reduced apoptosis in D1 cells deprived of IL-7 as indicated by the increased percentage of viable cells (Annexin-V/PI negative) detected (Fig. 11C). For this experiment, D1 cells were incubated with siRNAs for 72 hours, of which the first 24 hours were in presence of IL-7 and the last 48 hours were in the absence of IL-7. To determine whether IL-7 regulated the gene expression of Bim, we examined the levels of total Bim mRNA in D1 cells cultured with or without IL-7. Using quantitative PCR, we observed that Bim mRNA levels increased in the absence of IL-7 – specifically after 15-18 hours of cytokine withdrawal, indicating that the gene expression of Bim, was in part, IL-7 responsive (Fig. 11D). These results supported the conclusion that Bim was among the effectors of death in response to IL-7 deprivation.

To evaluate the biological consequence of Bim deficiency in IL-7-dependent T-cells and study the function of each major isoform without the limitations imposed by either primary lymphocyte cultures or siRNA treatments, we needed a Bim-deficient and IL-7-dependent T-cell line. To this end, we generated the SMoR T-cell line from BimKO mice as described in Materials and Methods. To demonstrate that the expression of Bcl-2 family members in D1 or SMoR cells was not altered by either the immortalization process or loss of p53 or Bim, we examined Bcl-2 and Bax, proteins whose expression or activity, respectively, is regulated by IL-7 [28, 29, 131]. As shown in Figure 12A, we found that the two cell lines displayed minimal differences in the total levels of Bcl-2 or Bax detected in response to IL-7. Bcl-2 levels decreased in the absence of IL-7 and Bax distributed between the cytosol and mitochondria (Fig. 12A). Next, we determined whether, lacking functional Bim, SMoR cells underwent death upon IL-7 withdrawal. Apoptosis was detected using Annexin-V/PI staining, and viability was determined by assessing changes in cell size and granularity. Shown in Figures 12B and 12C, we observed decreased numbers of Annexin-V/PI positive SMoR cells after 36 hours of IL-7 deprivation and sustained viability (50-60%) through 48 hours of IL-7 loss. These results indicated that IL-7-dependent, Bim-deficient SMoR cells are useful for the study of Bim function in IL-7 dependent T-cells and confirmed that Bim was contributing to death induced by IL-7 loss.

As shown and previously reported, D1 cells underwent death between 24-48 hours after IL-7 withdrawal (Fig. 12C) [28]. Stimuli that induce apoptosis can also trigger DNA damage and p53 is usually responsive to this mechanism [173]. To show that protection from IL-7-withdrawal-induced death in SMoR cells was likely due to loss of Bim and not the presence of a

possible p53-mediated activity, we treated cells with pifithrin-α, originally described as a p53 inhibitior [174], but also shown to protect from DNA-damaged induced apoptosis [175]. No differences in viability of SMoR cells or D1 cells, cultured with IL-7, were detected upon pifithrin treatment (Supplemental Figure 1). Withdrawal of IL-7 and the addition of pifithrin increased the death observed in D1 cells, suggesting that both p53–dependent and p53-independent death mechanisms were involved. In contrast, SMoR cells were resistant to death induced by increasing doses of pifithrin-α (Supplemental Figure 1), indicating that the loss of Bim was likely a key factor that contributed to protective effect observed upon IL-7 withdrawal (Fig. 12C). Note that upon extended IL-7 deprivation, SMoR cells eventually died after 4 days (data not shown). Hence, the loss of Bim did not prevent but delayed the death of cells deprived of IL-7.

Other parameters of importance are cytokine-driven proliferation and viability under conditions of nutrient deprivation. To measure the growth of D1 and SMoR cells in response to IL-7, we used the dye, CFSE. CFSE divides with each cell replication cycle and can be used to measure generation times as shown in Figure 12D. D1 cells rapidly divided in response to IL-7, replicating 1-2 times per day over the three days of evaluation, while SMoR cells divided 1-2 times over the same three day period (Fig. 12D). Therefore, loss of Bim, while providing protection from IL-7-induced cell death (Fig. 12C), decreased cell replication rate. The surface expression of the IL-7R was measured to determine whether the slow growth of SMoR cells was due to decreased IL-7R levels. This was not observed, as is shown in Figure 12E. Both D1 and SMoR cells displayed comparable levels of IL-7R that increased upon cytokine withdrawal, a pattern that is typical of what others have reported [11]. In fact, compared to D1 cells, SMoR

cells had slightly higher amounts of surface IL-7R relative to maximal receptor levels achieved in the absence of IL-7 (Fig. 12E). SMoR cells, but not D1 cells, were also more sensitive to glucose deprivation and decreased viability when cultured under conditions of minimal glucose (4 mM) (Fig. 12F). These results suggested that loss of Bim conferred partial protection from cell death caused by growth factor removal but also caused a growth disadvantage that resulted in reduced replication and sensitivity to nutrient loss that was not dependent on the levels of IL-7R.

Bim supports intracellular acidification and formation of acidic vesicles

In order to investigate the activity of Bim in IL-7 dependent T-cells that could account for the observed biological effects, changes in intracellular pH were examined. Cytosolic acidification can be a hallmark of apoptosis and has been linked with lysosomal proton release upon lysosomal permeabilization [176, 177]. Changes in pH can also correlate with proliferative status [178]. A time course experiment, measuring intracellular pH, showed that D1 cells acidify after 24-30 hrs of IL-7 withdrawal, consistent with morphological changes indicative of cell death (Fig. 13A). In SMoR cells, IL-7 deprivation did not induce acidification and cells remained more alkaline over the entire course of evaluation (Fig. 13A). These results were confirmed using LN T-cells from WT and BimKO mice (Fig. 13B). While we previously showed that D1 cells transiently alkalinize 6-8 hours after IL-7 withdrawal due to the activity of the sodium hydrogen exchanger 1 (NHE1) [29], this is an active mechanism induced by apoptotic stimulus [171]. In contrast, the increased intracellular pH of SMoR cells was detectable in the presence of IL-7 and did not change even during IL-7 withdrawal.

These data suggested that Bim loss was affecting a biological activity that impacted upon intracellular pH. One possibility could be that the loss of Bim disrupted normal lysosomal functioning. To determine whether the morphology of lysosomes was different in Bim-containing and Bim-deficient cells, endosomes and lysosomes were visualized using LysoSensor probe. LysoSensor measures the pH of acidic organelles and distinguishes more neutral vesicles of higher pH (i.e. endosomes) from acidic or lower pH vesicles (i.e. late endosomes/lysosomes). In parallel studies, the probe LysoTracker was used to visualize lysosomal content and show that no pH-dependent changes in the probe occurred in the organelles imaged, demonstrating that Lysotracker and LysoSensor staining were comparable (Supplemental Figure 2). Live cell imaging was performed to view results from lysosome probes. In Figure 13C, using LysoSensor, we observed a difference in the distribution and aggregation of less acidic (arbitrarily assigned a yellow color) compared to more acidic vesicles (arbitrarily assigned a blue color) in D1 cells grown with or without IL-7. The dispersed distribution of acidic vesicles within cells cultured with IL-7 became clumped and aggregated as IL-7 was deprived, indicating a potential increase in endosome/lysosome fusion. This is best observed in the 3-dimensional (3D) single-cell enlargement showing intense staining of merged fluorescent signals (appearing white in areas) from acidic vesicles (Fig 13C). When D1 cells were treated with Bim siRNA, a distinct change was observed in that aggregation was decreased (no intense staining of merged fluorescence or white areas) and increased detection of less acidic vesicles (Fig. 13D). This is most clearly seen in the merged 3D enlargement. These results suggested that loss of Bim had a negative effect upon the distribution of acidic vesicles (Fig. 13E) in the presence or absence of IL-7. In total,

increased intracellular alkalinity and decreased acidic vesicles in Bim deficient cells suggested that Bim could have a function in the maintenance of lysosomal activity.

The absence of Bim leads to impairment of the later degradative phase of autophagy

Our data showing that SMoR cells lacking Bim were less viable under conditions of limiting glucose (Fig. 12F) and has less acidic vesicles (Fig. 13E), suggested that Bim could be involved in a novel biological activity, that of self-eating or autophagy. Autophagic digestion can contribute to the recycling of cytoplasmic components and promote survival, inhibition of which accelerates apoptosis [179]. Alternatively, autophagy can directly lead to cell death [180]. To examine this, we used the class II PI3K inhibitor, 3-MA, which can inhibit autophagy under conditions of nutrient or cytokine deprivation [181]. We observed that 3-MA treatment accelerated cell death in the absence of IL-7 - from 32% (untreated) to 49% (3-MA) apoptotic/necrotic cells (Fig. 14). Treatment with 3-MA had only a minor impact in Bim deficient SMoR cells and did not greatly increase the percent of apoptotic/necrotic cells – from 8% (untreated) to 12% (3-MA) (Fig. 14). We also observed that treatment with 3-MA caused some death in the presence of IL-7 (Fig. 14), which could be due to the effect of this inhibitor on PI3 Kinases [181].

To assess autophagic activity, the levels of LC3-I and LC3-II were measured. LC3-I is cytosolic, while LC3-II, which is conjugated with phosphatidylethanolamine (PE), is associated with autophagosomes and less so with autolysosomes [182, 183]. Normally the amount of LC3-II correlates with the number of autophagosomes and is degraded as a result of autophagy. As shown in the representative experiment in Figure 15A, LC3-I and LC3-II levels varied slightly in

D1 cells cultured with IL-7 for 6 or 18 hours, with more LC3-I and less LC3-II detected at 18 hours. In contrast, D1 cells deprived of IL-7 for 6 hours (or at 18 hrs) had an increased ratio of LC3-II to LC3-I, suggesting an increased number of autophagosomes (Fig. 15A). In comparison, SMoR cells displayed higher amounts of both LC3-I and LC3-II, suggesting that either autophagosomes were increased in these cells or that degradation of LC3 was reduced, allowing the protein to accumulate (Fig. 15A). Note that by 18 hours of IL-7 deprivation, levels of LC3-I and II were negligible in both D1 and SMoR cells. Next, we examined the degradation of p62 (a.k.a. SQSTM1) as an indicator of autophagic flux. The targeting of p62 to the autophagosome formation site does not require LC3, however, once there, p62 binds to LC3 and is entrapped in autophagosomes where, upon fusion with lysosomes, it is degraded [184]. Hence, impairment of the degradative phase of autophagy can result in the accumulation of p62. We observed that in D1 cells, the levels of p62 declined when IL-7 was withdrawn, suggestive of increased autophagic degradation (Fig. 15A). This did not occur in SMoR cells where p62 levels remained elevated (Fig. 15A). We confirmed these results using freshly isolated LN T-cells from BimKO and WT mice. In comparison to WT cell, we detected elevated levels of LC3-II compared to LC3-I in BimKO cells, with a greatly increased ratio of LC3-II to LC3-I and increased accumulation of p62 (Fig. 15B). This data suggested that loss of Bim did not impair autophagosome formation, since LC3-II and p62 were detected, but could suggest a problem with the degradative phase of autophagy that allowed these proteins to accumulate.

To study lysosomal-mediated degradative activity, we used the inhibitor, chloroquine (CQ), to inhibit lysosomal acidification. As a comparison, we also used 3-MA. Within the timeframe of the experiment with freshly isolated LN cells, these inhibitors did not greatly

impact upon LC3 and p62 protein levels (Fig. 15B). However, inhibition of lysosomal acidification with CQ did increase LC3-II accumulation in D1 cells grown with or without IL-7 (Fig. 15C) and also increased the amount of p62 (Fig. 15D), indicating that these proteins were being degraded as a result of lysosomal activity. Treatment with 3MA had a similar, though slightly lesser, effect (Figs. 15C-D). This suggested that in Bim-containing D1 cells, autophagosome formation was occurring, followed by autolysosomal-mediated protein degradation. In SMoR cells CQ treatment also caused some accumulation of LC3-II but to a lesser extent than in D1 cells (Fig. 15C). As example, in D1 cells cultured with IL-7, CQ treatment caused an almost three-fold increase in LC3-II as compared to SMoR cells in which a slightly more than two-fold increase was observed (Fig. 15C). Note also that in SMoR cells, higher levels of LC3-I were found that resulted in lower ratios of LC3-II to LC3-I. The amount of p62 protein was also elevated in SMoR cells and was not significantly increased by CQ or 3MA treatments (Fig. 15D). These results supported the idea that Bim is needed to enable the degradative phase of autophagy, impairment of which could have a negative feedback upon the initiation of autophagy and LC3 conversion levels.

To strengthen the conclusion that the lysosomal/degradative phase of autophagy is defective in Bim-deficient cells, SMoR cells were treated with inhibitors of cathepsin activity or lysosomal acidification. The expectation was that Bim deficiency would render SMoR cells resistant to the effect of these inhibitors. In Figure 16A, a representative experiment with SMoR cells is shown in which treatments with a pan-cathepsin inhibitor (CI) had little effect on IL-7-withdrawal induced apoptosis. Results were confirmed with specific inhibitors of aspartic proteases, like cathepsin D (pepstatin A) and cathepsin B (Ca074) (Fig. 16B). With the

autophagy process intact, D1 cells showed the anticipated effect of accelerated cell death upon CI (Fig. 15A) and pepstatin A (Fig. 15B) treatments. Note that inhibitors of specific cathepsins were less effective than the pan-cathepsin inhibitor (CI) likely because the specific cathepsins inhibited were less active in these cells. To further examine the effect of Bim upon the lysosomal activity, CQ was used [185]. CQ is being tested as a therapeutic agent and is well-tolerated at treatment doses [186]. A CQ dose response curve was experimentally determined (data not shown). The representative experiment in Figure 16C revealed in the presence of IL-7, CQ caused less death in SMoR cells, and, upon IL-7 withdrawal, SMoR cells were resistant to the effects of CQ and did not accumulate large numbers of late-apoptotic/necrotic cells. As expected, Bim-containing, D1 cells underwent accelerated IL-7-induced apoptosis upon CQ treatment, with increased amounts of apoptotic/necrotic cells detected, as measured by Annexin-V/PI staining (Fig. 16C). These results suggested that the autophagy defect in Bim-deficient cells might be associated with the formation of degradative autolysosomes. Findings in Figure 13, that SMoR cells were more alkaline and accumulated fewer acidic vesicles provide additional support for this idea.

Studies performed with T-cell lines were extended to mice to determine whether inhibition of lysosome acidification accelerated the death of WT, but not BimKO, T-cells adoptively transferred to $Rag^{-/-}IL\text{-}7^{-/-}$ mice. Recipient $Rag^{-/-}$ (control) or $Rag^{-/-}IL\text{-}7^{-/-}$ mice were treated with CQ as described in Methods, and splenic CFSE-labeled T-cells were recovered for analysis. Generation or doubling time was determined by the number of cycles in which the CFSE label was halved during each cell division. Results are shown in Figures 16D-E. We observed that WT T-cells transferred to control $Rag^{-/-}$ mice proliferated equally well in the

absence or presence of CQ (Fig. 16D). The same was true with BimKO T-cells, although the total cell number was slightly reduced during CQ treatment (Fig. 16E). When WT cells were transferred to $Rag^{-/-}IL\text{-}7^{-/-}$ mice, proliferation was greatly reduced and a significant number of cells remained undivided (Fig. 16D). Moreover, loss of Bim did not rescue T-cell expansion in the absence of IL-7 (Fig. 16E). However, CQ treatment did complement Bim deficiency and restored T-cell growth in mice lacking IL-7 (Fig. 16E). Note that we observed a similar finding in that SMoR cells were more resistant to CQ treatment (Fig. 16C). CQ treated WT T-cells transferred to $Rag^{-/-}IL\text{-}7^{-/-}$ mice did not proliferate and fewer cells were recovered than was observed for untreated WT cells under IL-7-deficient conditions (Fig. 16D). These results confirmed the *in vitro* results described for T-cell lines (Fig. 16C) that inhibition of lysosomal activity can accelerate death during an apoptotic stimulus, like IL-7 withdrawal, and that this does not occur in cells lacking Bim.

Bim isoforms differentially contribute to apoptotic and lysosomal activities

Results obtained indicated that Bim could have possible roles supporting both apoptosis and the degradative, lysosomal-mediated phase of autophagy. The question remained – how can Bim function in both capacities? A possible answer could be that Bim isoforms have different functions in these processes. To determine this, we examined the expression of the major isoforms of Bim in response to IL-7. To localize the major Bim isoforms, BimEL, BimL and BimS, to organelles, density gradient separation of cell lysates was performed. This procedure allows the separation of organelles and membrane-encased vesicles based upon lipid and protein content. In Figure 17A, a representative experiment shows that in Bim-containing D1 cells,

cultured with IL-7, we detected BimL protein in fraction 3 that is associated with late endosomes/lysosomes and marked by the highest concentration of Lamp1 (fractions 1-4). Note that Lamp1 is diagnostic for lysosomal-associated disorders [187] and thus a marker for lysosome content. A small amount of the early endosome marker, Rab5, also associated with same fraction. As a control, we observed that Bcl-2 associated with those fractions in which Prohibitin, a mitochondrial marker, was found (fractions 3-5, but highest in fraction 4) as well as small amounts of the other major Bim isoforms (Fig. 17A).

Performing gradient centrifugation using cell lysates from IL-7-deprived D1 cells, we detected increased amounts of BimEL and BimS that associated with mitochondrial fractions marked by Bcl-2 and Prohibitin (fractions 3-6, but mostly in fraction 4) and decreased amounts of BimL that associated with lysosomes (Fig. 17A). Interestingly, more BimEL was seen across fractions 1-5, while BimL and BimS were concentrated in the mitochondrial-associated fractions. We also observed an increase in Lamp1 staining in the lightest density fraction (fraction 1) and a weak but dispersed distribution of Rab5. These results demonstrated that the isoforms of Bim could localize to different organelles based on the lipid/protein content in the presence of IL-7 as compared to the absence of IL-7. Significantly, we found that BimL was associated with lysosome fractions in the presence of IL-7.

In Figure 17B, similar density gradient experiments performed with SMoR cells are shown. Overall Lamp1 levels were reduced in the lighter density fractions (fraction 3 in the presence of IL-7 and fraction 1 in the absence of IL-7). While Lamp1 staining was decreased, Rab5 staining was increased, which supported the imaging experiments in Figure 3 and suggested that early endosomes (or more neutral vesicles) were more abundant in the absence of

Bim. Like in D1 cells, Bcl-2 in SMoR cells was mainly associated with mitochondrial fractions (Fig. 17B). Note that SMoR cells, like freshly isolated BimKO LN and spleen cells (see Supplemental Figure 3), express polypeptides that migrate in a gel at the same levels of endogenous BimL and BimS.

Results shown indicated that BimL may directly associate with lysosomes in IL-7 cultured cells. This could occur through association with the microtubule motor, dynein. Previous studies had shown an interaction between Bim and dynein that sequestered that BH3-only protein in non-apoptotic cells [77, 188]. To determine whether Bim facilitated the binding of lysosomes to dynein, we performed a co-immunoprecipitation experiment. Lysates were prepared from D1 cells cultured with IL-7 and immunoprecipated with an anti-dynein antibody. Blots were probed for Lamp-1 as indicator of lysosome cargo. As shown in Figure 17C, dynein co-immunoprecipated with Lamp1 in D1 cells grown with IL-7. We could not co-immunoprecipate dynein with Lamp1 in SMoR cells grown with or without IL-7 or with D1 cells deprived of IL-7 – basically cells lacking or with reduced content of BimL. As control, we found that Rab5 associated with dynein independently of IL-7 or Bim (Fig. 17C). Additionally, we observed that all the immunoprecipitated versions of Lamp1 and Rab5 ran slightly slower on the gels indicating possible modifications that enable complex formation. Also, the stronger detection of Lamp1 in the input lanes for SMoR cells as compared to other blots was due to significantly increased amount of protein input used to maximize detection of co-immunoprecipitates.

Next, BimEL and BimL were expressed in SMoR cells using a retroviral method. This method necessitated reduced numbers of cells as compared to blots in Figures 17A-C. Shown in

the representative experiment in Figure 17D, we found that expression of BimL, but not BimEL, was able to restore the interaction of dynein with Lamp1-containing vesicles in SMoR cells, significantly increasing the detection of Lamp1 (and some Rab5) well above endogenous levels. Thus, BimL could function as an adaptor for dynein to facilitate the loading and fusion of lysosomes within cells.

The role of BimL as the mediator of lysosomal positioning through its interaction with dynein, was examined by expressing the three isoforms of Bim in SMoR cells, and observing the effects upon lysosomal distribution and cell viability. To perform these experiments we used the probe, LysoTracker. Because we were imaging GFP positive cells to track those that were expressing the isoforms of Bim, we could not use LysoSensor as in Figure 13 since the fluorescent signals overlapped. We used the same live cell imaging technique as shown in Figure 13. In addition, in each image set, a dot plot displays cell death measured by Sytox uptake and membrane asymmetry. Images were collected at the final experimental time point. Results in Figure 18A, demonstrated that SMoR cells expressing the empty vector, pMIG, had dim LysoTracker staining, and viability upon retroviral expression was 62%. When BimEL was expressed, we noticed lysosomal staining with little or no vesicle aggregation evident (Fig. 18B), and viability decreased to 45%. In contrast, expression of BimL resulted in notable lysosomal aggregation, likely indicative of fusion (Fig. 18C), with viability stable at about 49-50%. For comparison, we also expressed BimS, which was the most toxic of the isoforms, causing rapid cell death with most of the GFP positive cells in the field acquiring a shrunken, and apoptotic morphology (Fig. 18D), and viability dropping to 30%.

Conclusions

In summary, our results revealed that the major isoforms of Bim has defined functions in the cell maintenance and the apoptotic processes occurring in T-cells responsive to IL-7. In T-cells receiving an IL-7 signal, BimL plays an essential role in lysosomal positioning through interactions with dynein that promote the formation of autolysosomes during the degradative phase of autophagy. BimEL associates with mitochondria in a pro-apoptotic manner, and expression of BimS further promotes the cell death process. BimL, therefore, functions in the presence of IL-7 to support lysosomal acidification, while BimEL and BimS are active during IL-7 deprivation to cause T-cell apoptosis.

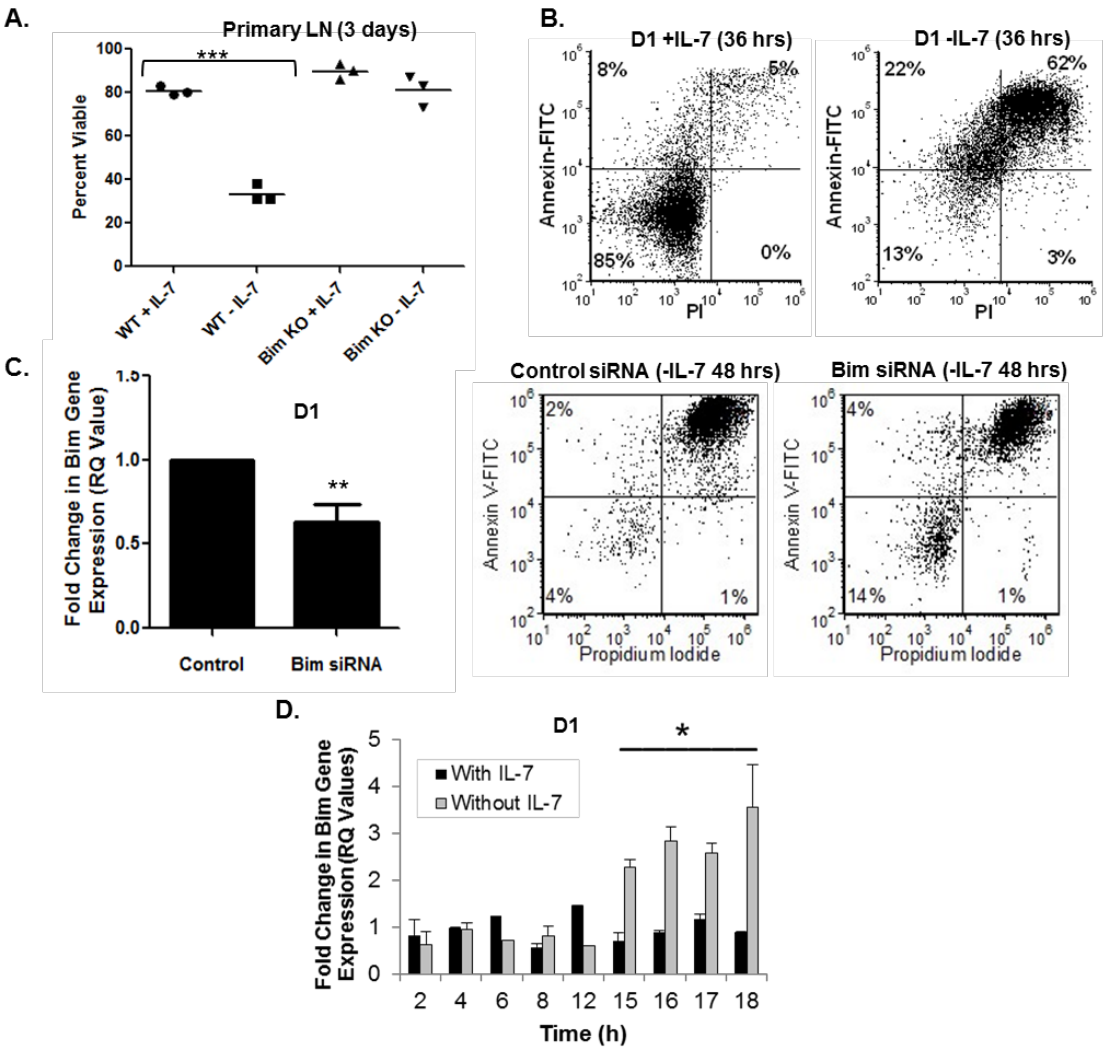

Figure 11. Loss of Bim partially protects IL-7 dependent cells from apoptosis.
(A) Lymph node T-cells, isolated from WT C57BL/6 or BimKO mice and cultured with or without 150 ng/ml of IL-7 for 3 days as described in Materials and Methods, were assessed for viability as determined by cell morphology, assessing size (forward scatter (FSC)) and granularity (side scatter (SSC)) by flow cytometry. (B) Cytokine withdrawal-induced death of D1 cells, grown with or without 50 ng/ml IL-7 (36 hours), was measured by surface expression of phosphatidyl serine using FITC-conjugated Annexin-V antibody. Membrane permeability was assessed by propidium iodide exclusion (PI), analyzed by flow cytometry. Dot plots show percentages representing the population of cells that are non-apoptotic (lower left quadrant), early apoptotic (upper left) or late apoptotic/necrotic (upper right). Quadrants were established using controls. (C) D1 cells were pre-treated with non-targeting control or BCL2L11 SMART pool siRNA (Dharmacon) for 24 hours with IL-7. Cells were then deprived of IL-7 for 48 hours. Efficacy of Bim siRNA upon Bim mRNA levels (graph) was established by measuring total Bim gene expression by quantitative PCR in which RQ value (or fold change in gene expression) = $2^{-\Delta\Delta Ct}$. IL-7-withdrawal-induced death in D1 cells, treated with either non-targeting control (Control) or Bim siRNA, is shown (dot plots) using Annexin-V/PI staining as described above. (D) Total Bim gene expression in D1 cells, in the presence or absence of IL-7, was measured for the times indicated by quantitative PCR. RQ (Fold change) = $2^{-\Delta\Delta Ct}$. Data shown in this figure are representative of a minimum of three independent experiments. * $P < 0.05$, ** $P < 0.0241$, *** $P < 0.0001$.

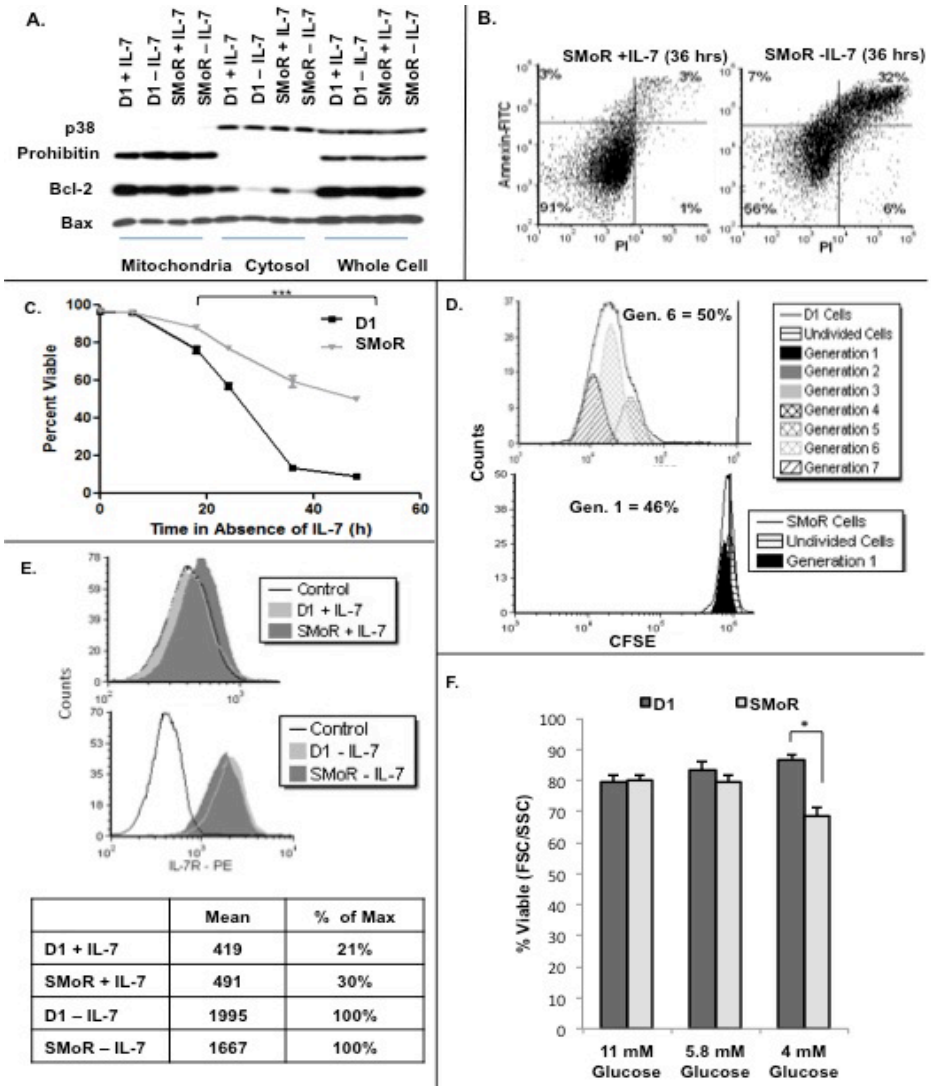

	Mean	% of Max
D1 + IL-7	419	21%
SMoR + IL-7	491	30%
D1 – IL-7	1995	100%
SMoR – IL-7	1667	100%

Figure 12. Characterization of SMoR cells.

(A) Bcl-2 and Bax expression in D1 and SMoR cells, cultured with or without IL-7 for 18 hours, was examined by immunoblot. Prohibitin and p38 MAPK shown are loading controls for mitochondrial and cytosolic content, respectively. (B) Cytokine-withdrawal-induced death of SMoR cells, grown with or without IL-7 (36 hours), was measured using FITC-conjugated Annexin-V antibody and PI as previously described. (C) Viability of D1 and SMoR cell lines, without IL-7 for the hours indicated, was determined by assessing morphological changes using FSC and SSC gating as previously described. (D) CFSE-labeled cells were cultured with IL-7 for 72 hours. Generation time, as indicated by loss of CFSE label, was assessed by flow cytometry as described in Methods. Histograms display the fluorescence profile of CFSE-labeled cells analyzed using proliferation software (DeNovo). The percent of cells in the peak generation for each cell line is shown. Lines indicate undivided cells and peaks indicate divided cells. Tables at the far right display the number of generations within the experimental period for each cell line. (E) Histograms show IL-7R surface expression in D1 and SMoR cells in the presence or absence of IL-7 for 18 hours, using a specific PE-conjugated anti-IL-7 antibody, analyzed by flow cytometry. Table shows the mean for each peak and the percent of IL-7R expression compared to the maximum level achieved in the absence of IL-7. (F) D1 and SMoR cells were cultured in the presence of IL-7 and limiting glucose concentrations for 114 hours. Viability was determined by cell morphology, assessing size (forward scatter (FSC)) and granularity (side scatter (SSC)) by flow cytometry. Results shown are representative of three experiments. * $P < 0.05$, *** $P < 0.0001$.

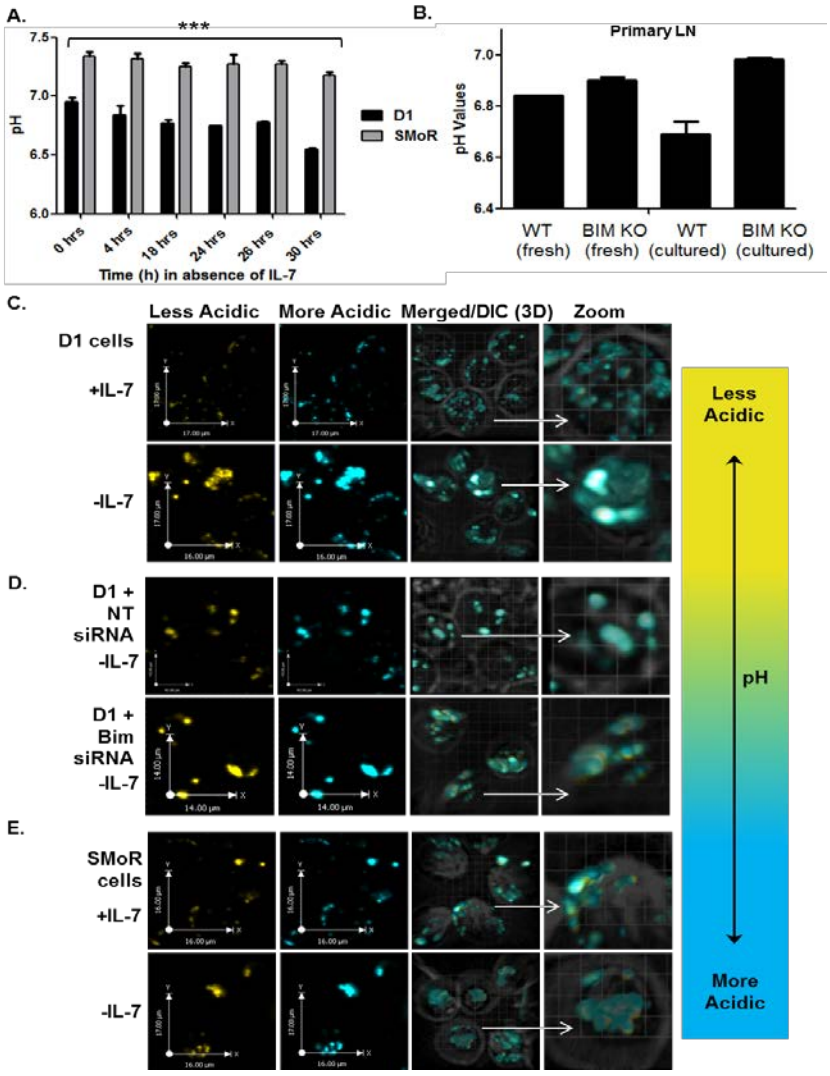

Figure 13. The distribution of acidic vesicles is altered in the absence of Bim.
(A) Intracellular pH of D1 and SMoR cell lines was measured in the absence of IL-7 at times indicated in the figure using flow cytometric analysis of BCECF-AM fluorescence, assessing the ratio at 525 nm and 610 nm. Results were determined from calibrated pH standards as described in Materials and Methods. (B) Lymph node T-cells isolated from WT C57BL/6 or BimKO mice, either freshly isolated (fresh) or cultured with 150 ng/ml of IL-7 (cultured) for 4 days, were assessed for pH, as determined by flow cytometric analysis of BCECF-AM fluorescence described above. (C-E) Live cell confocal microscopy images of D1 cells (C) in the presence or absence of IL-7 for 20 hours are shown. Cells were loaded with LysoSensor as described in Materials and Methods. IL-7-deprived D1 cells, containing either non-targeting control (NT) or Bim siRNA (D), were loaded with LysoSensor and imaged as described above. SMoR cells (E) grown with or without IL-7 were loaded with Lysosensor and imaged as described above. Yellow color indicates fluorescence of intracellular vesicles at a more neutral pH acquired at emissions 445/615, and blue color indicates fluorescence of vesicles at acidic pH acquired at 525/640 nm. Colors were arbitrarily chosen. Fluorescent images were obtained using the UltraView spinning disc confocal system (PerkinElmer) with AxioObserver.Z1 (Carl Zeiss) stand, and a Plan-Apochromat 40x/1.4 Oil DIC objective. For (C-E), images were obtained from Z-series collections and 3D projections developed using Velocity software. Arrows indicate regions of interest or intensity/merged vesicle staining. Images are representative "snapshots" of three or more independent experiments. ***$P < 0.001$

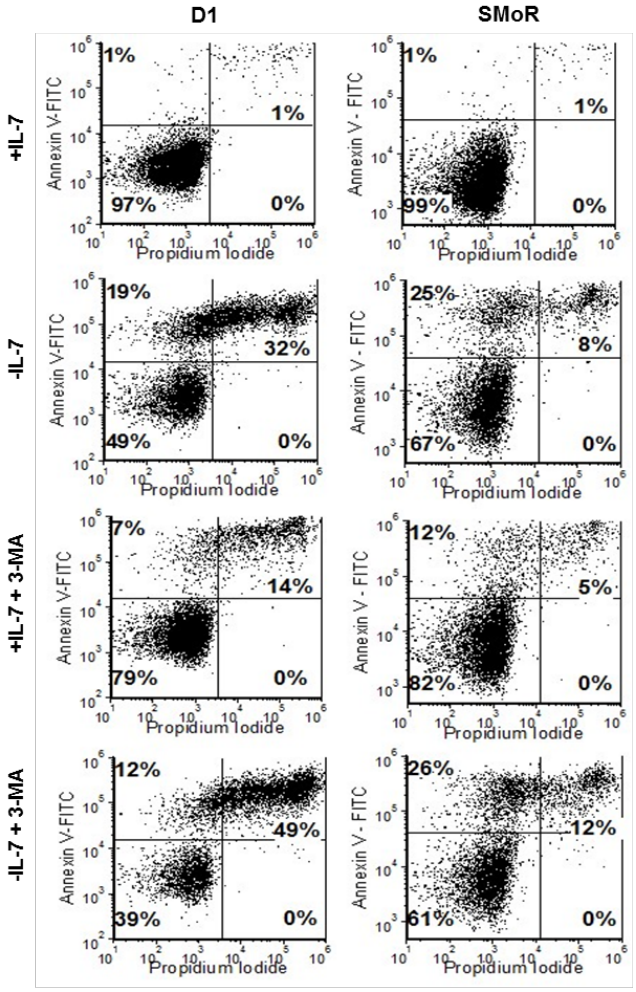

Figure 14. Treatment with 3-MA accelerated cell death induced by IL-7 withdrawal but not in Bim deficient cells.

D1 and SMoR cells, cultured with or without IL-7 for 18 hours, were treated with 3-MA (5 mM) as described in Materials and Methods. Cell death was assessed by measuring phosphatidyl serine surface exposure and membrane permeability with a FITC-conjugated Annexin-V antibody and PI staining using flow cytometry. Dot plots show percentages representing the population of cells that are non-apoptotic (lower right quadrant), early apoptotic (upper right quadrant) or late apoptotic/necrotic (upper left quadrant). Quadrants were established using controls. Results shown are representative of four independent assays.

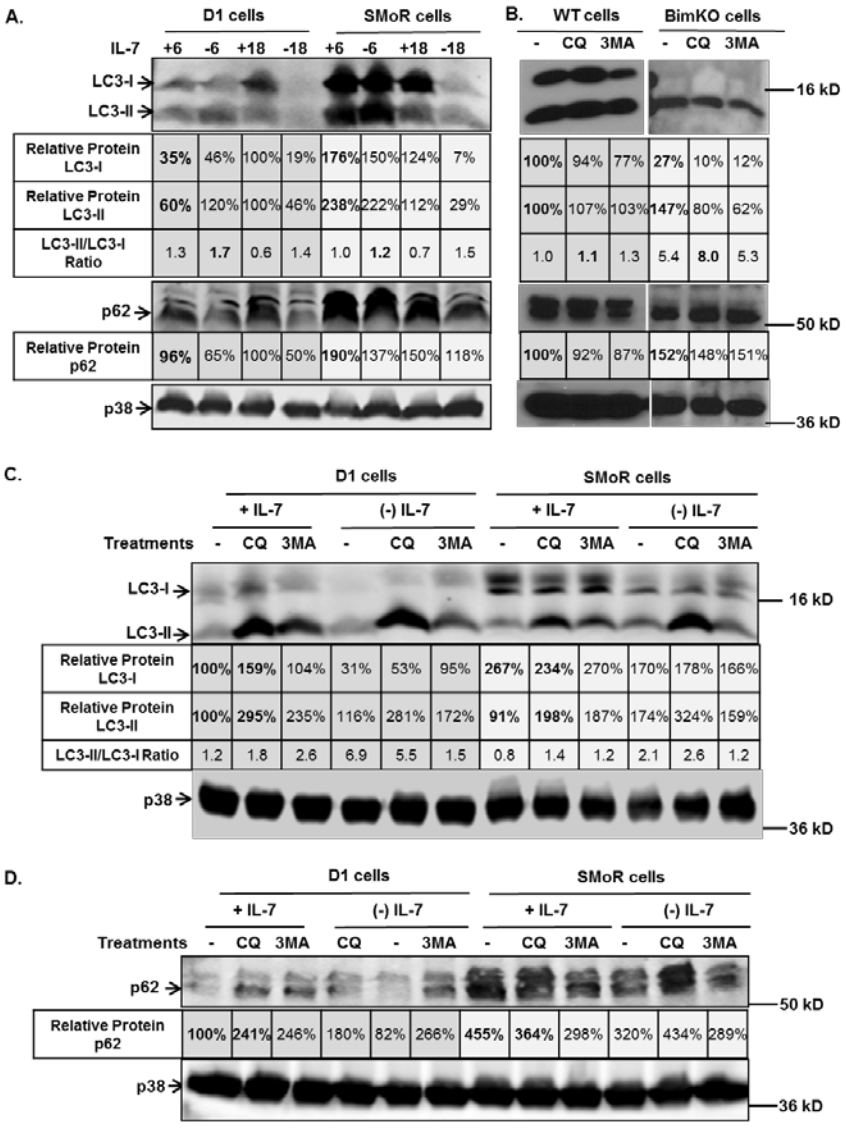

Figure 15. The degradative phase of autophagy is impaired by Bim loss.
(A) D1 and SMoR cells were grown with or without IL-7 for 6 or 18 hours, and whole cell lysates were prepared as described in Methods. Lysates were immunoblotted with specific antibodies for LC3 to examine levels of LC3-I and LC3-II as well as p62. Quantitation of bands was performed using ImageJ software and is the average of 3 measurements taken per band. p38 MAPK is included as a loading control. Protein levels of LC3 and p62 were normalized to p38 MAPK and percentages of protein detected shown are relative to samples from D1 cells cultured 18 hours with IL-7. (B) Whole cell lysates were prepared from primary LN cells freshly isolated from WT and BimKO mice and immunoblotted for LC3 and p62 as described above. Cells were treated with 3-MA (5 mM) or chloroquine (CQ) (25 μM) for six hours prior to lysis. p38 MAPK is shown as a loading control and quantitation of bands was performed as described in (A) with percentages of protein shown relative to untreated WT cells. (C-D) D1 and SMoR cells were cultured with or without IL-7 for 6 hours and treated with 3-MA or CQ as described above. Lysates were immunoblotted for LC3 (C) and p62 (D) following protocols described above. p38 MAPK is shown as a loading control for each blot and quantitation of bands was determined as described in (A) with percentages of proteins shown relative to D1 cells untreated and cultured with IL-7. Results are representative of three independent experiments. Images from full-length blots were cropped for concise presentation.

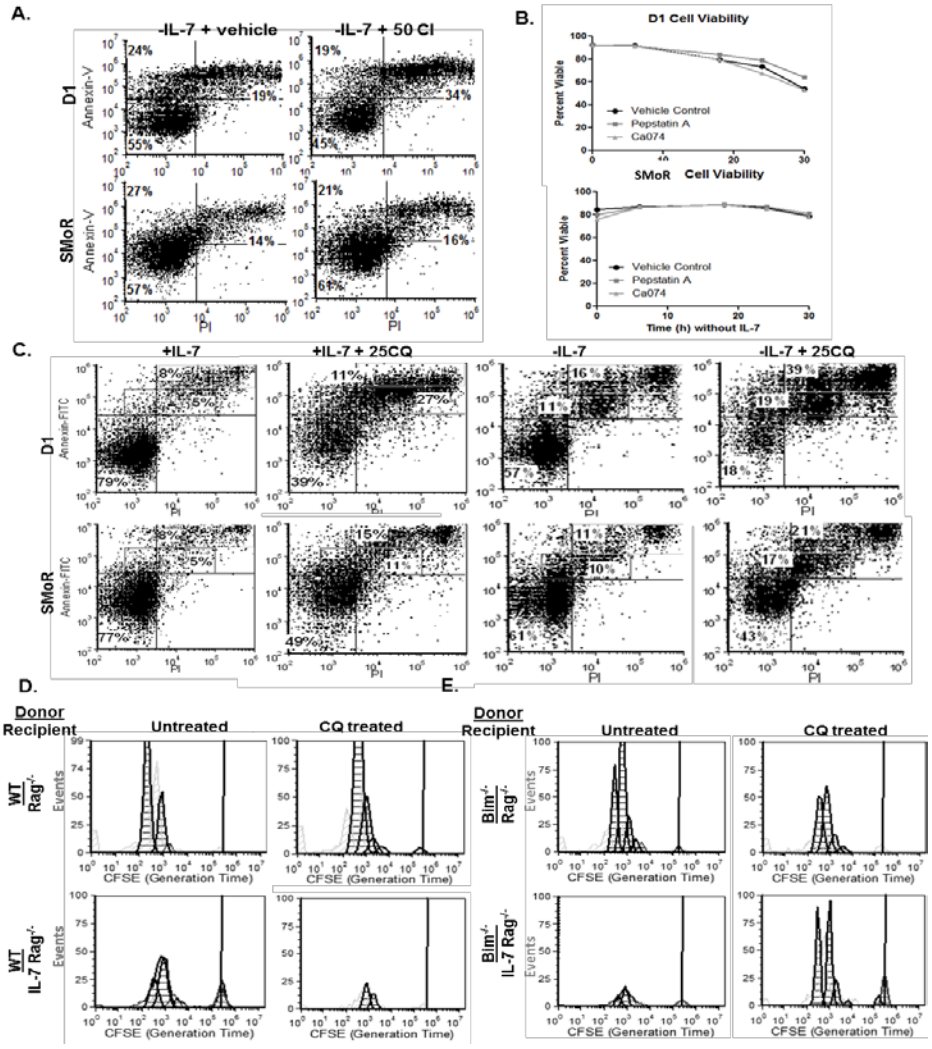

Figure 16. Bim deficient cells are resistant to inhibition of lysosomal activity.
(A) Cytokine-withdrawal induced death of D1 and SMoR cells cultured without IL-7 and either DMSO (vehicle control) or 50 μM pan-cathepsin inhibitor (Cathepsin inhibitor III (CI)) was measured by surface expression of phosphatidyl serine using a FITC-conjugated Annexin-V antibody. Membrane permeability was assessed by propidium iodide exclusion (PI) and analyzed by flow cytometry. Dot plots show percentages representing the population of cells that are non-apoptotic (lower left quadrant), early apoptotic (upper left) or late apoptotic/necrotic (upper right). Quadrants were established using controls. (B) D1 and SMoR cells cultured without IL-7 and either DMSO (vehicle control), 5 μM Pepstatin A (cathepsin D inhibitor), or 10 μM Ca074 (cathepsin B inhibitor) for times indicated, were assessed for viability as determined by cell morphology, assessing size (forward scatter (FSC)) and granularity (side scatter (SSC)) by flow cytometry. (C) D1 and SMoR cells cultured with IL-7 or without IL-7 and 25μM chloroquine (25CQ) were assayed for Annexin-V/PI staining by flow cytometry as described above. Percentages represent the population of cells indicated by the highlighted boxes of late apoptotic or necrotic cells. Results shown are representative of four experiments. (D-E) CFSE-labeled T-cells were adoptively transferred to either Rag knockout ($Rag^{-/-}$) or IL-7/Rag double knockout ($IL\text{-}7^{-/-}/Rag^{-/-}$) that were irradiated as described in Materials and Methods. Mice were untreated or treated with chloroquine (CQ) (i.p. 60 mg/kg/mouse) 24 and 48 hours after transfer of cells. Mice were sacrificed after 72 hours and organs analyzed for T-cell recovery. Number of generations recovered from transferred WT cells (D) and BimKO cells (E) were determined by loss of CFSE label using cell proliferation software (DeNovo). Representative results from duplicate experiments are shown.

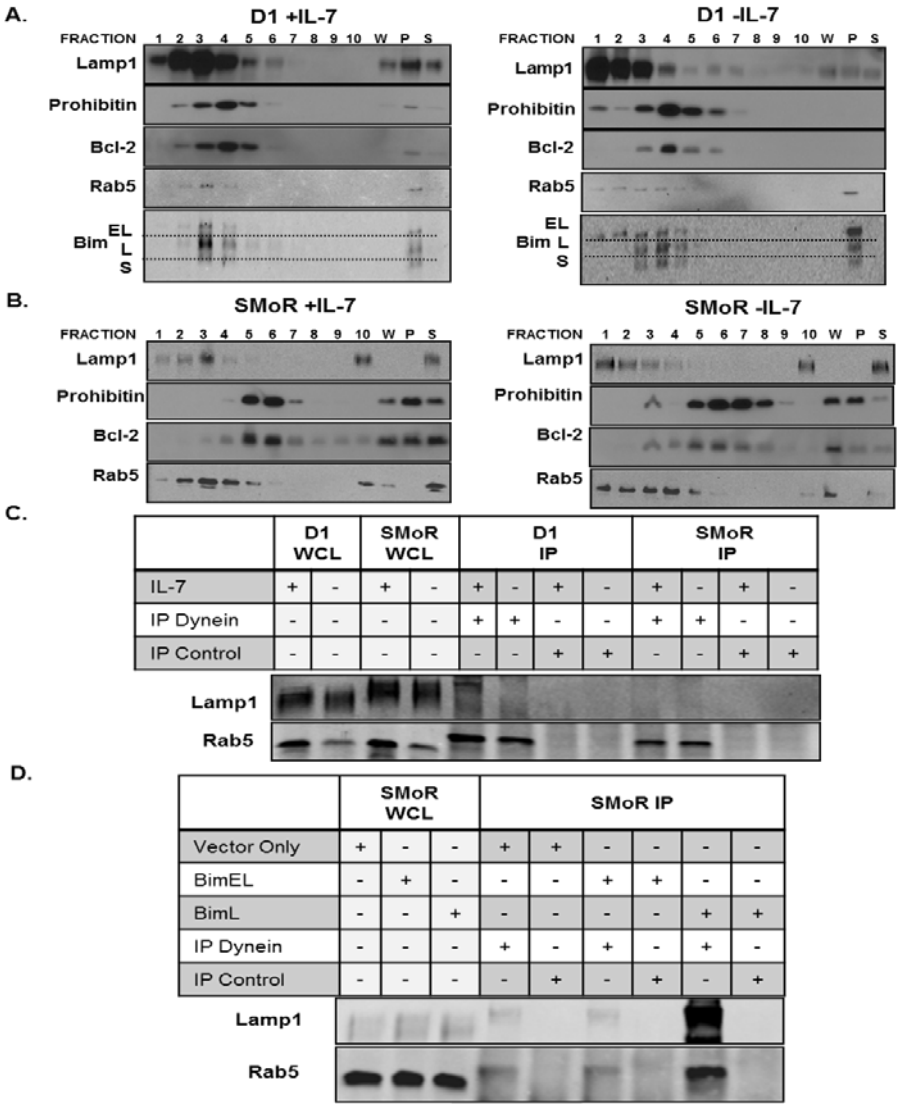

Figure 17. BimL associates with lysosomes through interactions with dynein.
(A) A representative immunoblot is shown of lysates enriched for lysosomal content from D1 cells. D1 cells were cultured in the presence or absence of IL-7 for 20 hours and subjected to differential ultracentrifugation. Gradient fractions (17-30% Optiprep, Fractions 1-10), whole cell lysate (W), pellets (P) and supernatant (S) after initial centrifugation step, were immunoblotted for Lamp1 (late endosome and lysosomal membrane), prohibitin (mitochondria), Rab5 (early endosome), Bcl-2, and Bim. (B) Immunoblot analysis of enriched lysosomal protein lysates were prepared from SMoR cells cultured in the presence or absence of IL-7 for 20 hours as described for D1 cells above. (A) Blots are representative of nine independent experiments. (C) Immunoblots show co-immunoprecipitation of dynein with Lamp1 upon presence of BimL. As input controls, the whole cell lysates before immunoprecipitation are included. Whole cell lysates of D1 and SMoR cells cultured were with or without IL-7 for 20 hours incubated with either dynein or control antibody to co-immunoprecipitate binding proteins, subjected to SDS-PAGE and immunoblotted for lysosomal/late endosomal protein (Lamp1), and early endosomal content (Rab5). (D) Whole cell lysates of SMoR cells transfected with retrovirus to express individual Bim isoforms as described in Methods, co-immunoprecipitated with either dynein or control antibody, were immunoblotted for lysosomal/late endosomal protein (Lamp1), early endosomal protein (Rab5), and Bim. A representative experiment of three performed is shown. Images from full-length blots were cropped for concise presentation.

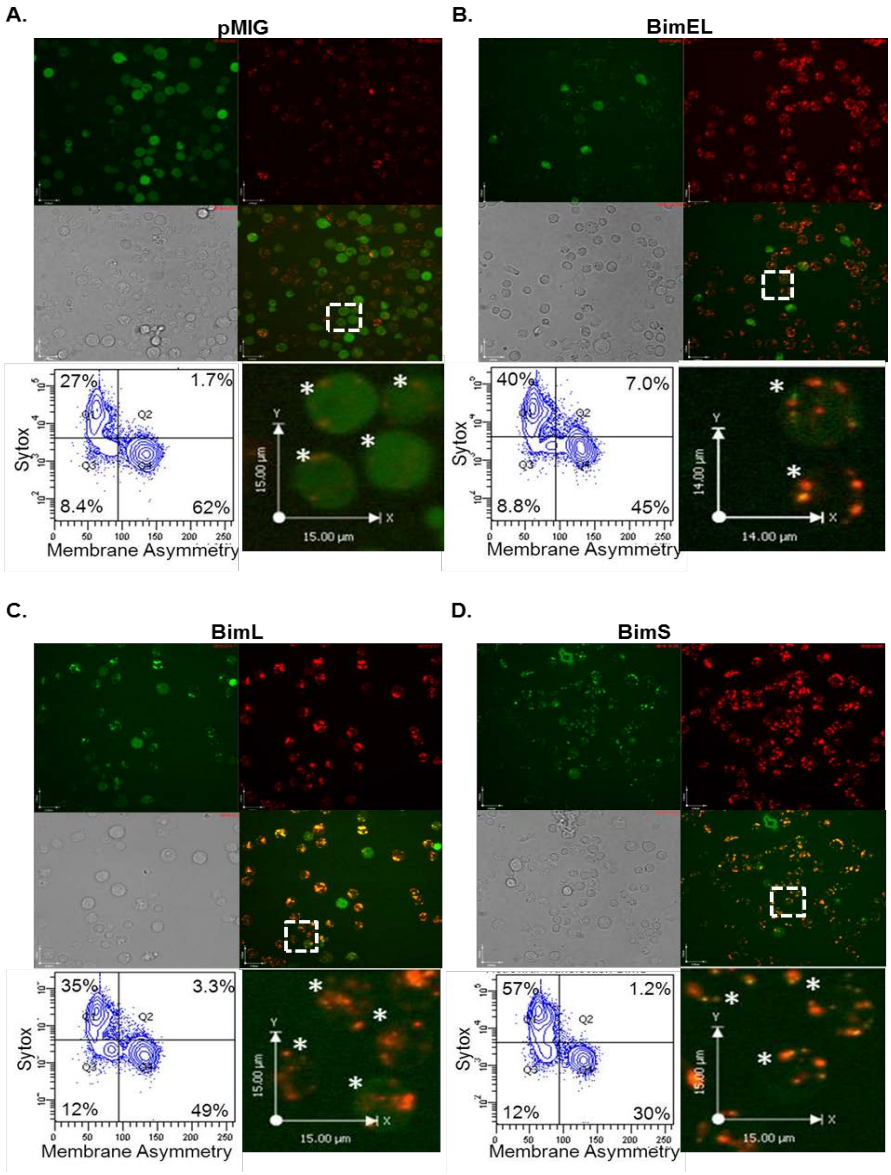

Figure 18. Expression of BimL restores lysosomal distribution in SMoR cells.
Live cell confocal microscopy images of SMoR cells are shown. Images are representative "snapshots" taken at the end of a 24 hour live-imaging experiment. SMoR cells were retrovirally transfected to express the control plasmid, pMIG (A), or the individual Bim isoforms, BimEL (B), BimL (C) and BimS (D), in the presence of IL-7, and loaded with 1µM LysoTracker. Images were acquired using the UltraView spinning disc confocal system (PerkinElmer) with AxioObserver.Z1 (Carl Zeiss) stand, and a Plan-Apochromat 40x/1.4 Oil DIC objective. Each field contains the same cells but with different fluorescent channels: GFP fluorescence (upper left), RFP (LysoTracker) fluorescence (upper right), DIC (lower left), and overlay of GFP and RFP fluorescence (lower right). Each panel also contains a larger, digitally magnified inset of the overlay, as indicated by a white cutout within the overlay panel. The magnification inset contains transfected cells indicated by (*). The bottom left panel of each figure section is a density plot displaying the viability of SMoR cells expressing control or Bim isoforms. Cell death was assessed by Sytox uptake (membrane permeability) and membrane asymmetry. Dot plots percentages represent the population of cells that are non-apoptotic (lower right quadrant), early apoptotic (lower left) or late apoptotic/necrotic (upper left). Quadrants were established using controls. Results shown are representative of three experiments.

Discussion

In this study, using Bim-containing and Bim-deficient T-cells, we examined the function of Bim during apoptosis and the degradative phase of autophagy controlled by IL-7 stimulation and determined that the major isoforms of Bim contribute independently to these processes. We found that BimL may facilitate lysosomal positioning in cells responding to IL-7 through interactions with dynein. We also observed that loss of IL-7 up-regulated total Bim transcription, and that Bim deficiency partially protected these cells from death induced by IL-7 withdrawal, suggesting that the other isoforms participated in the intrinsic pathway of apoptosis. In support, we found that T-cells lacking functional Bim had decreased growth rate, increased endosomal and reduced lysosomal content, and were resistant to the effects of cathepsin inhibition or impairment of lysosomal acidification. Over-expression of BimL in Bim deficient cells increased vesicular aggregation, while BimEL, and more so BimS, overexpression increased apoptotic morphology. Taken together, these results demonstrated that the major isoforms of Bim could have distinct activities in T-cells that were indicated by localization to different organelles.

Based on our studies, and others, it can be surmised that T-cells lacking Bim would be deficient in the ability of lysosomes to degrade intracellular contents. Hence Bim-deficient T-cells would not effectively degrade autophagic vesicles or initiate lysosome-mediated apoptotic events [189]. As a result, Bim deficient T-cells would be delayed undergoing cell death, but, lacking the lysosomal degradative machinery, would eventually succumb perhaps to nutrient deprivation or metabolic suicide. It is also possible that a limited form of autophagy could occur in the absence of Bim. Under some conditions, the contents of autophagic vesicles can be

degraded by amphisomes, autophagic vacuoles formed through the fusion of endosomes to autophagosomes [190]. In Bim-deficient cells, we detected increased amounts of Rab5, an early endosome marker, suggesting the fusion of early endosomes was possible and could, during autophagy, perhaps form amphisomes in the absence of forming autolysosomes. There is also the possibility that with reduced lysosomal activities, degradation via the proteosome could be impaired [191]. p62 is primarily degraded by lysosomes and proteasomes [192], hence, this could explain why incomplete degradation and accumulation of p62 occurs, and why CQ and 3-MA treatments have little effect on Bim deficient SMoR cells.

Previous studies demonstrated that Bim is sequestered by dynein in healthy cells, and dissociates upon an apoptotic stimulus; providing a possible regulatory mechanism [77, 193]. However, the viability of T-cells transfected with a BH3 domain mutant of BimL was increased [47]. This suggested a possibility that beyond sequestering Bim, the interaction of BimL with dynein facilitates the loading and perhaps fusion and positioning of lysosomes. In our study, IL-7 withdrawal induced vesicular aggregation in T-cells containing Bim, while this was not observed in Bim deficient T-cells. This result is supported by studies with dynein-deficient cells in which endosomal and lysosomal content became dispersed and lysosomes ceased to co-localize with microtubules [194, 195]. Moreover, knockdown of Huntingtin (Htt), a scaffolding protein that interacts with dynein, resulted in lysosomal accumulation and aggregation, indicating that Htt was involved in the movement of cargo. In contrast, we found that Bim deficiency resulted in dispersed vesicles and reduced aggregation, suggesting that Bim's role may not be in cargo movement but rather facilitating the fusion of late endosomes/lysosomes. An example similar to Bim deficiency was seen in a study using mice deficient in Snapin, a

SNARE-binding protein. Deletion of Snapin caused accumulation of endocytic organelles and impaired lysosomal function and maturity [196]. These results support the possibility that the dynein-binding motif on Bim, KXTQT [161], renders the protein accessible as an adaptor for dynein during normal T-cell function to facilitate the positioning and fusion of lysosomal cargo.

The regulation of Bim transcription is mediated by the forkhead transcription factor, FKHR-L1, in growth factor-deprived hematopoietic cells [49, 162]. This transcription factor, also known as Foxo3a, translocates to the nucleus when the PI3-kinase/Akt pathway is down-regulated in the absence of survival signals [58]. In neurons, under growth factor deprivation, Bim was up-regulated but required Jun N-terminal protein kinases (JNK) activation [57, 188]. We show that IL-7 induced basal levels of *bim* gene transcription, even in non-apoptotic cells, and that the withdrawal of IL-7 further amplified Bim synthesis. It may be that the JNK pathway and the PI3K pathway, both shown to be active in response to IL-7 signaling [30, 45, 90], may contribute to Bim expression in T-cells. Interestingly, engagement of IL-7 induces the internalization and further recycling of the IL-7R by proteasomes and lysosomes [197]. It is possible that Bim, by enabling lysosomal degradative activities, could play a role in regulating the amount of IL-7R available for membrane expression. In support, we found that in SMoR cells IL-7R levels were slightly higher. Further evidence comes from a study in which cells were cultured with IL-7 and treated with a clathrin formation inhibitor [197]. As a result, pAKT was reduced, which in turn, stimulated FKHR-1 translocation and increased Bim synthesis, perhaps to participate in the maintenance of IL-7R recycling [197].

Another way of controlling Bim levels includes regulation of alternative mRNA splicing. For example, in B cells, engagement of the B cell receptor (BCR) led to BimL expression not

through increased generation of BimL mRNA but rather through splicing of the BimEL mRNA. Hence BimEL was a pre-mRNA form of BimL [64]. Additionally, phosphorylation sites encoded by alternative splicing of exons within BimEL can contribute to BimL expression. As example, in BimEL mutant mice lacking exon 3, which encodes sites of MAPK phosphorylation, BimL expression resulted [68]. In our study, we observed more BimL protein compared to BimEL in the presence of IL-7, suggesting that BimL was being produced in preference to BimEL, perhaps through the splicing mechanism described above. In the absence of IL-7, we noted increased total Bim mRNA and more BimEL protein, indicating that the possible splicing of BimEL to make BimL was only occurring upon an IL-7 stimulus.

Our results indicate that the BimL isoform may have non-apoptotic activities that support lysosome maintenance. Bim and IL-7R double-deficient mice showed partial restoration of thymocyte development [44], while, in a bone marrow chimera, Bim deficiency failed to fully reconstitute thymocyte development [52]. Bim deficiency, in our studies, failed to rescue adoptively transferred T-cells in IL-$7^{-/-}$ hosts. The inability of Bim deficiency to completely restore an immunodeficient phenotype could in part be explained by the redundancy of other pro-apoptotic proteins like Bad or Bid. However, another perspective could be that Bim isoforms have both apoptosis (BimEL, and BimS) and cell maintenance or autophagic (BimL) activities. Other apoptosis-regulating proteins have been shown to contribute to autophagy. For example, anti-apoptotic Bcl-2 bound Beclin-1 and inhibited autophagic induction, but overexpression of pro-apoptotic protein, Bad, induced autophagy in human cells [198]. Additionally, the lone *C. Elegans* BH3-only protein, EGL-1, can trigger autophagy [199]. In studies examining the individual isoforms of Bim, in which both BimL and Bcl-2 were expressed, BimL could not non-

apoptotic function such as we have described. Moreover, expression of BimL did not cause release of cytochrome c [76].

The implications of Bim isoforms having different cellular activities for disease treatments are significant. In cancers with specific genetic mutations, Bim levels were found to be predictive of the effect of inhibitors targeting PI3K, HER2 or EGFR, but did not correlate with effectiveness to standard chemotherapeutics [200]. Efforts at developing inhibitory Bim BH3-like mimetics for therapy only consider the pro-apoptotic action of Bim mediated, for example, through the BH3 domain [201]. Our work suggests that Bim is more complex, having multiple isoforms and functions. An alternative approach could be the design of compounds that target the Bim isoform-splicing mechanisms. As a result, one could potentially control the generation of a specific isoform to elicit the desired apoptotic (BimEL/S>BimL) or autophagic (BimL>BimEL/S) outcome in a manner that is more effective than the targeting of total Bim.

CHAPTER 4: CONCLUSIONS

IL-7 is a pleotropic cytokine, and promising as a therapeutic agent to support the immune system. As of recently, IL-7 is being evaluated in 15 clinical trials as treatment for reconstitution in lymphopenic patients, or after chemotherapy, in addition to patients with depleted immune systems due to long term HIV infection. Unfortunately, assessment of the effects of IL-7 has been limited to cell survivability and expansion of certain T cell subsets. However, as we've shown here, IL-7 signaling mechanisms are more complex in T cells. Using our IL-7 dependent T cell line, D1, and *in vitro* and *in vivo* models, we have been able to study how IL-7 signaling contributes to the maintenance of T cells, specifically, in terms of metabolism and cell survival. Specifically, we've found that IL-7 promoted HXKII gene expression in a Stat5-independent manner, through the activity of JNK. JNK, in turn, drove the expression of JunD, a component of the AP-1 transcription factors, and JunD homodimerization. These findings were significant as both JNK and JunD are typically ascribed inhibitory characteristics, so how JNK and JunD could have both inhibitory and stimulatory functions necessitates further study. In addition to stimulating metabolism, we found that IL-7 promoted growth and proliferation through the activity of JunD, namely, in the expression of Pim-1. Finding that two factors involved in growth and proliferation of T cells, HXKII and Pim-1, are regulated in a Stat5-independent manner, establishes that IL-7 signaling pathways are more diverse than previously thought.

The studies that we have performed illustrate the wide-ranging possible effects of IL-7 signaling. Specifically, the bioinformatics completed demonstrates the large number of early-response genes activated within a two-hour pulse with IL-7, with a potential JunD binding site located within their promoter region. Some of these genes play critical roles in cell cycling,

suppressing inflammation, and cell adhesion, perhaps contributing to T-cell migration to areas of increased IL-7. We've also shown that increased glucose uptake occurs through JunD activation, perhaps leading to increased rates of glycolysis. Bioinformatics has provided a plethora of potentially IL-7-mediated, JunD-regulated genes to investigate, and future studies could reveal additional mechanisms involved in glucose consumption that were previously unknown.

Cancer cells preferentially metabolize glucose through aerobic glycolysis, termed the Warburg effect [202]. Recent studies have attempted to find methods in which to regulate cancer cell metabolism, and in turn, inhibit metastasis of invasive tumors. Cancer cells contain mutations to retain immortality, including abnormalities in tumor-suppressor p53 [203], among others. We and others have shown that JunD protects cells from both p53-dependent [145] and p53- independent apoptosis [140]. Therapies developed to target JunD, or its downstream effectors, could potentially eliminate the cancer cells that switch to glycolysis.

One future study should attempt to determine the involvement of JNK in IL-7 directed JAK/Stat pathway. In our first study, we presented a mechanism for HXKII gene expression, induced by IL-7 signaling, mediated through JNK activity, independent of Stat5. However, under IL-7 deprivation conditions, JNK has been found to phosphorylate BimEL to induce apoptosis [90]. One question to ask is why JNK can function in either the presence, or absence of IL-7, with both pro- and anti-apoptotic activities. Therefore it is necessary to determine what regulates JNK activity.

Previous studies have shown that in mice expressing constitutively active Stat5, IL-7 can induce Pim-1 transcription in pro-B cells [94]. In studies included here, we've shown that basal Pim-1 protein synthesis is IL-7 dependent, but independent of JNK. We also showed that IL-7

re-addition induced Pim-1 expression, and that JNK inhibition could ablate it. It is possible that Stat5 could regulate basal Pim-1 expression, and that JNK could initiate the synthesis of Pim-1. Pim-1, a kinase dysregulated in several cancers, can be transcribed through Stat5 [94], but Pim-1 can modulate Stat5 transcription by binding its inhibitor, SOCS1 [97, 204]. Taken together, these studies indicate that Pim-1 could potentially regulate its own expression. Since overexpression of Pim kinases result in lymphogenesis in mice [205], and Stat5 is a potential chemotherapeutic target [206, 207], further study is necessary to evaluate what stimulus maintains Pim-1 expression in these cancers, and if targeting a pathway other than Jak/Stat would be more beneficial.

In addition to mediating cell growth, we've shown that IL-7 can regulate the maintenance of T cell populations. Previous work has shown that Bim, a pro-apoptotic member of the Bcl-2 family, participates in activated T cell death [39]. However, those studying Bim have all but ceased further examination investigating the possibility of separate functions per individual isoform. In our own studies, we have confirmed the involvement of Bim in apoptosis, and furthermore, the binding Bim to the dynein light chain [77]. Conversely, we have established that individual isoforms of Bim have different functions, namely, BimL participates in the stabilization of lysosomes, and in progressing the process of autophagy, while BimEL and BimS participate in apoptotic activities. Instead of observing the sequestering of Bim as to prevent apoptosis, we found an unexpected protective function of BimL, helpful in stress conditions. Autophagy allows cell scavenging when the environment is deficient in essential nutrients, which is most often when a peripheral T cell is circulating until encountering IL-7 or other factors. These findings are significant in that they establish pro- and anti- survival properties of

Bim, and illustrate deleterious effects if Bim is targeted therapeutically. Hence, taken together, our studies clearly demonstrate the importance for an understanding on how IL-7 signal transduction consequently affects gene expression in T cells, to further therapeutic development of this cytokine.

We've shown that the lack of IL-7 up-regulates total Bim gene expression, and that the presence of IL-7 maintains basal Bim levels. Recently, Clybouw and colleagues found that BCR stimulation up-regulated the production of BimL, not transcriptionally, but rather, BimL mRNA resulted from intron retention within BimEL mRNA [64]. An interesting study to undertake would determine if IL-7 maintains basal Bim expression, specifically to increase BimL transcription and further, protein expression, and whether IL-7 directs BimL expression through the conversion of BimEL mRNA to BimL. As alternative splicing contributes to the expression of BimL, splicing can also be influenced by microRNA (miRNA) activity. MiRNA inhibits gene expression by associating with target mRNA, contributing to the degradation and silencing of its target [65]. In fact, epiblasts deficient in Dicer, an enzyme necessary for the creation of miRNA, have increased expression of Bim [208]. How miRNA regulation of Bim expression contributes to BimL protein stability, and its involvement in autophagy induction needs further study.

A recent study has concluded that BimEL and BimL are interchangeable for apoptotic function in homeostatic hematopoiesis [66], but have not evaluated the individual isoforms in other context other than degree of apoptosis upon treatment with immunosuppressors. In T cells where phosphorylation of Bim is impaired, these cells activate upon mitogen stimulation, and proliferate, to the same extent as wild type cells [66]. These results indicate that the integrity of

Bim could be essential for T cell activation and subsequently, mounting an immune response, and that BimEL degradation is not critical to the regulation of apoptosis.

Since the three major isoforms have different phosphorylation sites, regulatory targeting sequences, and lysosome recognition motifs, the question remains as to why BimL has pro-survival functions, while the other isoforms are pro-apoptotic. Furthermore, there is inconsistency as to whether phosphorylation stimulates Bim activity or targets these isoforms for ubiquitination, or other forms of degradation. Especially since a major phosphorylation site within BimL, Thr56, lies within a lysosomal targeting sequence, it is essential to determine whether the phosphorylation status of this region contributes to lysosomal stability or trafficking and the degradative phase of autophagy. It's interesting to note that this site can also be found in BimEL, but as of this writing, studies evaluating whether this site is physiologically significant to the function of BimEL have not been published. Additionally, it would be beneficial to determine whether the BH3 domain of BimL is modified in some manner, and whether this contributes to the possible pro-survival function of BimL.

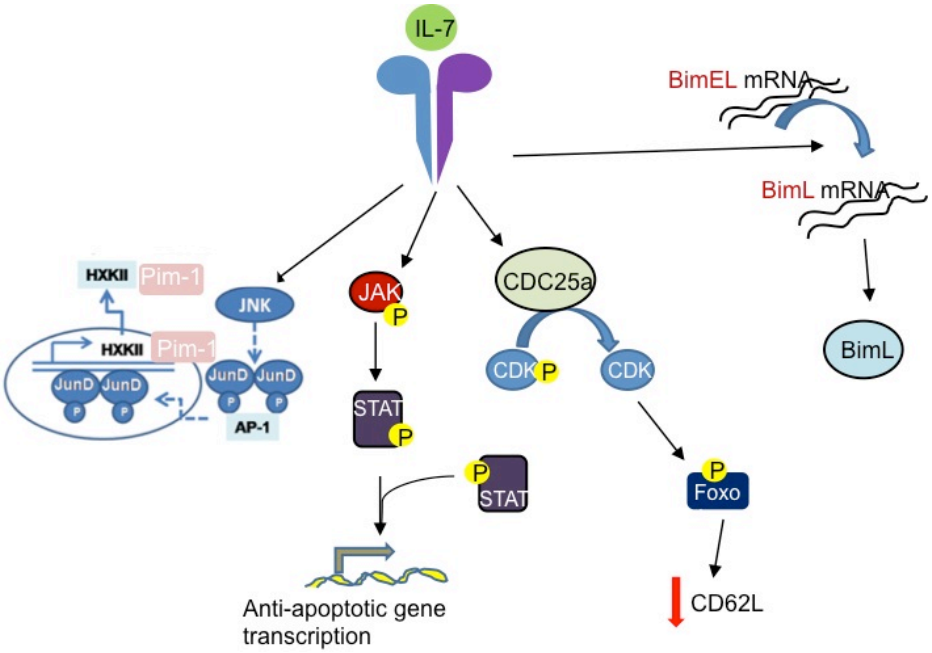

Figure 19. Novel IL-7-mediated signaling pathways.
IL-7 contributes to the survival of cells by mediating Jak/Stat5 activities and inducing synthesis of anti-apoptotic genes, such as Bcl-Xl, and SOCS1. IL-7 stimulates proliferation by activating CDC25A phosphatase, and initiates lymphocyte movement by down-regulating the extracellular adhesion molecule, CD62L. The studies included in this dissertation illustrate novel IL-7 signaling pathways that contribute to cell proliferation and survival that were previously unknown, including regulation of HXKII gene expression transduced JunD and JNK activity, and also, regulation of BimL and its potential contribution to lysosome trafficking or stability.

APPENDIX A:
IACUC APPROVAL LETTER

University of Central Florida

Office of Research & Commercialization

4/20/2011

Dr. Annette Khaled
Biomolecular Science Center
BRA
12722 Research Parkway
Orlando, FL 32826

Subject: Institutional Animal Care and Use Committee (IACUC) Protocol Submission

Dear Dr. Annette Khaled:

This letter is to inform you that your following animal protocol was re-approved by the IACUC. The IACUC Animal Use Renewal Form is attached for your records.

Animal Project #: 09-25

Title: IL-7 and Lymphocyte Homeostasis: Life versus Death.

First Approval Date: 6/16/2009

Please be advised that IACUC approvals are limited to one year maximum. Should there be any technical or administrative changes to the approved protocol, they must be submitted in writing to the IACUC for approval. Changes should not be initiated until written IACUC approval is received. Adverse events should be reported to the IACUC as they occur. Furthermore, should there be a need to extend this protocol, a renewal must be submitted for approval at least three months prior to the anniversary date of the most recent approval. If the protocol is over three years old, it must be rewritten and submitted for IACUC review.

Should you have any questions, please do not hesitate to call me at (407) 882-1164.

Please accept our best wishes for the success of your endeavors.

Best Regards,

Cristina Caamaño

Cristina Caamaño
IACUC Coordinator

Copies: Facility Manager (when applicable.)

12201 Research Parkway • Suite 501 • Orlando, FL 32826-3246 • 407-823-3778 • Fax 407-823-3299

THE UNIVERSITY OF CENTRAL FLORIDA
INSTITUTIONAL ANIMAL CARE and USE COMMITTEE (IACUC)
Re-Approval to Use Animals

Dear Dr. Annette Khaled,

Your application for IACUC Re-Approval has been reviewed and appproved by the UCF IACUC Committee Reviewers.

Approval Date: 4/18/2011

Title: IL-7 and Lymphocyte Homeostasis: Life versus Death.

Department: Biomolecular Science Center

Animal Project #: 09-25

Expiration: 6/15/2012

You may purchase and use animals according to the provisions outlined in the above referenced animal project. This project will expire as indicated above. You will be notified 2-3 months prior to your expriation date regarding your need to file another renewal.

Christopher Parkinson, Ph.D.
IACUC Chair

Approved ✓ Renewed ✓

University of Central Florida Institutional Animal Care and Use Committee (IACUC)
IACUC Coordinator: Cristina Caamaño, Email ccaamano@mail.ucf.edu Phone: (407) 882-1164 Fax: (407) 823-3299

APPENDIX B:
PLOS ONE COPYRIGHT APPROVAL

APPENDIX C:
BBA-MCR COPYRIGHT APPROVAL

ELSEVIER

http://www.elsevier.com
About Elsevier > Authors' Rights & Responsibilities

Authors' Rights & Responsibilities

At Elsevier, we are dedicated to protecting your rights as an author, and ensuring that any and all legal information and copyright regulations are addressed.

Whether an author is published with Elsevier or any other publisher, we hold ourselves and our colleagues to the highest standards of ethics, responsibility and legal obligation.

As a journal author, you retain rights for a large range of author uses of your article, including use by your employing institute or company. These rights are retained and permitted without the need to obtain specific permission from Elsevier.

- Intellectual property
- Your role
- Permissions
- Publishing ethics
- Other policies

Copyright
Intellectual property, in particular copyright (rights in editorial content), trademarks (rights in brands for services or journals), and database rights (rights in compilations of information), form the foundation of Elsevier's publishing services and communications businesses. We in Elsevier embrace the opportunities the digital environment offers for communication and access, while at the same time we recognize the new risks that this environment poses, that being the ease with which unauthorized copies can be made and distributed worldwide. Download your practical guide to Elsevier's copyright policy.

Our objective
We aim to manage digital rights and brands amidst the structural changes that the "information society" represents, while at the same time recognizing the shared goals we have with our customers and authors. These include providing the widest possible distribution of scientific and medical content and services in a financially sustainable business model.

Elsevier wants to ensure a proper balance between the scholarly rights which authors retain (or are granted/transferred back in some cases) and the rights granted to Elsevier that are necessary to support our mix of business models. We routinely analyse and modify our policies to ensure we are responding to authors' needs and concerns, and to the concerns in general of the research and scholarly communities.

What rights do I retain as a journal author*?

- the right to make copies (print or electronic) of the journal article for your own personal use, including for your own classroom teaching use;
- the right to make copies and distribute copies of the journal article (including via e-mail) to research colleagues, for personal use by such colleagues for scholarly purposes*;
- the right to post a pre-print version of the journal article on Internet websites including electronic pre-print servers, and to retain indefinitely such version on such servers or sites for scholarly purposes* (with some exceptions such as The Lancet and Cell Press. See also our information on electronic preprints for a more detailed

discussion on these points)*;

- the right to post a revised personal version of the text of the final journal article (to reflect changes made in the peer review process) on your personal or institutional website or server for scholarly purposes*, incorporating the complete citation and with a link to the Digital Object Identifier (DOI) of the article (but not in subject-oriented or centralized repositories or institutional repositories with mandates for systematic postings unless there is a specific agreement with the publisher. Click here for further information);
- the right to present the journal article at a meeting or conference and to distribute copies of such paper or article to the delegates attending the meeting;
- for your employer, if the journal article is a 'work for hire', made within the scope of the author's employment, the right to use all or part of the information in (any version of) the journal article for other intra-company use (e.g. training);
- patent and trademark rights and rights to any process or procedure described in the journal article;
- the right to include the journal article, in full or in part, in a thesis or dissertation;
- the right to use the journal article or any part thereof in a printed compilation of your works, such as collected writings or lecture notes (subsequent to publication of the article in the journal); and
- the right to prepare other derivative works, to extend the journal article into book-length form, or to otherwise re-use portions or excerpts in other works, with full acknowledgement of its original publication in the journal.

***Commercial purposes and systematic distribution**
Authors of Elsevier-published articles may use them only for scholarly purposes as set out above and may not use or post them for commercial purposes or under policies or other mechanisms designed to aggregate and openly disseminate manuscripts or articles or to substitute for journal-provided services. This includes the use or posting of articles for commercial gain or to substitute for the services provided directly by the journal including the posting by companies of their employee-authored works for use by customers of such companies (e.g. pharmaceutical companies and physician-prescribers); commercial exploitation such as directly associating advertising with such postings; the charging of fees for document delivery or access; the systematic distribution to others via e-mail lists or list servers (to parties other than known colleagues), whether for a fee or for free; the posting of links to sponsored articles by commercial third parties including pharmaceutical companies; institutional, funding body or government manuscript posting policies or mandates that aim to aggregate and openly distribute the accepted, peer reviewed manuscripts or published journal articles authored by its researchers or funded researchers; and subject repositories that aim to aggregate and openly distribute accepted peer reviewed manuscripts or published journal articles authored by researchers in specific subject areas.

For a more detailed discussion of our article posting policies and the different stages of a journal article development that are relevant from a policy perspective, please see the Article Posting Policies information page.

When Elsevier changes its journal usage policies, are those changes also retroactive?
Yes, when Elsevier changes its policies to enable greater academic use of journal materials (such as the changes several years ago in our web-posting policies) or to clarify the rights retained by journal authors, Elsevier is prepared to extend those rights retroactively with respect to articles published in journal issues produced prior to the policy change.

We are pleased to confirm that, unless explicitly noted to the contrary, all policies apply retrospectively to previously published journal content. If, after reviewing the material noted above, you have any questions about such rights, please contact Global Rights.

How do I obtain a Journal Publishing Agreement?
You will receive a form automatically by post or e-mail once your article is received by Elsevier's Editorial-Production Department. View a generic example of the agreement. Some

journals will use another variation of this form.

Why does Elsevier request transfer of copyright?
The research community needs certainty with respect to the validity of scientific papers, which is normally obtained through the editing and peer review processes. The scientific record must be clear and unambiguous. Elsevier believes that, by obtaining copyright transfer, it will always be clear to researchers that when they access an Elsevier site to review a paper, they are reading a final version of the paper which has been edited, peer-reviewed and accepted for publication in an appropriate journal. This eliminates any ambiguity or uncertainty about Elsevier's ability to distribute, sub-license and protect the article from unauthorized copying, unauthorized distribution, and plagiarism.

Can you provide me with a PDF file of my article?
Many Elsevier journals are now offering authors e-offprints – free electronic versions of published articles. E-offprints are watermarked PDF versions, and are usually delivered within 24 hours, much quicker than print copies. These PDFs may not be posted to public websites. For more information, please see your journal's Guide to Authors or contact sciencereprints@elsevier.com

REFERENCES

1. Bayer, A.L., et al., *Essential role for interleukin-2 for CD4(+)CD25(+) T regulatory cell development during the neonatal period.* J Exp Med, 2005. **201**(5): p. 769-77.
2. Kittipatarin, C. and A.R. Khaled, *Interlinking interleukin-7.* Cytokine, 2007. **39**(1): p. 75-83.
3. Park, J.H., et al., *Suppression of IL7Ralpha transcription by IL-7 and other prosurvival cytokines: a novel mechanism for maximizing IL-7-dependent T cell survival.* Immunity, 2004. **21**(2): p. 289-302.
4. Furtado, G.C., et al., *Interleukin 2 signaling is required for CD4(+) regulatory T cell function.* J Exp Med, 2002. **196**(6): p. 851-7.
5. Jankovic, D., et al., *Schistosome-infected IL-4 receptor knockout (KO) mice, in contrast to IL-4 KO mice, fail to develop granulomatous pathology while maintaining the same lymphokine expression profile.* J Immunol, 1999. **163**(1): p. 337-42.
6. Nakazato, K., et al., *Enforced expression of Bcl-2 partially restores cell numbers but not functions of TCRgammadelta intestinal intraepithelial T lymphocytes in IL-15-deficient mice.* J Immunol, 2007. **178**(2): p. 757-64.
7. Kaech, S.M., et al., *Selective expression of the interleukin 7 receptor identifies effector CD8 T cells that give rise to long-lived memory cells.* Nat Immunol, 2003. **4**(12): p. 1191-8.
8. Osborne, L.C., et al., *Impaired CD8 T cell memory and CD4 T cell primary responses in IL-7R alpha mutant mice.* J Exp Med, 2007. **204**(3): p. 619-31.

9. Noguchi, M., et al., *Interleukin-2 receptor gamma chain mutation results in X-linked severe combined immunodeficiency in humans.* Cell, 1993. **73**(1): p. 147-57.

10. Cao, X., et al., *Defective lymphoid development in mice lacking expression of the common cytokine receptor gamma chain.* Immunity, 1995. **2**(3): p. 223-38.

11. Mazzucchelli, R. and S.K. Durum, *Interleukin-7 receptor expression: intelligent design.* Nat Rev Immunol, 2007. **7**(2): p. 144-54.

12. von Freeden-Jeffry, U., et al., *Lymphopenia in interleukin (IL)-7 gene-deleted mice identifies IL-7 as a nonredundant cytokine.* J Exp Med, 1995. **181**(4): p. 1519-26.

13. Peschon, J.J., et al., *Early lymphocyte expansion is severely impaired in interleukin 7 receptor-deficient mice.* J Exp Med, 1994. **180**(5): p. 1955-60.

14. Schluns, K.S., et al., *Interleukin-7 mediates the homeostasis of naive and memory CD8 T cells in vivo.* Nat Immunol, 2000. **1**(5): p. 426-32.

15. Tan, J.T., et al., *IL-7 is critical for homeostatic proliferation and survival of naive T cells.* Proc Natl Acad Sci U S A, 2001. **98**(15): p. 8732-7.

16. Silva, A., et al., *IL-7 contributes to the progression of human T-cell acute lymphoblastic leukemias.* Cancer Res, 2011. **71**(14): p. 4780-9.

17. Funk, P.E., R.P. Stephan, and P.L. Witte, *Vascular cell adhesion molecule 1-positive reticular cells express interleukin-7 and stem cell factor in the bone marrow.* Blood, 1995. **86**(7): p. 2661-71.

18. Sasson, S.C., et al., *Increased plasma interleukin-7 level correlates with decreased CD127 and Increased CD132 extracellular expression on T cell subsets in patients with HIV-1 infection.* J Infect Dis, 2006. **193**(4): p. 505-14.

19. Sawa, Y., et al., *Hepatic interleukin-7 expression regulates T cell responses.* Immunity, 2009. **30**(3): p. 447-57.

20. Unsinger, J., et al., *Sepsis-induced apoptosis leads to active suppression of delayed-type hypersensitivity by CD8+ regulatory T cells through a TRAIL-dependent mechanism.* J Immunol, 2010. **184**(12): p. 6766-72.

21. Zubkova, I., H. Mostowski, and M. Zaitseva, *Up-regulation of IL-7, stromal-derived factor-1 alpha, thymus-expressed chemokine, and secondary lymphoid tissue chemokine gene expression in the stromal cells in response to thymocyte depletion: implication for thymus reconstitution.* J Immunol, 2005. **175**(4): p. 2321-30.

22. Jiang, Q., et al., *Distinct regions of the interleukin-7 receptor regulate different Bcl2 family members.* Mol Cell Biol, 2004. **24**(14): p. 6501-13.

23. Chetoui, N., et al., *Interleukin-7 promotes the survival of human CD4+ effector/memory T cells by up-regulating Bcl-2 proteins and activating the JAK/STAT signalling pathway.* Immunology, 2010. **130**(3): p. 418-26.

24. Huang, J., S.K. Durum, and K. Muegge, *Cutting edge: histone acetylation and recombination at the TCR gamma locus follows IL-7 induction.* J Immunol, 2001. **167**(11): p. 6073-7.

25. Huang, J. and K. Muegge, *Control of chromatin accessibility for V(D)J recombination by interleukin-7.* J Leukoc Biol, 2001. **69**(6): p. 907-11.

26. Roth, D.B. and N.L. Craig, *VDJ recombination: a transposase goes to work.* Cell, 1998. **94**(4): p. 411-4.

27. Barata, J.T., et al., *Activation of PI3K is indispensable for interleukin 7-mediated viability, proliferation, glucose use, and growth of T cell acute lymphoblastic leukemia cells.* J Exp Med, 2004. **200**(5): p. 659-69.

28. Kim, K., et al., *Characterization of an interleukin-7-dependent thymic cell line derived from a p53(-/-) mouse.* J Immunol Methods, 2003. **274**(1-2): p. 177-84.

29. Khaled, A.R., et al., *Withdrawal of IL-7 induces Bax translocation from cytosol to mitochondria through a rise in intracellular pH.* Proc Natl Acad Sci U S A, 1999. **96**(25): p. 14476-81.

30. Li, W.Q., et al., *Interleukin-7 inactivates the pro-apoptotic protein Bad promoting T cell survival.* J Biol Chem, 2004. **279**(28): p. 29160-6.

31. Candeias, S., et al., *Defective T-cell receptor gamma gene rearrangement in interleukin-7 receptor knockout mice.* Immunol Lett, 1997. **57**(1-3): p. 9-14.

32. Hernandez, J.B., R.H. Newton, and C.M. Walsh, *Life and death in the thymus--cell death signaling during T cell development.* Curr Opin Cell Biol, 2010. **22**(6): p. 865-71.

33. Bouillet, P., *Proapoptotic Bcl-2 Relative Bim Required for Certain Apoptotic Responses, Leukocyte Homeostasis, and to Preclude Autoimmunity.* Science, 1999. **286**(5445): p. 1735-1738.

34. Bouillet, P., et al., *BH3-only Bcl-2 family member Bim is required for apoptosis of autoreactive thymocytes.* Nature, 2002. **415**(6874): p. 922-6.

35. Sudo, T., et al., *Expression and function of the interleukin 7 receptor in murine lymphocytes.* Proc Natl Acad Sci U S A, 1993. **90**(19): p. 9125-9.

36. Wojciechowski, S., et al., *Bim mediates apoptosis of CD127(lo) effector T cells and limits T cell memory.* Eur J Immunol, 2006. **36**(7): p. 1694-706.

37. Hofmeister, R., et al., *Interleukin-7: physiological roles and mechanisms of action.* Cytokine Growth Factor Rev, 1999. **10**(1): p. 41-60.

38. Rathmell, J.C., et al., *IL-7 enhances the survival and maintains the size of naive T cells.* J Immunol, 2001. **167**(12): p. 6869-76.

39. Hildeman, D.A., et al., *Activated T cell death in vivo mediated by proapoptotic bcl-2 family member bim.* Immunity, 2002. **16**(6): p. 759-67.

40. Matsuzaki, Y., et al., *Role of bcl-2 in the development of lymphoid cells from the hematopoietic stem cell.* Blood, 1997. **89**(3): p. 853-62.

41. Kim, K., et al., *The trophic action of IL-7 on pro-T cells: inhibition of apoptosis of pro-T1, -T2, and -T3 cells correlates with Bcl-2 and Bax levels and is independent of Fas and p53 pathways.* J Immunol, 1998. **160**(12): p. 5735-41.

42. Gross, A., J.M. McDonnell, and S.J. Korsmeyer, *BCL-2 family members and the mitochondria in apoptosis.* Genes Dev, 1999. **13**(15): p. 1899-911.

43. Maraskovsky, E., et al., *Bcl-2 can rescue T lymphocyte development in interleukin-7 receptor-deficient mice but not in mutant rag-1-/- mice.* Cell, 1997. **89**(7): p. 1011-9.

44. Pellegrini, M., et al., *Loss of Bim increases T cell production and function in interleukin 7 receptor-deficient mice.* J Exp Med, 2004. **200**(9): p. 1189-95.

45. Khaled, A.R., et al., *Bax deficiency partially corrects interleukin-7 receptor alpha deficiency.* Immunity, 2002. **17**(5): p. 561-73.

46. Strasser, A., et al., *DNA damage can induce apoptosis in proliferating lymphoid cells via p53-independent mechanisms inhibitable by Bcl-2.* Cell, 1994. **79**(2): p. 329-39.

47. O'Connor, L., et al., *Bim: a novel member of the Bcl-2 family that promotes apoptosis.* EMBO J, 1998. **17**(2): p. 384-95.

48. Conradt, B. and H.R. Horvitz, *The C. elegans protein EGL-1 is required for programmed cell death and interacts with the Bcl-2-like protein CED-9.* Cell, 1998. **93**(4): p. 519-29.

49. Dijkers, P.F., et al., *Expression of the pro-apoptotic Bcl-2 family member Bim is regulated by the forkhead transcription factor FKHR-L1.* Curr Biol, 2000. **10**(19): p. 1201-4.

50. O'Reilly, L.A., et al., *The proapoptotic BH3-only protein bim is expressed in hematopoietic, epithelial, neuronal, and germ cells.* Am J Pathol, 2000. **157**(2): p. 449-61.

51. Zhu, Y., et al., *Constitutive association of the proapoptotic protein Bim with Bcl-2-related proteins on mitochondria in T cells.* Proc Natl Acad Sci U S A, 2004. **101**(20): p. 7681-6.

52. Li, W.Q., et al., *Interleukin-7 regulates Bim proapoptotic activity in peripheral T-cell survival.* Mol Cell Biol, 2010. **30**(3): p. 590-600.

53. Yano, T., et al., *The RUNX3 tumor suppressor upregulates Bim in gastric epithelial cells undergoing transforming growth factor beta-induced apoptosis.* Mol Cell Biol, 2006. **26**(12): p. 4474-88.

54. Ley, R., et al., *Extracellular signal-regulated kinases 1/2 are serum-stimulated "Bim(EL) kinases" that bind to the BH3-only protein Bim(EL) causing its phosphorylation and turnover.* J Biol Chem, 2004. **279**(10): p. 8837-47.

55. Snow, A.L., et al., *Critical role for BIM in T cell receptor restimulation-induced death.* Biol Direct, 2008. **3**: p. 34.

56. Stahl, M., et al., *The forkhead transcription factor FoxO regulates transcription of p27Kip1 and Bim in response to IL-2.* J Immunol, 2002. **168**(10): p. 5024-31.

57. Whitfield, J., et al., *Dominant-negative c-Jun promotes neuronal survival by reducing BIM expression and inhibiting mitochondrial cytochrome c release.* Neuron, 2001. **29**(3): p. 629-43.

58. Datta, S.R., A. Brunet, and M.E. Greenberg, *Cellular survival: a play in three Akts.* Genes Dev, 1999. **13**(22): p. 2905-27.

59. Wildey, G.M. and P.H. Howe, *Runx1 is a co-activator with FOXO3 to mediate transforming growth factor beta (TGFbeta)-induced Bim transcription in hepatic cells.* J Biol Chem, 2009. **284**(30): p. 20227-39.

60. Ramesh, S., et al., *TGF beta-mediated BIM expression and apoptosis are regulated through SMAD3-dependent expression of the MAPK phosphatase MKP2.* EMBO Rep, 2008. **9**(10): p. 990-7.

61. Lee, H.C., et al., *Transcriptional regulation of the mouse IL-7 receptor alpha promoter by glucocorticoid receptor.* J Immunol, 2005. **174**(12): p. 7800-6.

62. U, M., et al., *Molecular cloning and characterization of six novel isoforms of human Bim, a member of the proapoptotic Bcl-2 family.* FEBS Lett, 2001. **509**(1): p. 135-41.

63. Ley, R., et al., *Regulatory phosphorylation of Bim: sorting out the ERK from the JNK.* Cell Death Differ, 2005. **12**(8): p. 1008-14.

64. Clybouw, C., et al., *BimL upregulation induced by BCR cross-linking in BL41 Burkitt's lymphoma results from a splicing mechanism of the BimEL mRNA.* Biochem Biophys Res Commun, 2009. **383**(1): p. 32-6.

65. Su, H., et al., *Essential and overlapping functions for mammalian Argonautes in microRNA silencing.* Genes Dev, 2009. **23**(3): p. 304-17.

66. Clybouw, C., et al., *Alternative splicing of Bim and Erk-mediated Bim(EL) phosphorylation are dispensable for hematopoietic homeostasis in vivo.* Cell Death Differ, 2012. **19**(6): p. 1060-8.

67. Anczukow, O., et al., *The splicing factor SRSF1 regulates apoptosis and proliferation to promote mammary epithelial cell transformation.* Nat Struct Mol Biol, 2012. **19**(2): p. 220-8.

68. Hubner, A., et al., *Multisite phosphorylation regulates Bim stability and apoptotic activity.* Mol Cell, 2008. **30**(4): p. 415-25.

69. Becker, E.B., et al., *Characterization of the c-Jun N-terminal kinase-BimEL signaling pathway in neuronal apoptosis.* J Neurosci, 2004. **24**(40): p. 8762-70.

70. Bivik, C. and K. Ollinger, *JNK mediates UVB-induced apoptosis upstream lysosomal membrane permeabilization and Bcl-2 family proteins.* Apoptosis, 2008. **13**(9): p. 1111-20.

71. Cai, B., et al., *p38 MAP kinase mediates apoptosis through phosphorylation of BimEL at Ser-65.* J Biol Chem, 2006. **281**(35): p. 25215-22.

72. Luciano, F., et al., *Phosphorylation of Bim-EL by Erk1/2 on serine 69 promotes its degradation via the proteasome pathway and regulates its proapoptotic function.* Oncogene, 2003. **22**(43): p. 6785-93.

73. Ley, R., et al., *Activation of the ERK1/2 signaling pathway promotes phosphorylation and proteasome-dependent degradation of the BH3-only protein, Bim.* J Biol Chem, 2003. **278**(21): p. 18811-6.

74. Dehan, E., et al., *betaTrCP- and Rsk1/2-mediated degradation of BimEL inhibits apoptosis.* Mol Cell, 2009. **33**(1): p. 109-16.

75. Adams, J.M., et al., *Control of apoptosis in hematopoietic cells by the Bcl-2 family of proteins.* Cold Spring Harb Symp Quant Biol, 1999. **64**: p. 351-8.

76. Terradillos, O., et al., *Direct addition of BimL to mitochondria does not lead to cytochrome c release.* FEBS Lett, 2002. **522**(1-3): p. 29-34.

77. Puthalakath, H., et al., *The proapoptotic activity of the Bcl-2 family member Bim is regulated by interaction with the dynein motor complex.* Mol Cell, 1999. **3**(3): p. 287-96.

78. Lei, K. and R.J. Davis, *JNK phosphorylation of Bim-related members of the Bcl2 family induces Bax-dependent apoptosis.* Proc Natl Acad Sci U S A, 2003. **100**(5): p. 2432-7.

79. Swainson, L., et al., *IL-7-induced proliferation of recent thymic emigrants requires activation of the PI3K pathway.* Blood, 2007. **109**(3): p. 1034-42.

80. Wofford, J.A., et al., *IL-7 promotes Glut1 trafficking and glucose uptake via STAT5-mediated activation of Akt to support T-cell survival.* Blood, 2008. **111**(4): p. 2101-11.

81. Frauwirth, K.A. and C.B. Thompson, *Regulation of T lymphocyte metabolism.* J Immunol, 2004. **172**(8): p. 4661-5.

82. Chehtane, M. and A.R. Khaled, *Interleukin-7 mediates glucose utilization in lymphocytes through transcriptional regulation of the hexokinase II gene.* Am J Physiol Cell Physiol, 2010. **298**(6): p. C1560-71.

83. Chin, H., et al., *Lyn physically associates with the erythropoietin receptor and may play a role in activation of the Stat5 pathway.* Blood, 1998. **91**(10): p. 3734-45.

84. Seddon, B. and R. Zamoyska, *TCR signals mediated by Src family kinases are essential for the survival of naive T cells.* J Immunol, 2002. **169**(6): p. 2997-3005.

85. Crawley, J.B., J. Willcocks, and B.M. Foxwell, *Interleukin-7 induces T cell proliferation in the absence of Erk/MAP kinase activity.* Eur J Immunol, 1996. **26**(11): p. 2717-23.

86. Crawley, J.B., et al., *T cell proliferation in response to interleukins 2 and 7 requires p38MAP kinase activation.* J Biol Chem, 1997. **272**(23): p. 15023-7.

87. Seddon, B. and R. Zamoyska, *TCR and IL-7 receptor signals can operate independently or synergize to promote lymphopenia-induced expansion of naive T cells.* J Immunol, 2002. **169**(7): p. 3752-9.

88. Kittipatarin, C., N. Tschammer, and A.R. Khaled, *The interaction of LCK and the CD4 co-receptor alters the dose response of T-cells to interleukin-7.* Immunol Lett, 2010. **131**(2): p. 170-81.

89. Khaled, A.R., et al., *Cytokine-driven cell cycling is mediated through Cdc25A.* J Cell Biol, 2005. **169**(5): p. 755-63.

90. Rajnavolgyi, E., et al., *IL-7 withdrawal induces a stress pathway activating p38 and Jun N-terminal kinases.* Cell Signal, 2002. **14**(9): p. 761-9.

91. Khaled, A.R., et al., *Trophic factor withdrawal: p38 mitogen-activated protein kinase activates NHE1, which induces intracellular alkalinization.* Mol Cell Biol, 2001. **21**(22): p. 7545-57.

92. Li, W.Q., et al., *IL-7 promotes T cell proliferation through destabilization of p27Kip1.* J Exp Med, 2006. **203**(3): p. 573-82.

93. Mochizuki, T., et al., *Physical and functional interactions between Pim-1 kinase and Cdc25A phosphatase. Implications for the Pim-1-mediated activation of the c-Myc signaling pathway.* J Biol Chem, 1999. **274**(26): p. 18659-66.

94. Goetz, C.A., et al., *STAT5 activation underlies IL7 receptor-dependent B cell development.* J Immunol, 2004. **172**(8): p. 4770-8.

95. Jacobs, H., et al., *PIM1 reconstitutes thymus cellularity in interleukin 7- and common gamma chain-mutant mice and permits thymocyte maturation in Rag- but not CD3gamma-deficient mice.* J Exp Med, 1999. **190**(8): p. 1059-68.

96. Mikkers, H., et al., *Mice deficient for all PIM kinases display reduced body size and impaired responses to hematopoietic growth factors.* Mol Cell Biol, 2004. **24**(13): p. 6104-15.

97. Chen, X.P., et al., *Pim serine/threonine kinases regulate the stability of Socs-1 protein.* Proc Natl Acad Sci U S A, 2002. **99**(4): p. 2175-80.

98. Shaulian, E. and M. Karin, *AP-1 in cell proliferation and survival.* Oncogene, 2001. **20**(19): p. 2390-400.

99. Shaulian, E. and M. Karin, *AP-1 as a regulator of cell life and death.* Nat Cell Biol, 2002. **4**(5): p. E131-6.

100. Devary, Y., et al., *The mammalian ultraviolet response is triggered by activation of Src tyrosine kinases.* Cell, 1992. **71**(7): p. 1081-91.

101. Pfarr, C.M., et al., *Mouse JunD negatively regulates fibroblast growth and antagonizes transformation by ras.* Cell, 1994. **76**(4): p. 747-60.

102. Xiao, L., et al., *Induced JunD in intestinal epithelial cells represses CDK4 transcription through its proximal promoter region following polyamine depletion.* Biochem J, 2007. **403**(3): p. 573-81.

103. Macaire, H., et al., *Tax Protein-induced Expression of Antiapoptotic Bfl-1 Protein Contributes to Survival of Human T-cell Leukemia Virus Type 1 (HTLV-1)-infected T-cells.* J Biol Chem, 2012. **287**(25): p. 21357-70.

104. Storek, J., et al., *Interleukin-7 improves CD4 T-cell reconstitution after autologous CD34 cell transplantation in monkeys.* Blood, 2003. **101**(10): p. 4209-18.

105. Fry, T.J., et al., *A potential role for interleukin-7 in T-cell homeostasis.* Blood, 2001. **97**(10): p. 2983-90.

106. Mackall, C.L., et al., *IL-7 increases both thymic-dependent and thymic-independent T-cell regeneration after bone marrow transplantation.* Blood, 2001. **97**(5): p. 1491-7.

107. Colombetti, S., F. Levy, and L. Chapatte, *IL-7 adjuvant treatment enhances long-term tumor-antigen-specific CD8+ T-cell responses after immunization with recombinant lentivector.* Blood, 2009. **113**(26): p. 6629-37.

108. Li, C.R., et al., *IL-7 uniquely maintains FoxP3(+) adaptive Treg cells that reverse diabetes in NOD mice via integrin-beta7-dependent localization.* J Autoimmun, 2011. **37**(3): p. 217-27.

109. Sportes, C., et al., *Administration of rhIL-7 in humans increases in vivo TCR repertoire diversity by preferential expansion of naive T cell subsets.* J Exp Med, 2008. **205**(7): p. 1701-14.

110. Mackall, C.L., T.J. Fry, and R.E. Gress, *Harnessing the biology of IL-7 for therapeutic application.* Nat Rev Immunol, 2011. **11**(5): p. 330-42.

111. Alpdogan, O., et al., *IL-7 enhances peripheral T cell reconstitution after allogeneic hematopoietic stem cell transplantation.* J Clin Invest, 2003. **112**(7): p. 1095-107.

112. Unsinger, J., et al., *IL-7 promotes T cell viability, trafficking, and functionality and improves survival in sepsis.* J Immunol, 2010. **184**(7): p. 3768-79.

113. Sereti, I., et al., *IL-7 administration drives T cell-cycle entry and expansion in HIV-1 infection.* Blood, 2009. **113**(25): p. 6304-14.

114. Sakata, T., et al., *Constitutive expression of interleukin-7 mRNA and production of IL-7 by a cloned murine thymic stromal cell line.* J Leukoc Biol, 1990. **48**(3): p. 205-12.

115. Mazzucchelli, R.I., et al., *Visualization and identification of IL-7 producing cells in reporter mice.* PLoS One, 2009. **4**(11): p. e7637.

116. Repass, J.F., et al., *IL7-hCD25 and IL7-Cre BAC transgenic mouse lines: new tools for analysis of IL-7 expressing cells.* Genesis, 2009. **47**(4): p. 281-7.

117. Kovanen, P.E. and W.J. Leonard, *Cytokines and immunodeficiency diseases: critical roles of the gamma(c)-dependent cytokines interleukins 2, 4, 7, 9, 15, and 21, and their signaling pathways.* Immunol Rev, 2004. **202**: p. 67-83.

118. Venkitaraman, A.R. and R.J. Cowling, *Interleukin 7 receptor functions by recruiting the tyrosine kinase p59fyn through a segment of its cytoplasmic tail.* Proc Natl Acad Sci U S A, 1992. **89**(24): p. 12083-7.

119. Seckinger, P. and M. Fougereau, *Activation of src family kinases in human pre-B cells by IL-7.* J Immunol, 1994. **153**(1): p. 97-109.

120. Shaulian, E., *AP-1--The Jun proteins: Oncogenes or tumor suppressors in disguise?* Cell Signal, 2010. **22**(6): p. 894-9.

121. Eychene, A., N. Rocques, and C. Pouponnot, *A new MAFia in cancer.* Nat Rev Cancer, 2008. **8**(9): p. 683-93.

122. Hess, J., P. Angel, and M. Schorpp-Kistner, *AP-1 subunits: quarrel and harmony among siblings.* J Cell Sci, 2004. **117**(Pt 25): p. 5965-73.

123. Gao, Y., et al., *JNK1 is essential for CD8+ T cell-mediated tumor immune surveillance.* J Immunol, 2005. **175**(9): p. 5783-9.

124. Kallunki, T., et al., *c-Jun can recruit JNK to phosphorylate dimerization partners via specific docking interactions.* Cell, 1996. **87**(5): p. 929-39.

125. Short, J.D. and C.M. Pfarr, *Translational regulation of the JunD messenger RNA.* J Biol Chem, 2002. **277**(36): p. 32697-705.

126. Ryseck, R.P., et al., *Transcriptional activation of c-jun during the G0/G1 transition in mouse fibroblasts.* Nature, 1988. **334**(6182): p. 535-7.

127. Ryder, K., L.F. Lau, and D. Nathans, *A gene activated by growth factors is related to the oncogene v-jun.* Proc Natl Acad Sci U S A, 1988. **85**(5): p. 1487-91.

128. Schutte, J., J.D. Minna, and M.J. Birrer, *Deregulated expression of human c-jun transforms primary rat embryo cells in cooperation with an activated c-Ha-ras gene and transforms rat-1a cells as a single gene.* Proc Natl Acad Sci U S A, 1989. **86**(7): p. 2257-61.

129. Castellazzi, M., et al., *Overexpression of c-jun, junB, or junD affects cell growth differently.* Proc Natl Acad Sci U S A, 1991. **88**(20): p. 8890-4.

130. von Freeden-Jeffry, U., et al., *The earliest T lineage-committed cells depend on IL-7 for Bcl-2 expression and normal cell cycle progression.* Immunity, 1997. **7**(1): p. 147-54.

131. Khaled, A.R. and S.K. Durum, *Death and Baxes: mechanisms of lymphotrophic cytokines.* Immunol Rev, 2003. **193**: p. 48-57.

132. Kittipatarin, C. and A.R. Khaled, *Ex vivo expansion of memory CD8 T cells from lymph nodes or spleen through in vitro culture with interleukin-7.* J Immunol Methods, 2009. **344**(1): p. 45-57.

133. Rahman, Z., et al., *Down-regulation of Pim-1 and Bcl-2 is accompanied with apoptosis of interleukin-6-depleted mouse B-cell hybridoma 7TD1 cells.* Immunol Lett, 2001. **75**(3): p. 199-208.

134. Zou, T., et al., *Polyamines regulate the stability of JunD mRNA by modulating the competitive binding of its 3' untranslated region to HuR and AUF1.* Mol Cell Biol, 2010. **30**(21): p. 5021-32.

135. Azfer, A., et al., *Activation of endoplasmic reticulum stress response during the development of ischemic heart disease.* Am J Physiol Heart Circ Physiol, 2006. **291**(3): p. H1411-20.

136. Jaganathan, S., P. Yue, and J. Turkson, *Enhanced sensitivity of pancreatic cancer cells to concurrent inhibition of aberrant signal transducer and activator of transcription 3 and epidermal growth factor receptor or Src.* J Pharmacol Exp Ther, 2010. **333**(2): p. 373-81.

137. Dignam, J.D., R.M. Lebovitz, and R.G. Roeder, *Accurate transcription initiation by RNA polymerase II in a soluble extract from isolated mammalian nuclei.* Nucleic Acids Res, 1983. **11**(5): p. 1475-89.

138. Storey, J.D. and R. Tibshirani, *Statistical significance for genomewide studies.* Proc Natl Acad Sci U S A, 2003. **100**(16): p. 9440-5.

139. Boyle, E.I., et al., *GO::TermFinder--open source software for accessing Gene Ontology information and finding significantly enriched Gene Ontology terms associated with a list of genes.* Bioinformatics, 2004. **20**(18): p. 3710-5.

140. Ruppert, S.M., et al., *JunD/AP-1-Mediated Gene Expression Promotes Lymphocyte Growth Dependent on Interleukin-7 Signal Transduction.* PLoS One, 2012. **7**(2): p. e32262.

141. Heikkinen, S., et al., *Mouse hexokinase II gene: structure, cDNA, promoter analysis, and expression pattern.* Mamm Genome, 2000. **11**(2): p. 91-6.

142. Kang, J., et al., *STAT5 is required for thymopoiesis in a development stage-specific manner.* J Immunol, 2004. **173**(4): p. 2307-14.

143. Morcinek, J.C., et al., *Activation of STAT5 triggers proliferation and contributes to anti-apoptotic signalling mediated by the oncogenic Xmrk kinase.* Oncogene, 2002. **21**(11): p. 1668-78.

144. Cen, B., et al., *Regulation of Skp2 levels by the Pim-1 protein kinase.* J Biol Chem, 2010. **285**(38): p. 29128-37.

145. Weitzman, J.B., et al., *JunD protects cells from p53-dependent senescence and apoptosis.* Mol Cell, 2000. **6**(5): p. 1109-19.

146. Lamb, J.A., et al., *JunD mediates survival signaling by the JNK signal transduction pathway.* Mol Cell, 2003. **11**(6): p. 1479-89.

147. Meixner, A., et al., *JunD regulates lymphocyte proliferation and T helper cell cytokine expression.* EMBO J, 2004. **23**(6): p. 1325-35.

148. Hernandez, J.M., et al., *Multiple facets of junD gene expression are atypical among AP-1 family members.* Oncogene, 2008. **27**(35): p. 4757-67.

149. Hartman, T.R., et al., *RNA helicase A is necessary for translation of selected messenger RNAs.* Nat Struct Mol Biol, 2006. **13**(6): p. 509-16.

150. Musti, A.M., et al., *Differential regulation of c-Jun and JunD by ubiquitin-dependent protein degradation.* Biol Chem, 1996. **377**(10): p. 619-24.

151. Yazgan, O. and C.M. Pfarr, *Regulation of two JunD isoforms by Jun N-terminal kinases.* J Biol Chem, 2002. **277**(33): p. 29710-8.

152. Sasson, S.C., J.J. Zaunders, and A.D. Kelleher, *The IL-7/IL-7 receptor axis: understanding its central role in T-cell homeostasis and the challenges facing its utilization as a novel therapy.* Curr Drug Targets, 2006. **7**(12): p. 1571-82.

153. Rathmell, J.C., et al., *In the absence of extrinsic signals, nutrient utilization by lymphocytes is insufficient to maintain either cell size or viability.* Mol Cell, 2000. **6**(3): p. 683-92.

154. Kim, G.Y., C. Hong, and J.H. Park, *Seeing is believing: illuminating the source of in vivo interleukin-7.* Immune Netw, 2011. **11**(1): p. 1-10.

155. Jiang, Q., et al., *Cell biology of IL-7, a key lymphotrophin.* Cytokine Growth Factor Rev, 2005. **16**(4-5): p. 513-33.

156. Maraskovsky, E., et al., *Impaired survival and proliferation in IL-7 receptor-deficient peripheral T cells.* J Immunol, 1996. **157**(12): p. 5315-23.

157. Lai, S.Y., J. Molden, and M.A. Goldsmith, *Shared gamma(c) subunit within the human interleukin-7 receptor complex. A molecular basis for the pathogenesis of X-linked severe combined immunodeficiency.* J Clin Invest, 1997. **99**(2): p. 169-77.

158. Rich, B.E., et al., *Cutaneous lymphoproliferation and lymphomas in interleukin 7 transgenic mice.* J Exp Med, 1993. **177**(2): p. 305-16.

159. Yamanaka, K., et al., *Skin-derived interleukin-7 contributes to the proliferation of lymphocytes in cutaneous T-cell lymphoma.* Blood, 2006. **107**(6): p. 2440-5.

160. Maraskovsky, E., et al., *Overexpression of Bcl-2 does not rescue impaired B lymphopoiesis in IL-7 receptor-deficient mice but can enhance survival of mature B cells.* Int Immunol, 1998. **10**(9): p. 1367-75.

161. Benison, G., P.A. Karplus, and E. Barbar, *Structure and dynamics of LC8 complexes with KXTQT-motif peptides: swallow and dynein intermediate chain compete for a common site.* J Mol Biol, 2007. **371**(2): p. 457-68.

162. Dijkers, P.F., et al., *FKHR-L1 can act as a critical effector of cell death induced by cytokine withdrawal: protein kinase B-enhanced cell survival through maintenance of mitochondrial integrity.* J Cell Biol, 2002. **156**(3): p. 531-42.

163. Seward, R.J., et al., *Phosphorylation of the pro-apoptotic protein Bim in lymphocytes is associated with protection from apoptosis.* Mol Immunol, 2003. **39**(16): p. 983-93.

164. Weston, C.R., et al., *Activation of ERK1/2 by deltaRaf-1:ER* represses Bim expression independently of the JNK or PI3K pathways.* Oncogene, 2003. **22**(9): p. 1281-93.

165. Leung, K.T., et al., *Activation of the JNK pathway promotes phosphorylation and degradation of BimEL--a novel mechanism of chemoresistance in T-cell acute lymphoblastic leukemia.* Carcinogenesis, 2008. **29**(3): p. 544-51.

166. Adachi, M., X. Zhao, and K. Imai, *Nomenclature of dynein light chain-linked BH3-only protein Bim isoforms.* Cell Death Differ, 2005. **12**(2): p. 192-3.

167. Hubbard, V.M., et al., *Macroautophagy regulates energy metabolism during effector T cell activation.* J Immunol, 2010. **185**(12): p. 7349-57.

168. Li, C., et al., *Autophagy is induced in CD4+ T cells and important for the growth factor-withdrawal cell death.* J Immunol, 2006. **177**(8): p. 5163-8.

169. Kittipatarin, C., et al., *Cdc25A-driven proliferation regulates CD62L levels and lymphocyte movement in response to interleukin-7.* Exp Hematol, 2010. **38**(12): p. 1143-56.

170. Franck, P., et al., *Measurement of intracellular pH in cultured cells by flow cytometry with BCECF-AM.* J Biotechnol, 1996. **46**(3): p. 187-95.

171. Grenier, A.L., et al., *Apoptosis-induced alkalinization by the Na+/H+ exchanger isoform 1 is mediated through phosphorylation of amino acids Ser726 and Ser729.* Am J Physiol Cell Physiol, 2008. **295**(4): p. C883-96.

172. Willis, S.N. and J.M. Adams, *Life in the balance: how BH3-only proteins induce apoptosis.* Curr Opin Cell Biol, 2005. **17**(6): p. 617-25.

173. Reinhardt, H.C. and B. Schumacher, *The p53 network: cellular and systemic DNA damage responses in aging and cancer.* Trends Genet, 2012. **28**(3): p. 128-36.

174. Komarov, P.G., et al., *A chemical inhibitor of p53 that protects mice from the side effects of cancer therapy.* Science, 1999. **285**(5434): p. 1733-7.

175. Sohn, D., et al., *Pifithrin-alpha protects against DNA damage-induced apoptosis downstream of mitochondria independent of p53.* Cell Death Differ, 2009. **16**(6): p. 869-78.

176. Nilsson, C., et al., *Cytosolic acidification and lysosomal alkalinization during TNF-alpha induced apoptosis in U937 cells.* Apoptosis, 2006. **11**(7): p. 1149-59.

177. Turk, B. and V. Turk, *Lysosomes as "suicide bags" in cell death: myth or reality?* J Biol Chem, 2009. **284**(33): p. 21783-7.

178. Pedersen, S.F., *The Na+/H+ exchanger NHE1 in stress-induced signal transduction: implications for cell proliferation and cell death.* Pflugers Arch, 2006. **452**(3): p. 249-59.

179. Gonzalez-Polo, R.A., et al., *Inhibition of paraquat-induced autophagy accelerates the apoptotic cell death in neuroblastoma SH-SY5Y cells.* Toxicol Sci, 2007. **97**(2): p. 448-58.

180. Shen, H.M. and P. Codogno, *Autophagic cell death: Loch Ness monster or endangered species?* Autophagy, 2011. **7**(5): p. 457-65.

181. Wu, Y.T., et al., *Dual role of 3-methyladenine in modulation of autophagy via different temporal patterns of inhibition on class I and III phosphoinositide 3-kinase.* J Biol Chem, 2010. **285**(14): p. 10850-61.

182. Kabeya, Y., et al., *LC3, a mammalian homologue of yeast Apg8p, is localized in autophagosome membranes after processing.* EMBO J, 2000. **19**(21): p. 5720-8.

183. Kabeya, Y., et al., *LC3, GABARAP and GATE16 localize to autophagosomal membrane depending on form-II formation.* J Cell Sci, 2004. **117**(Pt 13): p. 2805-12.

184. Komatsu, M. and Y. Ichimura, *Physiological significance of selective degradation of p62 by autophagy.* FEBS Lett, 2010. **584**(7): p. 1374-8.

185. Gonzalez-Noriega, A., et al., *Chloroquine inhibits lysosomal enzyme pinocytosis and enhances lysosomal enzyme secretion by impairing receptor recycling.* J Cell Biol, 1980. **85**(3): p. 839-52.

186. He, Y., et al., *Identification of a lysosomal pathway that modulates glucocorticoid signaling and the inflammatory response.* Sci Signal, 2011. **4**(180): p. ra44.

187. Meikle, P.J., et al., *Diagnosis of lysosomal storage disorders: evaluation of lysosome-associated membrane protein LAMP-1 as a diagnostic marker.* Clin Chem, 1997. **43**(8 Pt 1): p. 1325-35.

188. Putcha, G.V., et al., *JNK-mediated BIM phosphorylation potentiates BAX-dependent apoptosis.* Neuron, 2003. **38**(6): p. 899-914.

189. Droga-Mazovec, G., et al., *Cysteine cathepsins trigger caspase-dependent cell death through cleavage of bid and antiapoptotic Bcl-2 homologues.* J Biol Chem, 2008. **283**(27): p. 19140-50.

190. Berg, T.O., et al., *Isolation and characterization of rat liver amphisomes. Evidence for fusion of autophagosomes with both early and late endosomes.* J Biol Chem, 1998. **273**(34): p. 21883-92.

191. Qiao, L. and J. Zhang, *Inhibition of lysosomal functions reduces proteasomal activity.* Neurosci Lett, 2009. **456**(1): p. 15-9.

192. Isogai, S., et al., *Crystal structure of the ubiquitin-associated (UBA) domain of p62 and its interaction with ubiquitin.* J Biol Chem, 2011. **286**(36): p. 31864-74.

193. Day, C.L., et al., *Localization of dynein light chains 1 and 2 and their pro-apoptotic ligands.* Biochem J, 2004. **377**(Pt 3): p. 597-605.

194. Caviston, J.P., et al., *Huntingtin coordinates the dynein-mediated dynamic positioning of endosomes and lysosomes.* Mol Biol Cell, 2011. **22**(4): p. 478-92.

195. Harada, A., et al., *Golgi vesiculation and lysosome dispersion in cells lacking cytoplasmic dynein.* J Cell Biol, 1998. **141**(1): p. 51-9.

196. Cai, Q., et al., *Snapin-regulated late endosomal transport is critical for efficient autophagy-lysosomal function in neurons.* Neuron, 2010. **68**(1): p. 73-86.

197. Henriques, C.M., et al., *IL-7 induces rapid clathrin-mediated internalization and JAK3-dependent degradation of IL-7Ralpha in T cells.* Blood, 2010. **115**(16): p. 3269-77.

198. Maiuri, M.C., et al., *Functional and physical interaction between Bcl-X(L) and a BH3-like domain in Beclin-1.* EMBO J, 2007. **26**(10): p. 2527-39.

199. Maiuri, M.C., et al., *BH3-only proteins and BH3 mimetics induce autophagy by competitively disrupting the interaction between Beclin 1 and Bcl-2/Bcl-X(L).* Autophagy, 2007. **3**(4): p. 374-6.

200. Faber, A.C., et al., *BIM Expression in Treatment-Naive Cancers Predicts Responsiveness to Kinase Inhibitors.* Cancer Discov, 2011. **1**(4): p. 352-365.

201. Labelle, J.L., et al., *A stapled BIM peptide overcomes apoptotic resistance in hematologic cancers.* J Clin Invest, 2012. **122**(6): p. 2018-31.

202. Warburg, O., *On respiratory impairment in cancer cells.* Science, 1956. **124**(3215): p. 269-70.

203. Zhao, J., Y. Lu, and H.M. Shen, *Targeting p53 as a therapeutic strategy in sensitizing TRAIL-induced apoptosis in cancer cells.* Cancer Lett, 2012. **314**(1): p. 8-23.

204. Peltola, K.J., et al., *Pim-1 kinase inhibits STAT5-dependent transcription via its interactions with SOCS1 and SOCS3.* Blood, 2004. **103**(10): p. 3744-50.

205. Allen, J.D., et al., *Pim-2 transgene induces lymphoid tumors, exhibiting potent synergy with c-myc.* Oncogene, 1997. **15**(10): p. 1133-41.

206. Nelson, E.A., et al., *The STAT5 inhibitor pimozide decreases survival of chronic myelogenous leukemia cells resistant to kinase inhibitors.* Blood, 2011. **117**(12): p. 3421-9.

207. Warsch, W., et al., *High STAT5 levels mediate imatinib resistance and indicate disease progression in chronic myeloid leukemia.* Blood, 2011. **117**(12): p. 3409-20.

208. Spruce, T., et al., *An early developmental role for miRNAs in the maintenance of extraembryonic stem cells in the mouse embryo.* Dev Cell, 2010. **19**(2): p. 207-19.